Regulation of PIN-FORMED-mediated auxin transport and the role of auxin and cytokinin responses in plant-nematode interactions

UR

DISSERTATION

UNIVERSITÄT REGENSBURG

Vorgelegt von

Birgit Absmanner

aus Göming

im Juni 2013

Das Promotiongesuch wurde eingereicht am: 21.06.2013

Die Arbeit wurde angeleitet von: Dr. Ulrich Hammes

Table of contents

3 Phytohormone responses during vascular development in nematode induced feeding sites..47

1 General introduction

1.1 Auxin – a major regulator of plant growth and development

In order to compensate for their sessile lifestyle, plants exhibit enormous developmental plasticity which allows them to adapt to changing environmental conditions and nutrient supply. Phytohormones act as mobile signals between cells, tissues and organs and play a crucial role in the regulation and coordination of plant growth and development. They include the five "classical" phytohormones auxin, cytokinin, giberellic acid, abscisic acid and ethylene as well as compounds that have been identified more recently like brassinosteroids, jasmonic acid, salicylic acid and strigolactones. Processes that are influenced by phytohormone action include the control of plant size and architecture, tropisms, responses to biotic and abiotic stresses, organismic interactions as well as flower and embryo development (Davies, 2010).

The most investigated phytohormone and also the first one to be described is auxin. Based on classical experiments studying the phototropism of canary grass coleoptiles, Charles Darwin postulated the existence of a transmissible signal (Darwin and Darwin, 1880) which was later chemically identified as indole-3-acetic acid (IAA) and termed auxin (Kögl *et al.*, 1934; Went and Thimann, 1937). Nowadays, the term auxin does not only describe IAA but also several other chemical compounds - naturally occurring and synthetic ones - that exhibit auxin activity. However, IAA is by far the most prominent endogenous auxin in plants (Sauer *et al.*, 2013).

Since its discovery, extensive research revealed that auxin is involved in the regulation of an enormous variety of biological processes. On a cellular level, auxin influences cell division, elongation and differentiation. Additionally, it plays a role in a seemingly never-ending list of developmental and growth processes including embryogenesis, organogenesis, flower development, root meristem maintenance, vascular tissue differentiation, apical dominance as well as various growth responses to environmental stimuli like light, gravity and pathogen attack (Vanneste and Friml, 2009; Sauer *et al.*, 2013).

How is it possible that the rather simple indolic molecule auxin is such a crucial determinant for the plant's structure and functioning? The unique property of auxin that distinguishes it from other plant hormones is that its action is not only mediated through signaling and transcriptional changes but also through the formation of local maxima and gradients within

tissues. This differential distribution is interpreted on the level of the individual cell via a signaling pathway that can lead to distinct outputs, depending on temporal and spatial context. Therefore, auxin is probably better described as a morphogen rather than a hormone because very often a concentration gradient within a tissue governs the developmental output (Friml, 2003). An overview of the mode of action of auxin including metabolism, transport and signaling will be given in the following chapters.

1.2 Auxin - the mode of action

1.2.1 Metabolism

Cellular auxin levels are strongly influenced by the complex interplay between biosynthesis, storage by conjugation and degradation. IAA, which is structurally related to tryptophan, is synthesized mainly in rapidly dividing and growing tissues of the shoot, but also in the meristematic root tip by several redundant biosynthetic pathways (Ljung *et al.*, 2001; Ljung *et al.*, 2005). So far, one tryptophan-independent as well as four tryptophan-dependent synthesis pathways have been described (Woodward and Bartel, 2005; Mano and Nemoto, 2012). Characterization of mutants with defects in key enzymes of the different biosynthetic pathways and analyses of their distinct expression patterns suggest that local biosynthesis contributes to differential auxin distribution. Additionally, IAA can be catabolized or conjugated to various amino acid and sugar moieties, which allows temporal inactivation and storage of the hormone. Finally, excess cellular auxin is degraded by several different oxidation pathways (Woodward and Bartel, 2005; Sauer *et al.*, 2013).

1.2.2 Polar transport

Although local differences in auxin metabolism contribute to its asymmetric distribution within the plant body, it has become obvious over the last years that the major determinant for establishing auxin maxima and gradients is cell-to-cell transport. From the places of synthesis, auxin is distributed *via* two different pathways. Long distance transport throughout the plant occurs in the phloem (Cambridge and Morris, 1996). The local accumulation observed in different developmental contexts on the other hand is controlled by directional intercellular transport of the phytohormone termed polar auxin transport

(PAT). PAT is mediated by a system of influx and efflux carriers, whose differential and often polar subcellular localization defines the direction of auxin flow (Tanaka *et al.*, 2006; Vieten *et al.*, 2007).

IAA is a weak acid which is partly protonated at the apoplastic pH of ~ 5.5. In this form, it can enter the plant cell via lipophilic membrane diffusion. Additionally, proton symporters of the AUXIN-RESISTANT1 (AUX1) / LIKE-AUX1 (LAX1) family mediate the uptake of the anionic form of IAA. Auxin influx carrier activity can exceed diffusive influx enormously in certain cell types and is essential for developmental processes like gravitropism or lateral root formation (Marchant *et al.*, 1999; Marchant *et al.*, 2002; Yang *et al.*, 2006; Swarup *et al.*, 2008). At neutral cytosolic pH, IAA is predominantly dissociated and is therefore unable to pass through the plasma membrane. Consequently, export of auxin from cells is fully dependent on efflux carriers. Members of the P-GLYCOPROTEIN/MULTIDRUG-RESISTANCE subfamily of ATP-binding cassette proteins (MDR/PGP/ABCB) play a role both in auxin influx and efflux (Geisler *et al.*, 2005; Santelia *et al.*, 2005; Terasaka *et al.*, 2005). However, ABCB transporters generally exhibit apolar localization and high stability at the plasma membrane (Blakeslee *et al.*, 2007; Titapiwatanakun *et al.*, 2009). Their efflux activity is therefore mainly nondirectional and they might rather fulfill more general functions in auxin transport like controlling the amount of auxin that is available on certain transport routes (Zazimalova *et al.*, 2007; Vanneste and Friml, 2009). The main players in PAT-related auxin efflux are the PIN-FORMED (PIN) proteins which facilitate vectorial auxin transport and, by their distinct expression and dynamic polar localization, provide the molecular basis for the establishment of auxin maxima and gradients during different developmental processes (Tanaka *et al.*, 2006; Zazimalova *et al.*, 2007). A detailed introduction to PIN-mediated auxin efflux will be given in Chapter 2.1.

1.2.3 Perception and transcriptional output

Biosynthesis, metabolism and transport ensure appropriate and distinct auxin levels within plant tissues. In order to trigger a biological response, auxin signals must be perceived and interpreted at the level of the individual cell. Several independent auxin receptors and their corresponding signaling systems have been described in Arabidopsis, adding further flexibility to the great variety of auxin responses. The best-studied receptor is the F-box protein TRANSPORT INHIBITOR RESISTANT 1 (TIR1) which is a subunit of a Skp1-Cullin-F-box

(SCF) class E3 ubiquitin ligase complex (Ruegger *et al.*, 1998; Dharmasiri *et al.*, 2005). Upon binding of auxin, this ubiquitin ligase promotes the degradation of AUXIN / INDOLE ACETIC ACID (Aux/IAA) transcriptional repressors via the proteasome pathway by enhancing their ubiquitination. In the absence of auxin, the Aux/IAAs form inhibitory heterodimers with AUXIN RESPONSE FACTOR (ARF) transcription factors. Therefore, auxin-enhanced proteolysis of the Aux/IAA repressors leads to release and thus activation of the ARFs and subsequent early auxin-responsive gene expression (Chapman and Estelle, 2009). These auxin-responsive genes contain specific sequence motifs, so called auxin response elements (AuxRE) in their promoters, which are recognized and bound by the ARFs (Ulmasov *et al.*, 1995). The components of the described pathway belong to large protein families. There are 5 homologs of TIR1, AUXIN SIGNALIN F-BOX-PROTEIN 1 (AFB) to AFB5. Additionally, 29 Aux/IAAs and 23 ARFs provide a huge number of combinatorial possibilities and consequently of potential transcriptional outputs (Santner and Estelle, 2009). It seems likely that defined pairs of ARFs and Aux/IAAs can mediate specific developmental responses by acting on distinct sets of target genes. One such a pair is for example formed by the auxin response factor MONOPTEROS (MP) / ARF5 and its corresponding AUX/IAA protein BODENLOS (BDL) /IAA12 which are involved in the initiation of the root meristem, the specification of provascular cells in the embryo and vascular differentiation in the post-embryonic plant (Berleth and Jürgens, 1993; Przemeck *et al.*, 1996; Hardtke and Berleth, 1998; Hamann *et al.*, 1999; Hamann *et al.*, 2002).

1.2.4 Crosstalk with other hormones

Auxin action is very often dependent on input provided by other hormones. A famous example is the modulation of auxin responses by cytokinin and *vice versa*. Cytokinins are adenine derivates originally identified in the 1950ies as compounds which promote cell division and act antagonistically to auxin by promoting shoot growth from tobacco suspension cultured cells (Skoog and Miller, 1957). Since then they were shown to be involved in the regulation of numerous aspects of development like root growth, root architecture and vascular development, all of which are also influenced by auxin (To and Kieber, 2008). Several studies provide evidence for the extensive crosstalk and feedback loops between the auxin and cytokinin signaling pathways on the molecular level and further substantiate their role as regulatory opponents (Ioio *et al.*, 2008; Müller and Sheen, 2008;

Moubayidin *et al.,* 2010; Bishopp *et al.,* 2011b).

Apart from cytokinins, a number of other phytohormones, among them gibberelic acid, ethylene and brassinosteroids, have been shown to be closely linked to auxin (Woodward and Bartel, 2005), adding further complexity and flexibility to the hormonal control of plant life.

1.3 The role of auxin in vascular development

1.3.1 Vascular development in the embryo

The delicate auxin regulatory network plays a crucial role in many – if not all – aspects of plant development. A well characterized example is the initiation of vascular development during embryogenesis and the development of the root.

In the course of embryogenesis, the basic organization of the plant body is established, resulting in a seedling that consists of shoot apical meristem, cotelydons, hypocotyl, embryonic root and root meristem. The correct arrangement of these organs and the different cell types within them is tightly regulated and strongly dependent on auxin (Weijers and Jürgens, 2005). Vascular precursor cells, also termed procambial cells, are initiated during the globular stage of embryogenesis and subsequently develop as continuous files through the embryo, providing the basis for the vascular network of the mature plant. Specification of xylem and phloem from the vascular initials starts either during embryogenesis or after germination, depending on the plant species (Esau, 1965; Scheres *et al.,* 1995). The above mentioned auxin responsive transcription factor MP (see 1.2.3) plays a critical role in the initiation of the procambium. Mutations in the genes encoding for MP and also its corresponding repressor BDL result in rootless seedlings with strongly reduced vascular systems and occasionally fused cotyledons (Berleth and Jürgens, 1993; Hamann *et al.,* 1999). These phenotypes are partially caused by a lack of polar auxin transport in the procambial cells of the embryo. Indeed, MP positively regulates expression of the auxin efflux carrier PIN1, which by its polar localization mediates basally directed auxin flow in the preprocambial cells of the proembryo from the globular stage on. Therefore, a positive feedback loop between auxin, MP and PINs defines the auxin fluxes in the embryo (Friml, 2003, Wenzel). Such a feedback loop was also found to be essential during vein formation in leaves where likewise auxin flow directed by the polar localization

of PIN1 precedes procambium differentiation (Scarpella *et al.*, 2006b). The so called auxin-canalization hypothesis that was formulated over 30 years ago (Sachs and Woolhouse, 1981) states that directional auxin flow in a self-reinforcing canalization defines the position of future vein strands. This means that auxin maxima which are established in procambial cells enhance the transport to adjacent cells in a polar manner. These adjacent cells consequently perceive high auxin levels and, turn into procambium cells and repeat the process with the next cell. Like in the embryo, MP plays an important role in the canalization of auxin flow in the leaves. Additionally, it was shown that in leaves the auxin dependent regulatory network is complemented by the HD-ZIP III family transcription factor ARABIDOPSIS THALIANA HOMEOBOX 8 (ATHB8). ATHB8 acts in the specification of the procambial cell fate and its expression is directly activated by MP via binding of an AuxRe in the promoter. The described auxin flows lead to the formation of continuous and interconnected veins which are arranged in a specific pattern (Scarpella *et al.*, 2006a; Wenzel *et al.*, 2007; Donner and Scarpella, 2009)

After establishing procambial strands and thereby the sites of vascular tissue formation, the tissue is patterned, defining the domains of the future xylem, phloem and intervening pluripotent procambium in an organ specific manner. In the embryo, the vascular initials devide periclinally, thereby giving rise to the radial pattern that is highly similar to that of the primary root (Scheres *et al.*, 1994). After germination the primary vascular pattern is propagated by the apical meristems, i.e. the shoot apical meristem and the root apical meristem.

1.3.2 Vascular development in the primary root

In the root apical meristem, a single layer of multipotent stem cells surrounds the quiescent center, a population of slowly dividing cells that represents the organizing center of the meristem. After stem cell division, the daughter cell that is located next to the quiescent center retains stem cell identity while the second daughter cell acquires a specific cell fate depending on its position. As the root grows, this daughter cell undergoes several rounds of division before it enters a stage of elongation and differentiation (Dolan *et al.*, 1993; van den Berg *et al.*, 1995). The activity and maintenance of the stem cell population are strongly dependent on an apical-basal auxin gradient which is brought about and maintained by the concerted action of PIN proteins (Blilou *et al.*, 2005). Additionally, other hormonal inputs

contribute to meristem size and function. For example, cytokinin and auxin have antagonistic functions in the root meristem, thereby balancing cell differentiation with cell division and determining meristem size. While auxin supports cell proliferation in the division zone of the meristem, cytokinin promotes cell differentiation in the transition zone (Dello Ioio *et al.*, 2007; Perilli *et al.*, 2012).

Vascular tissues which are continuously produced from the respective procambial stem cells are organized in a cylindrical structure which is schematically depicted in Figure 1.1. The Arabidopsis root exhibits a diarch vascular pattern with a central xylem axis and two phloem poles in perpendicular positions. The phloem and xylem cell lineages are separated by cambial cells. Xylem vessels that are formed in the primary root are termed according to their position. The first xylem elements to be specified, the so called protoxylem elements, are located at the outermost position of the stele adjacent to the pericycle and can be identified due to their annular cell wall thickenings. Metaxylem elements, which are characterized by their reticulate cell wall thickenings, are located between the protoxylem elements, thereby forming the central xylem axis of the primary root. The phloem which develops at the positions perpendicular to the xylem axis, can also be divided in proto- and metaphloem. Phloem generally comprises two cell types, sieve elements and companion cells which in angiosperms are derived from one common mother cell. The protophloem elements of the primary root exhibit sieve element characteristics but do not contain
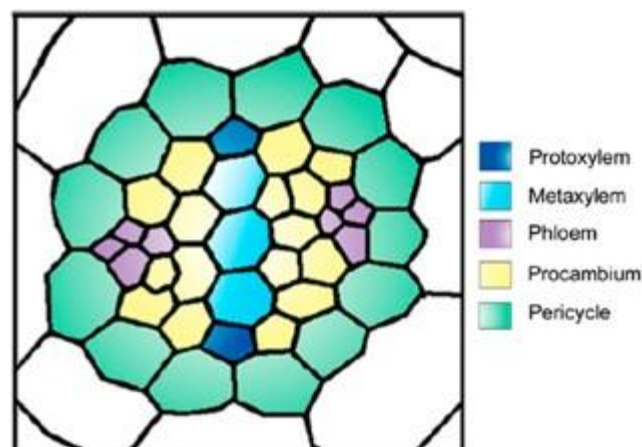
Figure 1-1 Schematic representation of a cross-section through an Arabidopsis root showing the vascular organization during the primary development. The stele consists of a central xylem axis and two phloem poles. The different cell lineages are separated by procambium and surrounded by the pericycle. Picture taken from Elo *et al.* (2009).

companion cells. In contrast, the metaphloem elements which are specified slightly later during root growth consist of both sieve elements and companion cells (Esau, 1969; Scheres *et al.*, 1995; Bauby *et al.*, 2007)

It is a complex regulatory network that controls the specification and patterning of the vascular tissues, however a number of key players have been identified. Most of these so far characterized regulators, for example the members of the HD-ZIP III and GRAS transcription factor family, work in xylem cell type specification, while little is known about how phloem identity is defined (reviewed in Cano-Delgado *et al.*, 2010). The *wooden leg* (*wol*) mutant which carries an amino acid exchange in the cytokinin receptor protein WOL/CRE1/AHK4, is characterized by a stele that consists of fewer cells which exclusively possess protoxylem identity (Mähönen *et al.*, 2000). These observations suggest that cytokinins are required for cell divisions in the stele and suppress protoxylem identity. Phloem initiation does not appear to require cytokinins because the introduction of *fass*, a mutant that restores the cell division defect but has no impact on cytokinin signalling, results in the protophloem specification (Torres-Ruiz and Jürgens, 1994; Scheres *et al.*, 1995). Recently, it has been described that the combinatorial effects of auxin and cytokinin in the primary root meristem contribute to the specification of the xylem axis, thereby defining spatial constraints in which phloem development can take place (Bishopp *et al.*, 2011b). ALTERED PHLOEM DEVELOPMENT (APL), a MYB-type transcription factor, is the only known regulator of phloem identity so far. An *apl* mutant fails to specify phloem. APL seems to be essential for the first asymmetric cell divisions that lead to phloem formation. Apart from that, it obviously also suppresses xylem differentiation, as in the mutant, cells with xylem characteristics are found at the phloem positions (Bonke *et al.*, 2003). The question how the different cell types within the phloem are specified and whether their differentiation is under hormonal control remains unsolved.

1.3.3 Vascular development in organismic interactions

In contrast to the initiation of vascular tissues from the apical meristems, little is known about how existing vascular systems are connected to each other for example after wounding, during the formation of lateral organs or during organismic interactions, including symbiotic and parasitic ones.

Nodules which are formed during the beneficial interaction between legumes and nitrogen

fixing bacteria are vascularized to ensure the exchange of assimilates and fixation products between the plant and the bacteria (Schultze and Kondorosi, 1998).

Among the parasitic interactions, haustoria formed by plants like *Cuscuta sp.* or *Viscum sp.* or crown galls induced by *A. tumefaciens* display a high degree of vascularization. The tissue in crown galls for a long time was considered an unorganized mass with varying degrees of organization reflecting the random movement of stimulating substances within the tumorous tissue (Sachs, 1975, 1991). However, it is now generally accepted that crown galls exhibit a well-organized vascular system to satisfy the high demand of the tumor for nutrients (Aloni *et al.*, 1995). A further agronomically important organismic interaction during which sophisticated vascularization occurs is the interaction of sedentary plant parasitc nematodes and their host plant`s roots. The plant parasitic nematodes will be introduced in detail in chapter 3.1.

It is well known that parasites as well as symbionts interfere with the phytohormone households of their host plant in order to serve their purposes. This can be achieved by secretion of phytohormones, by transfer of hormone biosynthesis genes like in the case of *A. tumefaciens* or by manipulation of the hosts signaling and transport machinery. In the first instance, the modification of phytohormone pathways serves the induction and establishment of the symbiont- or parasite induced tissues, for example nodules or galls. The vascularization events that take place during these organismic interactions also seem to depend on phytohormone action, with auxin as the most important determinant. (Aloni *et al.*, 1995; Ullrich and Aloni, 2000). However, detailed studies on the latter aspect are missing and nothing is known about whether and how auxin is involved in the vascularization of nematode induced tissues.

1.4 Aims of the work

The phytohormone auxin is involved in the regulation of numerous aspects of growth and development in plants. The basis for its multiple functions is provided by its complex mode of action. Asymmetric distribution of the molecule between and within tissues leads to different downstream responses in individual cells. In this work, two different aspects of auxin biology were studied.

In the first part of the thesis, new insights into the regulation of PIN-mediated polar auxin

transport by phosphorylation should be gained. Therefore, the impact of PIN phosphorylation by several members of the plant specific AGCVIII kinase family should be studied in the heterologous *X. laevis* oocyte expression system.

A second goal of this thesis was to shed light on the role of phytohormone responses during the vascularization of nematode-induced feeding sites. Therefore, auxin and cytokinin responses in infected Arabidopsis plants should be studied with the help of reporter constructs and responsive tissues should be identified in order to gain first insights about possible functions of the two phytohormones in the specification of the vascular tissues around the feeding sites.

2 Regulation of PIN-FORMED-mediated auxin transport by the AGCVIII kinases D6 and PINOID

Parts of the data presented in this chapter will be included in the following publication: Zourelidou[#], M., Absmanner[#], B., Weller, B., Barbosa, I., Willige, B. C., Fastner, A., Streit, V., Port, S., Colcombet, J., van Bentem, S., Hirt, H., Küster, B., Schulze, W. X., Hammes, U. Z. and Schwechheimer, C.: PIN-FORMED-mediated auxin efflux is activated by D6 PROTEIN KINASE. ([#]contributed equally. Manuscript in preparation).

2.1 Introduction

2.1.1 The PIN protein family of auxin efflux carriers

A function of the PIN proteins in mediating auxin efflux was first proposed based on a phenotypic analysis of the Arabidopis *pin1* mutant which is defective in organ initiation and phyllotaxy, resulting in the eponymous pin-shaped influorescence that does not form flowers. The mutant shows drastically reduced PAT and its phenotypes can be mimicked by application of auxin efflux inhibitors (Okada *et al.*, 1991). Cloning of the gene lead to the identification of PIN1, a transmembrane protein that shares limited similarity to some bacterial transporters and localizes polarly to the basal end of cells in the vasculature (Gälweiler *et al.*, 1998).

PIN1 belongs to a land plant specific protein family which, in Arabidopsis, consists of eight members that can be subdivided into two clades distinguished by their predicted structure and their subcellular localization. The long PINs, PIN1-4 and PIN7, are characterized by a central hydrophilic loop separating two hydrophobic domains of five transmembrane regions each (Gälweiler *et al.*, 1998; Paponov *et al.*, 2005; Zazimalova *et al.*, 2007). These PINs are localized at the plasma membrane in a polar manner which corresponds to the direction of auxin flow (Palme and Gälweiler, 1999). Functional analysis of the long PINs revealed that they act in tropic responses, meristem patterning, vascular differentiation, lateral root formation and early embryogenesis (Chen *et al.*, 1998; Luschnig *et al.*, 1998; Friml *et al.*, 2002a; Friml *et al.*, 2002b; Benkova *et al.*, 2003; Friml *et al.*, 2003; Scarpella *et al.*, 2006b).

The three PINs that form the second clade of the family, PIN5, 6 and 8, have a strongly

reduced central hydrophilic loop and are localized to the endomembrane system, suggesting a function in intracellular auxin distribution and the regulation of cellular auxin homeostasis (Mravec *et al.*, 2009; Ding *et al.*, 2012). A similar function was also proposed for the members of the recently identified family of the PINL-LIKE (PILS) proteins that are structurally similar to the short PINs (Barbez *et al.*, 2012).

The fact that *pin* mutants are defective in PAT, their asymmetric subcellular localization as well as the observation that auxin transport inhibitors such as naphthylphthalamic acid (NPA) can phenocopy loss-of-function *pin* mutants strongly pointed towards a common molecular function of PINs as efflux carriers. According to predictions derived from sequence analysis, PINs work as secondary transporters which gain the energy for the transport process from an electrochemical gradient. Consequently, none of the PIN sequences contains an ATP-binding domain (Zazimalova *et al.*, 2007; Zazimalova *et al.*, 2010).

First biochemical evidence for an actual transport activity of PINs came from heterologous expression of *PIN2* in yeast which resulted in reduced accumulation of auxin as well as in decreased sensitivity towards toxic auxin-like molecules, suggesting that PIN2 is involved in the export of these compounds (Chen *et al.*, 1998; Luschnig *et al.*, 1998). In 2006, Petrasek *et al.* used different plant cell cultures as well as the heterologous expression systems *S. cerevisiae* and HeLa in order to prove the direct role of PINs as efflux carriers. Indeed they could show that overexpression of different PINs resulted in reduced accumulation or retention of auxin compounds and that this effect was partially sensitive to auxin transport inhibitors. Similar findings were described by Yang and Murphy (2009) who used *S. pombe* for heterologous expression of PIN1 and PIN2.

Although different systems have been used to characterize single PINs it seems that none of them is appropriate for the analysis of all PINs under controlled conditions. This highlights the fact that very little is known about the actual mechanism of the transport, about additional factors that might be required and about processes that differentially control the efflux activity of PIN proteins.

2.1.2 Polarity dynamics of PIN proteins

The differential polar localization of PIN proteins at apical, basal or lateral cell faces depends on the protein itself, on the cell type as well as the developmental context. The complexity and dynamics can be illustrated impressively by looking at auxin streams and PIN localization in the root apex (Figure 2-1). Here, the concerted action of the different PIN proteins provides the basis for the establishment and maintenance of a stable auxin maximum around the quiescent center that is required for root meristem organization and growth (Sabatini *et al.*, 1999; Blilou *et al.*, 2005; Petrasek and Friml, 2009). Localization of certain PINs can even differ in neighboring cell files as seen for PIN2 which is found at the basal cell face in cortical cells and is localized apically in the epidermis and the lateral root cap (see arrows in Figure 2-1, Müller *et al.*, 1998). Dynamic changes of PIN localization in the root apex can be observed for example during gravitropic response as was shown for PIN3. After a gravitropic stimulus, PIN3 localization in the columella rapidly changes from non-polar to polar, facing the lower side of the cells. As a consequence, auxin flow is redirected which results in asymmetric growth and ultimately in downward bending of the root (Friml *et al.*, 2002b).
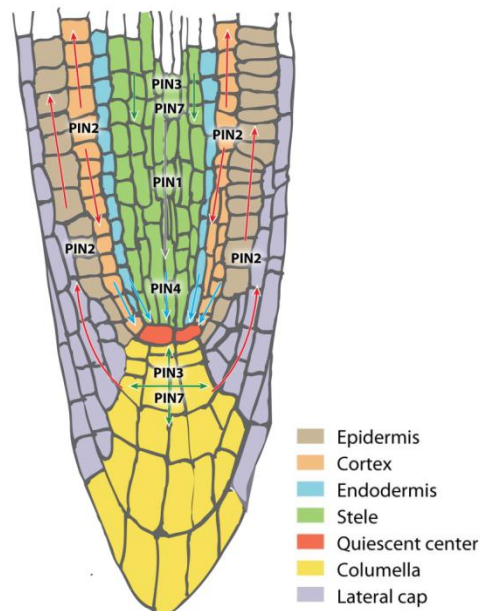
Figure 2-1 Schematic overview of the pattern of PIN protein localization in the *Arabidopsis* root tip.

Arrows indicate polar PIN localization at the plasma membrane and direction of auxin flow. Picture taken from Kleine-Vehn and Friml (2008).

How is PIN polarity regulated? It was shown that, following protein synthesis, PINs are delivered to the membrane in a nonpolar fashion, are then internalized and subsequently sorted polarly (Dhonukshe *et al.*, 2008). The rapid dynamic switches observed during responses to developmental or environmental stimuli are achieved by constant endocytosis, transcytosis and exocytosis which allow polar retargeting after each internalization event. Depending on the destination of the specific PIN, different pathways are used (Feraru and Friml, 2008). Brefeldin A (BFA) is an inhibitor of subcellular vesicle trafficking. In its presence, PIN1 is no longer found at the plasma membrane but aggregates in so-called BFA-compartments inside the cell (Steinmann *et al.*, 1999; Geldner *et al.*, 2001). One of the molecular targets of BFA is GNOM, which belongs to the so ARF-GEFs. ARF-GEFs are GDP-GTP exchange factors and activate ADP-ribosylation factor (ARF) GTPases, thereby mediating vesicle budding processes at different subcellular compartments (Donaldson and Jackson, 2000; Geldner *et al.*, 2001). The endosomal ARF-GEF GNOM is crucial for trafficking of PINs to basal membranes. Consequently, a pharmacological or genetical reduction of GNOM activity leads to dynamic basal-to-apical PIN transcytosis. Apical or lateral cargo on the other hand seems to use alternative pathways that require distinct sets of BFA-insensitive ARF-GEFs (Kleine-Vehn *et al.*, 2008).

2.1.3 Regulation of polar targeting by phosphorylation

The decision whether a specific PIN protein is recruited into the apical or basal sorting pathway is strongly dependent on its phosphorylation status (Michniewicz *et al.*, 2007; Kleine-Vehn *et al.*, 2008; Dhonukshe *et al.*, 2010). The Ser/Thr kinase PINOID was the first identified molecular determinant in PIN polar targeting (Friml *et al.*, 2004). It was shown to phosphorylate PIN proteins in their hydrophilic loop region and this phosphorylation was antagonized by the action of the protein phosphatase subunit PP2A (Michniewicz *et al.*, 2007; Dai *et al.*, 2012). Overexpression of PID as well as inhibition of PP2A causes apicalization of PIN proteins whereas loss-of function *pid* mutants exhibit preferentially basal PIN targeting. The mislocalization of PINs in these mutants goes along with strong phenotypes that correlate with the changes in the direction of auxin flow (Benjamins *et al.*, 2001; Friml *et al.*, 2004; Michniewicz *et al.*, 2007).

The recruitment of PINs to the apical recycling pathway is instructed by a phosphorylation of the serine residues in three conserved TPRXS(N/S) motifs which are highly conserved among

the long PIN proteins. Analysis of loss-of phosphorylation and phosphomimicking mutants of PIN1 and PIN2 revealed that the reversible phosphorylation of these three residues is required and sufficient for proper PIN localization. Consequently, lack of phosphorylation leads to basal localization due to higher affinity of these variants to the GNOM-dependent sorting pathway (Dhonukshe *et al.*, 2010; Huang *et al.*, 2010). The current model for the phosphorylation-dependent sorting of PIN proteins is depicted in Figure 2-2. Two closely related kinases WAVY ROOT GROWTH 1 (WAG1) and WAG2, have been shown to target the same residues and act redundantly to PID in the apical targeting of PINs (Dhonukshe *et al.*, 2010).
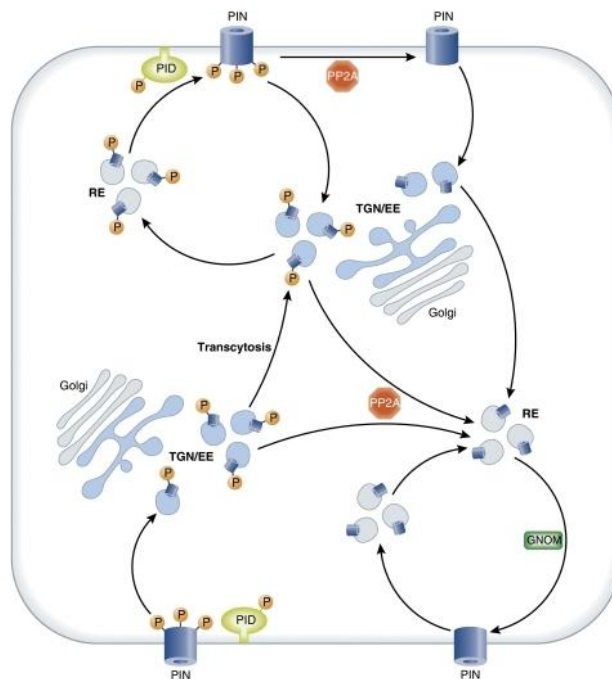
Figure 2-2 Schematic illustration of phosphorylation-dependent polarity changes of PIN proteins. Unphosphorylated PINs are constantly recycled to the basal cell face. PIN-dependent phosphorylation results in apicalization by transcytosis. The phosphatase PP2A acts as a PID –antagonist. TGB/EE: trans-golgi-network / early endosomes, RE: recycling endosomes. Picture taken from Grunewald and Friml (2010).

2.1.4 The AGCVIII kinase family

PID, WAG1 and WAG2 belong to the plant specific AGCVIII family of Ser/Thr protein kinases (Galvan-Ampudia and Offringa, 2007). The AGC kinases were named based on their homology to the mammalian protein kinase A, cyclic GMP-dependent protein kinase G and protein kinase C, which are all involved in receptor-mediated growth factor signal transduction in animals. They contain a highly conserved catalytic core consisting of two lobes which are interconnected by a linker domain. The binding sites for ATP, Mg^{2+} and for the substrate are localized in this catalytic core. AGC kinase activity is regulated by (auto-)phosphorylation in a specific loop as well as by interacting proteins (Bögre *et al.*, 2003; Rademacher and Offringa, 2012). The characteristic features of the AGCVIII subfamily are a substitution of DFG to DFD in the conserved catalytic domain VII as well as a specific insertion between the subdomains VII and VIII which was speculated to be essential for the proper subcellular localization of the kinases that ranges from cytosolic, nuclear to plasma membrane associated (Zegzouti *et al.*, 2006; Galvan-Ampudia and Offringa, 2007; Rademacher and Offringa, 2012). In Arabidopsis, the AGCVIII family consists of 23 members which can be divided into four subgroups, one of which includes the above mentioned PID and WAG kinases. The members of this clade are the only AGCVIII kinases demonstrated to be involved in the regulation of PIN polarity. However, the D6 protein kinases, which belong to the largest subclade of the AGCVIII kinases, have also been shown to phosphorylate PINs and to regulate auxin transport (Zourelidou *et al.*, 2009).

2.1.5 The AGCVIII kinase D6PK regulates auxin transport

The family of the D6 protein kinases consists of the founding member D6PK and its three close homologs D6PKL1, D6PKL2 and D6PKL3. First indications for a role of the D6PKs in auxin transport came from a phenotypic analysis of *d6pk* mutants which exhibit a number of developmental defects that are typically associated with reduced auxin transport, among them fused cotyledons, impaired lateral root initiation, agravitropic root growth as well as defects in phototropic responses. Consistently, auxin transport in stems of mutant plants is strongly decreased (Zourelidou *et al.*, 2009; Willige *et al.*, 2013). A synergistic genetic interaction between *PIN1* and the *D6PK* genes as well as a colocalization of D6PK and different PINs at the basal sides of cells in various tissues suggested a functional link

between PINs and D6 kinases and indeed it could be shown that PIN proteins are phosphorylation targets of D6PK *in vitro* (Zourelidou *et al.*, 2009). However, unlike the related PID and WAG kinases, D6PKs do not influence the polar targeting of PIN proteins (Zourelidou *et al.*, 2009; Dhonukshe *et al.*, 2010; Willige *et al.*, 2013). Also, PID and D6PK overexpression results in different phenotypes, further suggesting different molecular functions of the two kinases.

As D6PK phosphorylates PINs and regulates auxin transport efficiency without influencing PIN polarity, a function in the regulation of transport activity of PIN proteins was suggested (Zourelidou *et al.*, 2009). This hypothesis is further substantiated by the recent finding that lateral auxin transport during phototropic bending of hypocotyls is dependent on D6PKs (Willige *et al.*, 2013). An essential process in phototropism is redirection of the auxin flow to the shaded side of hypocotyls which is achieved by a relocalization of PIN3 to lateral cell faces (Friml *et al.*, 2003; Ding *et al.*, 2011). In *d6pk* mutants, a gradual loss of PIN3 phosphorylation and a loss in lateral auxin transport was observed, however PIN3 lateralization took place normally. The data suggested that PIN3 transport activity was stimulated by D6PK mediated phosphorylation (Willige *et al.*, 2013).

The major phosphorylation targets of PID that are required for apical sorting of PIN proteins have been characterized and are located within conserved sequence motifs (Dhonukshe *et al.*, 2010; Huang *et al.*, 2010). Recently, candidate residues that are phosphorylated by D6PK *in vitro* and *in vivo* were identified in PIN1, however their relevance for PIN1 activity and activation was not clarified to date (Zoureidou *et al.,* unpublished).

2.1.6 Aims of the project

The D6 protein kinases have been implicated in the regulation of PIN protein function by phosphorylation (Zourelidou *et al.*, 2009, Zourelidou *et al.*, unpublished, Willige *et al.*, 2013). However, biochemical proof that D6PK phosphorylation directly influences the efflux activity of PIN proteins was missing. The main goal of this project therefore was to establish an auxin transport assay that would allow the investigation of the activatory effect of D6PK and possibly also of other AGCVIII kinases on PIN proteins in the heterologous *X. laevis* oocyte expression system.

Amino acids that are targeted by D6PK have been identified *in vitro* and *in vivo (*Zourelidou *et al.,* unpublished). Focussing on PIN1, the importance of these amino acid residues in

terms of transport activity should be addressed by quantifying auxin efflux in oocytes upon co-expression of the respective mutants with D6PK.

Moreover, as a functional link between D6PK and PIN3 was recently shown (Willige *et al.*, 2013), the heterologous system should also be used to demonstrate activation of PIN3 by D6PK.

2.2 Results

2.2.1 Co-expression of PIN1 and YFP-D6PK leads to enhanced IAA efflux in *X. laevis* oocytes

The D6 Ser/Thr kinases have been implicated in the regulation of PIN-mediated auxin efflux (Zourelidou *et al.*, 2009). In order to find out whether D6PK directly regulates PIN1 transport activity by phosphorylation, an IAA efflux assay was established in *X. laevis* oocytes. Oocytes are a versatile and well established expression system especially for membrane proteins. As they store large amounts of protein, they do not depend on extracellular resources for nutrition and therefore express only a very limited number of own membrane proteins. Consequently, background activity of endogenous transporters is low (Bröer, 2010). Additionally, no PIN-related genes or compounds of the auxin signaling and transport pathways that might interact with the proteins of interest in any way are present. The auxin importer AUX1 has been characterized successfully in this system (Yang *et al.*, 2006), but no data for PIN mediated auxin efflux in *X. laevis* oocytes were available so far.

For heterologous expression of proteins in oocytes, mRNAs including a 5'-cap and a poly-A-tail (synthesized *in vitro* as described in 7.7.2) encoding for PIN1 and a YFP tagged version of D6PK (YFP-D6PK) which was shown to be functional (Zourelidou *et al.*, 2009) were injected into oocytes which were then incubated for 5 days to allow production of the mature proteins. First, it had to be confirmed that the proteins were produced and correctly localized in the oocytes. In case of the D6PK, the protein could be detected by fluorescence microscopy due to the N-terminal YFP-tag. Figure 2-3 A and B shows confocal images of oocytes expressing YFP-D6PK in absence (Figure 2-3 A) or presence of PIN1 (Figure 2-3 B). In either case, YFP fluorescence was detected in the periphery of the oocytes. D6PK does not contain any transmembrane domains, but it is localized polarly in plant cells and appears to be associated with the plasma membrane in a so far unknown fashion (Zourelidou *et al.*, 2009). It seems likely that the attachment of the kinase to the membrane is needed for the correct function of the protein. To confirm the membrane association also in oocytes, protein extracts were prepared and microsomal and cytosolic fractions were separated by ultracentrifugation (see 7.7.5). Figure 2-3 C shows a Western Blot where YFP-D6PK was detected in protein extracts from oocytes that were co-expressing PIN1 and YFP-D6PK. Before loading samples of microsomal and cytosolic fractions on a SDS gel, they are typically

solubilized in a different way, i.e. cytosolic proteins are boiled at 95 °C for 5 min while membrane proteins which are more temperature sensitive are solubilized at 42 °C for 15 min. If gels containing samples that were treated like this were blotted and decorated with an anti-GFP antibody to detect the fusion protein which has a calculated size of 82 kDa, strong signals were observed both in the microsomal and in the cytosolic fraction (Figure 2-3 C, panel 1 and 2). An additional band with higher mobility appeared in the microsomal fraction. However, this band disappeared when the microsomal fraction was boiled at 95 °C prior to loading (Figure 2-3 C, panel 1 and 3). Therefore, the additional band in the microsomal fraction that was incubated at 42 °C most likely represents incompletely solubilized protein. Taken together it can be concluded that at least a part of the fusion protein YFP-D6PK is associated with membranes in *X. laevis* oocytes like it is the case in the plant and can consequently act in direct proximity to membrane localized proteins.
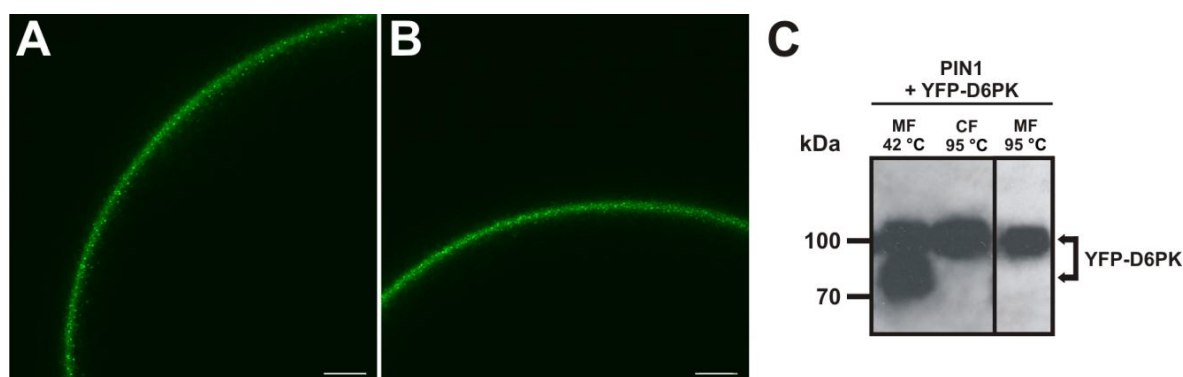
Figure 2-3 Expression and subcellular localization of YFP-D6PK in *X. laevis* oocytes 5 days after mRNA injection. (A,B) YFP fluorescence in oocytes expressing YFP-D6PK (A) or PIN1 + YFP-D6PK (B). In both cases, the kinase is localized in the periphery of the oocyte. Scale bars in (A) and (B) represent 50 µm. (C) Western blot analysis of YFP-D6PK in protein extracts. The fusion protein was detected with an anti-GFP antibody. Membrane fraction (MF) and cytosolic fraction (CF) were incubated at 42 °C or 95 ° prior to protein separation. The fusion protein was detected both in the MF and in the CF. The lower band in panel 1 results from incomplete solubilization of the protein and disappeared when the sample was treated like the CF (panels 2 and 3).

PIN1 was used in an untagged version for the transport assay and was therefore only detected on a Western Blot. Figure 2-4 shows the analysis of protein extracts from oocytes that were separated into microsomal and cytosolic fractions and labeled with an anti-PIN1 antibody by western blotting (see 7.7.5, 7.7.6). As expected, PIN1 which contains 10 transmembrane domains was mainly found in the microsomal fractions in protein extracts

from oocytes expressing PIN1 exclusively as well as in extracts from oocytes co-expressing PIN1 and YFP-D6PK. In the microsomal fraction of protein extracts from the latter samples, a smear of additional bands of higher mobility was observed that was not seen in the corresponding fraction from oocytes lacking the kinase (asterisks in Figure 2-4). This is the typical pattern described for phosphorylated PIN1 (Michniewicz *et al.*, 2007; Zourelidou *et al.*, 2009) indicating that PIN1 is phosphorylated by YFP-D6PK in *X. laevis* oocytes.
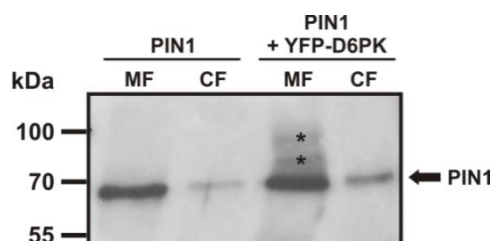
Figure 2-4 Western blot analysis of PIN1 in protein extracts from *X. laevis* oocytes expressing PIN1 or PIN1 + YFP-D6PK. PIN1 was detected with an anti-PIN1 antibody and was found mainly in the microsomal fraction (MF), only weak signals were detected in the cytosolic fraction (CF). The additional bands with lower mobility (asterisks) in protein extracts from oocytes co-expressing PIN1 + YFP-D6PK represent phosphorylated PIN1.

After the five day incubation period of the mRNA-injected oocytes, efflux assays were performed as described in 7.7.4. Briefly, oocytes were injected with defined amounts of the [^{3}H]-labeled auxin IAA, resulting in an internal concentration of 1 - 1.5 µM IAA which corresponds to a physiologically relevant concentration (Petersson *et al.*, 2009). Directly after injection, oocytes were incubated on ice for 10 min to allow homogenous distribution of the IAA inside the cell and the closure of the injection wound. The reduction of the IAA content over time was then determined by sampling 10-12 oocytes at 5 different time points and measuring the residual radioactivity in each cell by liquid scintillation counting. Initial experiments were performed with oocytes expressing PIN1 or the YFP-D6PK alone or co-expressing both proteins. Water-injected oocytes were used as a control. At least 5 biological replicates were analyzed for each tested construct. Figure 2-5 clearly shows that co-expression of PIN1 and YFP-D6PK in oocytes resulted in a much higher decrease of the IAA content than expression of PIN1 or the kinase alone which in turn could not enhance auxin efflux at all as the respective samples were indistinguishable from water-injected cells. While in water, PIN1- or YFP-D6PK injected oocytes, about 65 % of the initially injected amount of [^{3}H]-IAA was retained after 60 min, [^{3}H]-IAA content in the PIN1 / YFP-D6PK

co-expressing oocytes was reduced to app. 44 %. This means that while PIN1 alone is obviously not able to actively efflux auxin from oocytes, it can do so upon co-expression of the D6PK kinase. As it was shown that PIN1 is a phosphorylation target of the D6PK (Zourelidou *et al.*, 2009) and is also phosphorylated by YFP-D6PK in oocytes (Figure 2-4), it can be assumed that phosphorylation of PIN1 is crucial for its auxin transport activity.
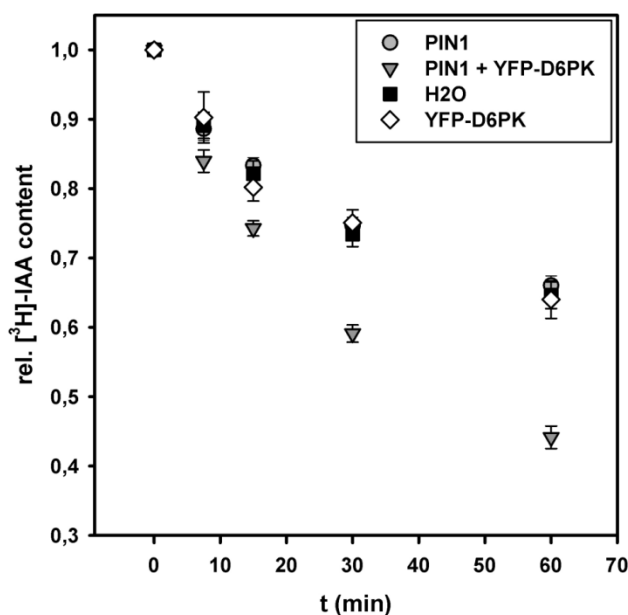
Figure 2-5 Co-expression of PIN1 and YFP-D6PK leads to enhanced IAA efflux in *X. laevis* oocytes. Reduction of [^{3}H]-IAA content in oocytes after direct injection of the substrate. CPM at time point 0 min were set to 1. Oocytes expressing PIN1 or YFP-D6PK alone were indistinguishable from water-injected control oocytes, whereas oocytes co-expressing PIN1 + YFP-D6PK contained app. 20 % less [^{3}H]-IAA after 60 min. Error bars show SEM of biological replicates (n=23 for PIN1 and PIN1 + YFP-D6PK, n=17 for H_2O, n=5 for YFP-D6PK). 10-12 technical replicates per time point were analyzed in every biological replicate.

2.2.2 Efflux is sensitive to the auxin transport inhibitor NPA

Auxin transport inhibitors are important tools in studying the role of polar auxin transport in plant developmental processes. One well known inhibitor of auxin efflux is naphthylphthalamic acid (NPA) which belongs to the so-called phytotropins (Katekar and Geissler, 1980; Rubery, 1990). The molecular mechanism of NPA action is still unclear, but its application causes increased auxin accumulation in tobacco suspension cultured cells (Delbarre *et al.*, 1996) and leads to *pin1* like phenotypes in Arabidopsis (Okada *et al.*, 1991;

Gälweiler *et al.*, 1998), suggesting that it acts in close proximity to PINs. Additionally, phenotypes of *d6pk* mutants can be mimicked by NPA application (Zourelidou *et al.*, 2009). In order to test whether NPA has an influence on auxin efflux from oocytes mediated by D6PK-activated PIN1, changes in the IAA content in oocytes expressing PIN1, PIN1 + YFP-D6PK and in control water-injected oocytes were determined under different conditions. mRNA injection and efflux assays were basically performed as described in 7.7.3 and 7.7.4. Oocytes were incubated in Barth's solution supplemented with 10 µM NPA out of a 10 mM stock in DMSO or with the equivalent amount of DMSO only as a control. After 60 min, residual IAA content was determined by liquid scintillation counting. The relative IAA content after 60 min compared to time point 0 min was normalized to the data for water-injected oocytes incubated in buffer without NPA. As Figure 2-6 A shows, the relative IAA content in oocytes co-expressing PIN1 and YFP-D6PK was not affected by 10 µM NPA in the buffer. Both in the presence and in the absence of NPA the IAA content was about 20 % lower than in PIN1 expressing oocytes or in water-injected control oocytes. However, the observation that NPA had no effect when present in the buffer is very likely due to the inability of the chemical to enter the cells under the given experimental conditions, i.e. a pH of 7.4 in the incubation solution. NPA is a weak acid with a pKa of 4.6 which is mainly present in the deprotonated form at neutral pH and can therefore not pass the plasma membrane by diffusion. Consistently, different results were obtained when NPA, instead of adding it to the buffer, was co-injected into the oocytes together with the substrate [3H]-IAA (Figure 2-6 B). Control oocytes were injected with [3H]-IAA supplemented with the respective amount of DMSO. While the rel. IAA content in water-injected and PIN1-expressing oocytes, which do not actively transport auxin, was not altered by co-injection of NPA, a clear effect was observed for oocytes co-expressing PIN1 and YFP-D6PK. As expected, IAA content in oocytes that were injected with [3H]-IAA only was about 20 % lower than in PIN1- or water-injected oocytes after 60 min, reflecting the enhanced auxin efflux from these cells. Co-injection of NPA leading to a concentration of app. 1 µM inside the oocytes caused a slight increase in residual IAA, while 10 µM NPA resulted in a very strong increase of the residual IAA content. Unexpectedly, the IAA retention in these cells was even slightly higher than in the corresponding PIN- or water-injected oocytes. The last observation cannot be explained at the moment, however the experiments on NPA inhibition were performed with only one biological replicate and should be repeated in order to verify the data.
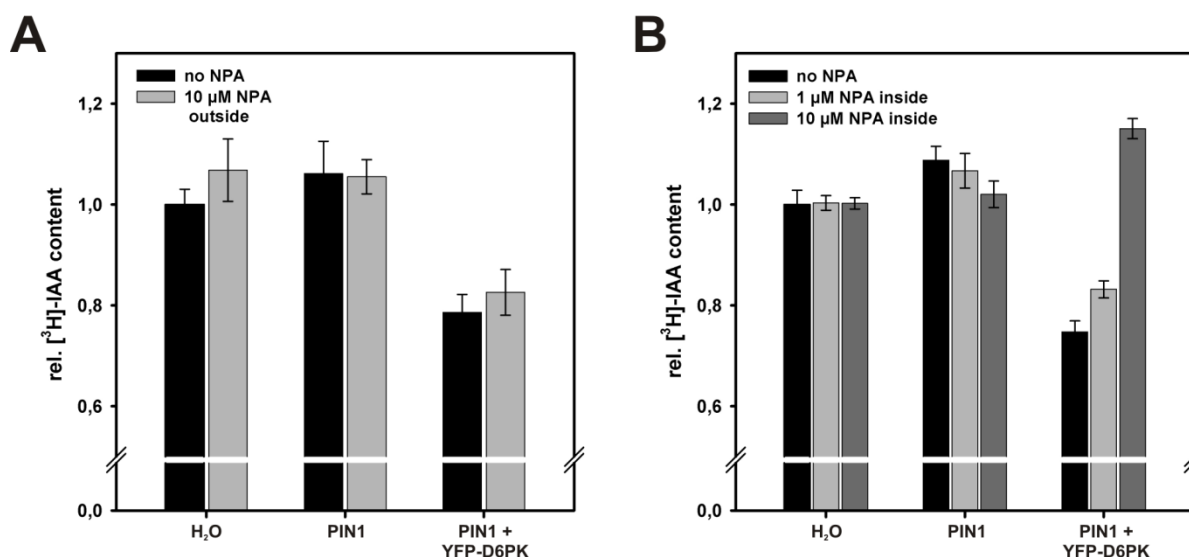
Figure 2-6 Effect of NPA on PIN1 mediated IAA efflux from *X. laevis* oocytes. (A) Rel. [^{3}H]-IAA content in oocytes after 60 min incubation in buffer without (black bars) or with 10 µM NPA (NPA outside, grey bars). Rel. IAA content in water-injected oocytes incubated in buffer without NPA was set to 1. 10 µM NPA in the buffer had no effect on the IAA content in water-injected oocytes, PIN1-expressing oocytes or oocytes co-expressing PIN1 + YFP-D6PK. Co-expression of PIN1 + YFP-D6PK resulted in significantly enhanced IAA export under both tested conditions. 10-12 oocytes were collected for each sampling point. (B) Rel. [^{3}H]-IAA content in oocytes 60 min after co-injection of different amounts of NPA together with the substrate (no NPA: black bars, 1 µM NPA inside: light grey bars, 10 µM NPA inside: dark grey bars). Rel. IAA content in water-injected oocytes injected with [^{3}H]-IAA only was set to 1. Co-injection of 10 µM NPA caused a strong increase o the rel. IAA content in oocytes co-expressing PIN1 and YFP-D6PK indicating that IAA export was reduced.

2.2.3 Determination of transport rates

The establishment of the transport assay in the *X. laevis* oocyte expression system and the presented evidence that PIN1 needs to be phosphorylated in order to efficiently mediate auxin efflux (see chapter 2.2.1) provided a basis for addressing a number of further questions for example about the influence of other kinases on PIN1 activity and of course the effect of mutations at target phosphorylation sites. In order to be able to compare results from different experiments efficiently and to present the data more clearly, transport rates were calculated from the obtained time courses. Therefore, only those parts of the curve in which the auxin content decreased in a linear fashion, i.e. all time points up to 30 min, were considered. A representative experiment for PIN1 and PIN1 co-expressed with YFP-D6PK including the corresponding linear regressions is shown in Figure 2-7 A. Transport

rates were determined from the negative value of the slopes. Blotting of the rates from the data sets shown in Figure 2-5 and subsequent normalization to "PIN1 without kinase" results in a graph as shown in Figure 2-7 B. Hence, auxin efflux is increased app. 1.6 fold when PIN and YFP-D6PK are co-expressed compared to PIN1 or the kinase expressed alone or when oocytes were injected with water only. This efflux in the latter samples is considered as background caused by diffusion or endogenous transporters that might transport auxin unspecifically. The difference in the transport rates was highly significant ($p<0.001$).
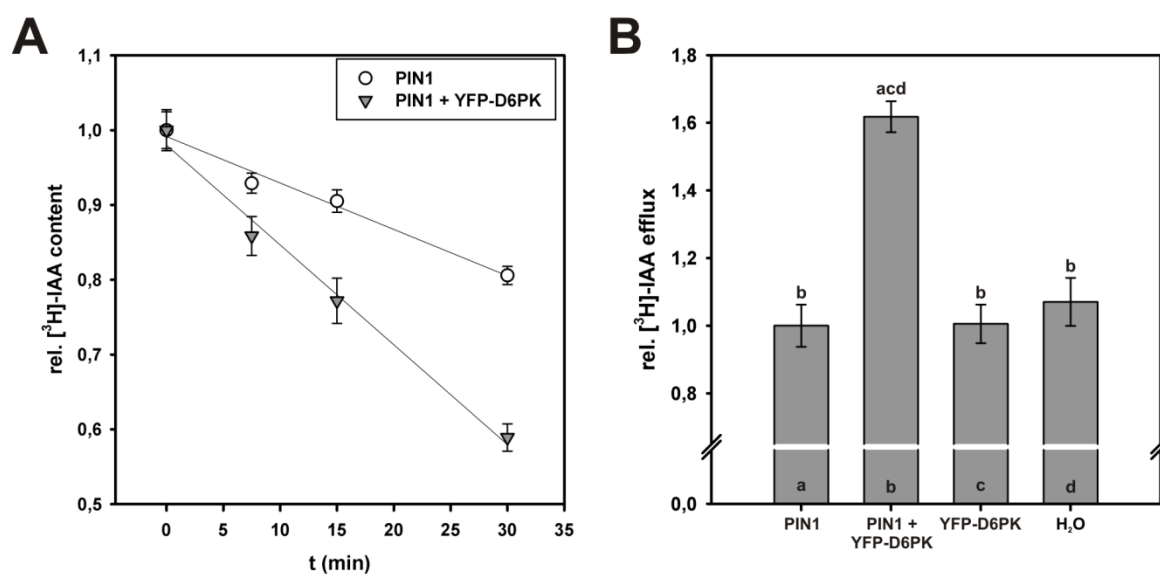
Figure 2-7 Determination of transport rates from efflux assays in *X. laevis* oocytes. (A) Reduction of [^{3}H]-IAA content in oocytes after direct injection of the substrate. Exemplary linear regression graph showing measurements of one biological replicate for PIN1 (r^2 = 0.981) and PIN1 + YFP-D6PK (r^2 = 0.988). The linear regression graphs served as a basis for the calculation of transport rates and hence rel. IAA efflux. Error bars show SEM of technical replicates (n=12). (B) Rel. [^{3}H]-IAA efflux in oocytes after direct injection of the substrate. Rel. efflux from oocytes expressing PIN1 alone was set to 1. Error bars show SEM of biological replicates (n=23 for PIN1 and PIN1 + YFP-D6PK, n=17 for H_2O, n=5 for YFP-D6PK). Different letters indicate significant differences. Statistical analysis was performed by means of a one way ANOVA followed by Bonferroni's post hoc test ($p<0.001$).

2.2.4 A kinase-inactive version of D6PK does not activate PIN1

In order to make sure that the activation of PIN1 upon co-expression with D6PK was indeed due to the phosphorylation and not to a phosphorylation-independent interaction between the two proteins, oocytes were co-injected with mRNAs encoding for PIN1 and a mutant version of YFP-D6PK which carries an amino acid substitution of K to E in the ATP-binding pocket, leading to total loss of the kinase activity (YFP-D6PK$_{in}$, (Zourelidou *et al.*, 2009). Western Blot analysis of protein extracts from oocytes five days after mRNA injection confirmed the expression of YFP-D6PK$_{in}$ and showed that the protein was localized to the microsomal as well as in the cytosolic fraction, indicating a membrane association of at least part of the protein (Figure 2-8 A). A double band that was observed in the microsomal fraction disappeared upon boiling the sample at 95 °C prior to SDS gel loading like it is typically done with the cytosolic fraction. The observed pattern was identical to the one described for the functional version of YFP-D6PK in chapter 2.2.1 (compare Figure 2-8 A to Figure 2-3 C). Additionally, an identical localization of YFP-D6PK (Figure 2-3 A,B) and YFP-D6PK$_{in}$ in the periphery of oocytes was confirmed by confocal microscopy (data not shown). In oocytes co-expressing PIN1 and the kinase-dead version of YFP-D6PK, no phosphorylated PIN1 which is represented by a smear of lower mobility bands as seen in samples derived from PIN1 / YFP-D6PK co-expressing oocytes was detected (Figure 2-8 B, compare panels 2 and 3).

In efflux assays with [^{3}H]-labeled IAA (Figure 2-8 C), oocytes co-expressing PIN1 and YFP-D6PK$_{in}$ did not show any differences in IAA efflux compared to cells expressing PIN1 alone, but differed significantly from PIN1 / YFP-D6PK co-expressing oocytes ($p<0.001$). Taken together, these results clearly show that the activation of PIN1 which leads to enhanced auxin efflux depends on phosphorylation by D6PK.
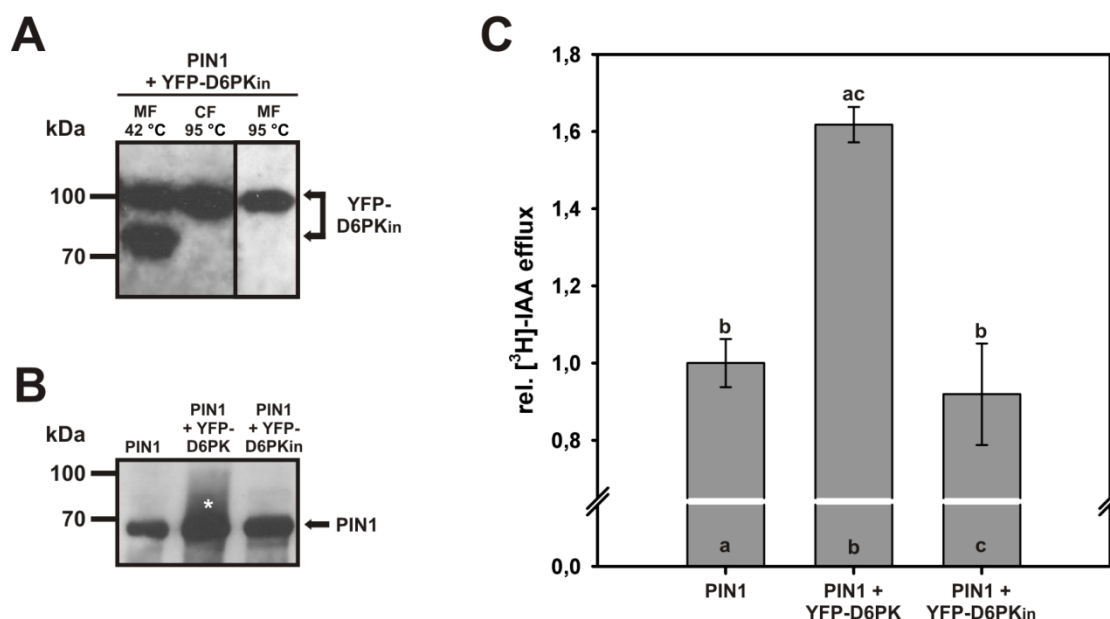
Figure 2-8 A kinase-inactive version of YFP-D6PK does not activate PIN1. (A) Western blot analysis of YFP-D6PK$_{in}$ in protein extracts 5 days after mRNA injection co-expressing the YFP-D6PK$_{in}$ + PIN1. The fusion protein was detected with an anti-GFP antibody. Membrane fraction (MF) and cytosolic fraction (CF) were incubated at 42 °C or 95 ° prior to SDS gel loading. The fusion protein was detected both in the MF and in the CF. The lower band in panel 1 results from incomplete denaturation of the protein and disappeared when the sample was treated like the CF (panels 2 and 3). (B) Western blot analysis of PIN1 in the MF of protein extracts 5 days after mRNA injection expressing PIN1 alone or PIN1 in combination with YFP-D6PK and YFP-D6PK$_{in}$, respectively. The smear of bands with lower mobility (asterisk) in protein extracts from oocytes co-expressing PIN1 + YFP-D6PK represents phosphorylated PIN1. (C) Rel. [^{3}H]-IAA efflux in oocytes after direct injection of the substrate. Rel. efflux from oocytes expressing PIN1 alone was set to 1. Co-expression of YFP-D6PK, but not of YFP-D6PK$_{in}$ resulted in enhanced IAA efflux. Error bars show SEM of biological replicates (n=23 for PIN1 and PIN1 + YFP-D6PK, n=4 for PIN1 + YFP-D6PK$_{in}$). Different letters indicate significant differences. Statistical analysis was performed by means of a one way ANOVA followed by Bonferroni's post hoc test (p<0.001).

2.2.5 PINOID also enhances PIN1 mediated IAA export from oocytes, while other tested AGCVIII kinases have no effect

The AGCVIII kinase family comprises 23 members in Arabidopsis which can be subdivided into four groups. D6PK and its three close homologs D6PKL1, D6PKL 2 and D6PKL3 belong to the AGC1 group (Bögre *et al.*, 2003; Galvan-Ampudia and Offringa, 2007). The AGC3 group includes PID as well as WAG1 and WAG2 which are, apart from D6PKs, the only AGCVIII

kinases shown to directly phosphorylate PIN proteins, thereby regulating PIN polar localization (Michniewicz *et al.*, 2007; Dhonukshe *et al.*, 2010; Huang *et al.*, 2010). PHOTOTROPIN1 (PHOT1) and PHOT2, which form the AGC4 group, are blue light receptors and play an important role in phototropic response (Sakai *et al.*, 2001). In this context, they act upstream of PIN proteins, as relocalization of the auxin efflux carriers leads to lateral auxin transport and consequently to bending (Friml *et al.*, 2002b; Ding *et al.*, 2011). However, there is no evidence that PINs are direct phosphorylation targets of phototropins. The fourth group of the AGCVIII kinases includes the recently characterized UNICORN (UNC), which is involved in the regulation of cell growth and division in various organs, but has not been implicated in auxin transport regulation so far (Enugutti *et al.*, 2012).

In order to find out more about the specificity of the activatory effect of D6PK on PIN1, representative members of each subgroup of the AGCVIII kinases, i.e. PID, PHOT1 and UNC, were chosen and the respective mRNAs were injected into oocytes together with the PIN1-encoding mRNA. Efflux assays revealed that co-expression of PIN1 with PHOT1 or UNC did not have any effect on auxin efflux, whereas co-expression with PID lead to a significant
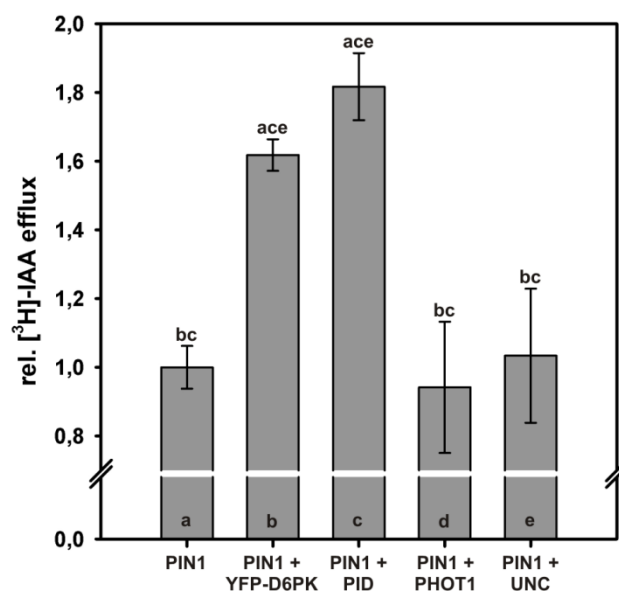
Figure 2-9 Influence of other AGCVIII kinases on PIN1 transport activity in *X. laevis* oocytes. Rel. [3H]-IAA efflux in oocytes after direct injection of the substrate. Rel. efflux from oocytes expressing PIN1 without a kinase was set to 1. Co-expression of YFP-D6PK or PID, but not of PHOT1 or UNC resulted in enhanced IAA efflux. Error bars show SEM of biological replicates (n=23 for PIN1 and PIN1 + YFP-D6PK, n=14 for PIN1 + PID, n=5 for PIN1 + PHOT1, n=3 for PIN1 + UNC). Different letters indicate significant differences. Statistical analysis was performed by means of a one way ANOVA followed by Bonferroni's post hoc test (p<0.05).

increase in auxin efflux from oocytes compared to the samples where no kinase was co-expressed with PIN1 (Figure 2-9). The extent of the induction caused by PID was even slightly stronger than for YFP-D6PK (app. 1.8 fold vs. 1.6 fold increase compared to the control without kinase).

In agreement with the activation of PIN1 observed by YFP-D6PK and PID, a smear of lower mobility bands was observed on a Western Blot when protein extracts from the respective oocytes were labeled with a PIN1 antibody. The smear represents phosphorylated PIN1 and was not present in samples of oocytes expressing PIN1 alone, PIN1 + PHOT1 or PIN1 + UNC (Figure 2-10 A).

An antibody against PID was not available in this work, but the fact that it activates and phosphorylates PIN1 may serve as a proof for its correct expression. Expression of PHOT1 and UNC on the other hand had to be verified to make sure that the lack of PIN1 activation was indeed due to the fact that it was not phosphorylated rather than that the kinases were not expressed. PHOT1 exists in an inactive form in the dark and is activated by auto-phosphorylation upon a blue light stimulus. Phosphorylation of the residue Ser-851 which is localized in the activation loop of the kinase is crucial for PHOT1 activity (Inoue *et al.*, 2008). To check whether the active form of PHOT1 (PHOT1-pSer851) was present in oocytes, protein extracts from oocytes expressing PIN1 or co-expressing PIN1 and PHOT1 were prepared as described in 7.7.5. Prior to the extraction, cells were placed in daylight for 15 min which corresponds to the time the oocytes are exposed to light during injection of [^{3}H]-IAA before the start of the efflux assays. The protein extracts were then analyzed on a Western Blot using antibodies that allowed the discrimination of unphosphorylated PHOT1 and PHOT1-pSer851 (Inoue *et al.*, 2008). The upper panel of Figure 2-9 B shows that unphosphorylated PHOT1 could be detected in the microsomal as well as in the cytosolic fraction of protein extracts from oocytes co-expressing PIN1 and PHOT1. Additionally, a weak signal was detected in the cytosolic fraction of the same protein extracts when using an antibody that specifically recognizes PHOT1-pSer851 (Figure 2-10 B lower panel). This indicates that at least part of PHOT1 was in the active, i.e. auto-phosphorylated state in the oocytes used for the efflux assays. Consequently, it can be stated that PIN1 is not activated / phosphorylated by PHOT1.

UNC, which was also not able to activate PIN1 in the oocyte system (Figure 2-9), was detected in the cytosolic fraction of protein extracts from PIN1 and UNC co-expressing

oocytes (Figure 2-10 C). This result corresponds to its described subcellular localization to the nucleus and the cytoplasm in plants (Enugutti *et al.*, 2012).
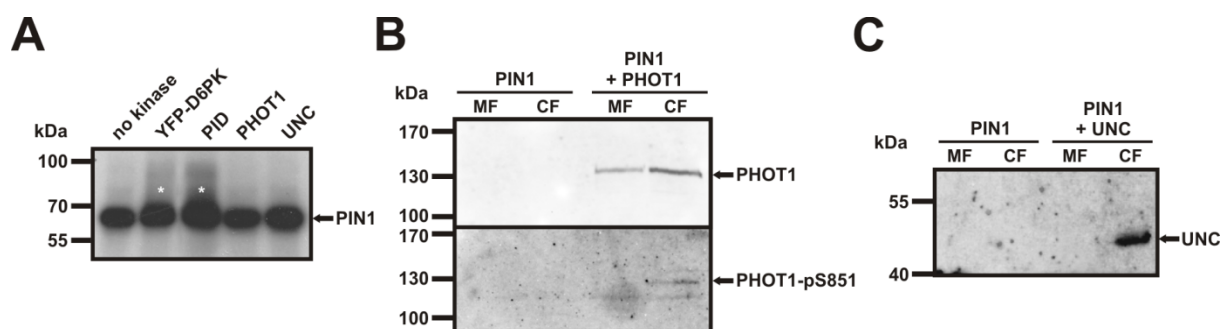
Figure 2-10 Western Blot analysis of PIN1, PHOT1 and UNC in protein extracts from *X. laevis* oocytes 5 days after mRNA injection. (A) Western blot analysis of PIN1 in microsomal fractions of protein extracts from oocytes expressing PIN1 alone or PIN1 in combination with different kinases. The smear of bands with lower mobility (asterisks) in samples from PIN1 + YFP-D6PK and PIN1 + PID represents phosphorylated PIN1. (B) Western Blot analyisis of PHOT1 and PHOT1-pSer851. Unphosphorylated PHOT1 was detected both in the microsomal fraction (MF) and in the cytosolic fraction (CF) of oocytes co-expressing PIN1 and PHOT1 (upper panel). PHOT1-pSer851 was detected in the CF of oocytes co-expressing PIN1 and PHOT1 (lower panel). (C) Western Blot analyisis of UNC. UNC was detected in the CF of oocytes co-expressing PIN1 and UNC.

The fact that two of the four tested kinases were not able to activate PIN1 in the oocyte system shows that the activation mediated by PID and D6PK is a specific feature of certain subgroups of the AGCVIII family. It is very interesting that PID which was so far mainly implicated in the polar targeting of PIN proteins (Friml *et al.*, 2004; Michniewicz *et al.*, 2007; Dhonukshe *et al.*, 2010; Huang *et al.*, 2010) is obviously also able to stimulate their transport activity, although the question whether this is of relevance in plants remains open. The activation of PIN1 by PID was therefore studied in more detail. First of all, the possibility that PID might act on *X. laevis*-specific transporters and enhance IAA efflux independently of PIN1 had to be ruled out by expressing the kinase without PIN1. As expected, PID alone could not induce IAA efflux (Figure 2-11). An interesting question was whether D6PK and PID activate PIN1 in a different way, i.e. by phosphorylating distinct target sites. It can be hypothesized that phosphorylation of different serine or threonine residues within the hydrophilic loop of PINs by PID and D6PK could cause an additive effect on the transport activity of PIN1. To test this, PIN1 was co-expressed with both PID and D6PK simultanously and IAA efflux from oocytes was measured. Figure 2-11 shows that expression of both activating kinases

together with PIN1 does not lead to a significantly stronger rise of PIN1 transport activity compared to when only one kinase was present. After setting the background efflux in PIN1-expressing oocytes to 1, an app. 1.9 fold induction for oocytes co-expressing PIN1 + YFP-D6PK + PID compared to a factor of 1.8 for PIN1 + PID and 1.6 for PIN1 + YFP-D6PK was observed. This indicates that – even if D6PK and PID use different phosphorylation sites in their target protein - the effect on IAA transport activity is the same.
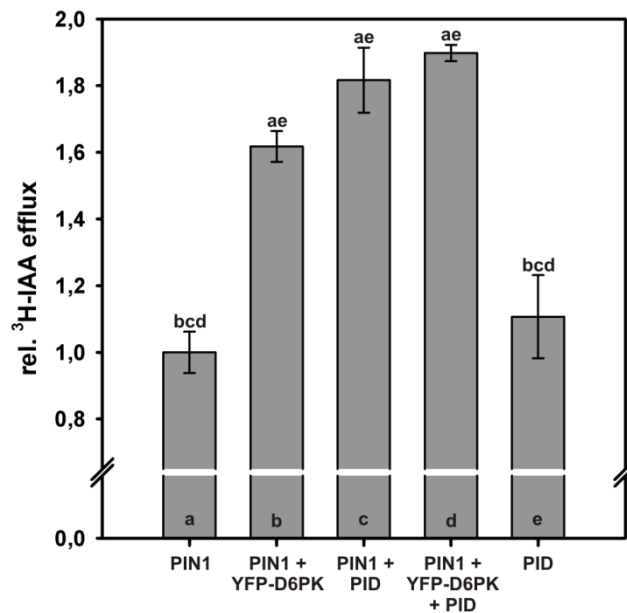
Figure 2-11 YFP-D6PK and PID do not have an additive effect on PIN1 mediated IAA efflux. Rel. [^{3}H]-IAA efflux in oocytes after direct injection of the substrate. Rel. efflux from oocytes expressing PIN1 was set to 1. Error bars show SEM of biological replicates (n=23 for PIN1 and PIN1 + YFP-D6PK, n=14 for PIN1 + PID, n=2 for PIN1 + YFP-D6PK + PID, n=5 for PID). Different letters indicate significant differences. Statistical analysis was performed by means of a one way ANOVA followed by Bonferroni's post hoc test (p<0.001).

2.2.6 D215 and S271 are important for PIN1 activation

While three serine residues in a conserved TPRXS(N/S) motif were described as targets of PID before (Dhonukshe *et al.*, 2010; Huang *et al.*, 2010), the serine at position 271 was identified as a preferential target for D6PK in PIN1 in an *in vitro* phosphorylation assay with synthetic peptides. Furthermore it was shown by mass spectrometry analysis of protein extracts from different plant lines that PIN1 is phosphorylated at position S271 *in vivo* and that PIN1-pSer271 is completely absent in higher order *d6pk* mutants (Zourelidou,

unpublished). In order to find out whether S271 phosphorylation is essential for PIN1 activation, a mutant version of PIN1 in which the serine at position 271 was substituted by an alanine (PIN1$_{S271A}$, Zourelidou, unpublished) was analyzed in the oocyte expression system. Looking at alignments of the hydrophilic loops of long PINs, yet another amino acid residue attracted attention. At position 215 PIN1 contains an aspartate, while in the other PINs (PIN2, 3, 4 and 7), a serine is found at the respective position. This raised the question whether D215 in PIN1 represents a natural phosphomimicking variant that leads to higher basic activity compared to a D215A mutant or compared to other PINs. However, wild type PIN1 does not exhibit any measurable transport activity in the oocyte system (Figure 2-5) indicating that D215 is not sufficient to confer higher activity to the protein. Still, the negative charge of D215 might contribute to the transport activity upon phosphorylation of S271 or other relevant residues. Therefore, both PIN1$_{D215A}$ and PIN1$_{S271A}$ as well as a double mutant PIN1$_{D215A/S271A}$ were analyzed concerning their activation upon co-expression with YFP-D6PK and also with PID. All the variants were expressed in oocytes either alone or in combination with the kinases, YFP-D6PK or PID. Expression of the mutant versions was confirmed by Western Blot analysis of protein extracts from oocytes that were injected with the respective mRNAs (Figure 2-12 B). Like for wild type PIN1, the strongest signal was always detected in the microsomal fraction of the protein extracts, indicating that the mutant versions are correctly localized to the membrane. Figure 2-12 A shows that compared to wild type PIN1, the activation by YFP-D6PK is reduced for the mutant versions (light gray bars). While in oocytes co-expressing PIN1 and YFP-D6PK, a 1.6 fold increase in IAA efflux was observed compared to the "no-kinase" control, this factor was reduced to app. 1.3 for the single mutants PIN1$_{D215A}$ and PIN1$_{S271A}$ and to 1.2 for the double mutant PIN1$_{D215A/S271A}$. In case of PID, the situation was different (Figure 2-12, dark gray bars). While activation of PIN1$_{D215A}$ and the double mutant PIN1$_{D215AS271A}$ seemed to be impaired compared to wild type PIN1 (factor of app. 1.4 versus 1.8 for wild type PIN1), the PIN1$_{S271A}$ was activated almost as well as the wild type version by the PINOID kinase (1.7 fold increase versus 1.8 fold increase in rel. IAA efflux). When the transport rates of the different PIN1 variants expressed alone or in combination with one of the kinases were statistically compared, activation of PIN1 and PIN1$_{S271A}$ by both YFP-D6PK and PID was significant ($p<0.001$ for PIN1 and $p<0.05$ for PIN1$_{S271A}$), while the increase in auxin efflux observed for PIN1$_{D215A}$ and PIN1$_{D215A/S271A}$ was not significant. However, this is most likely due to the
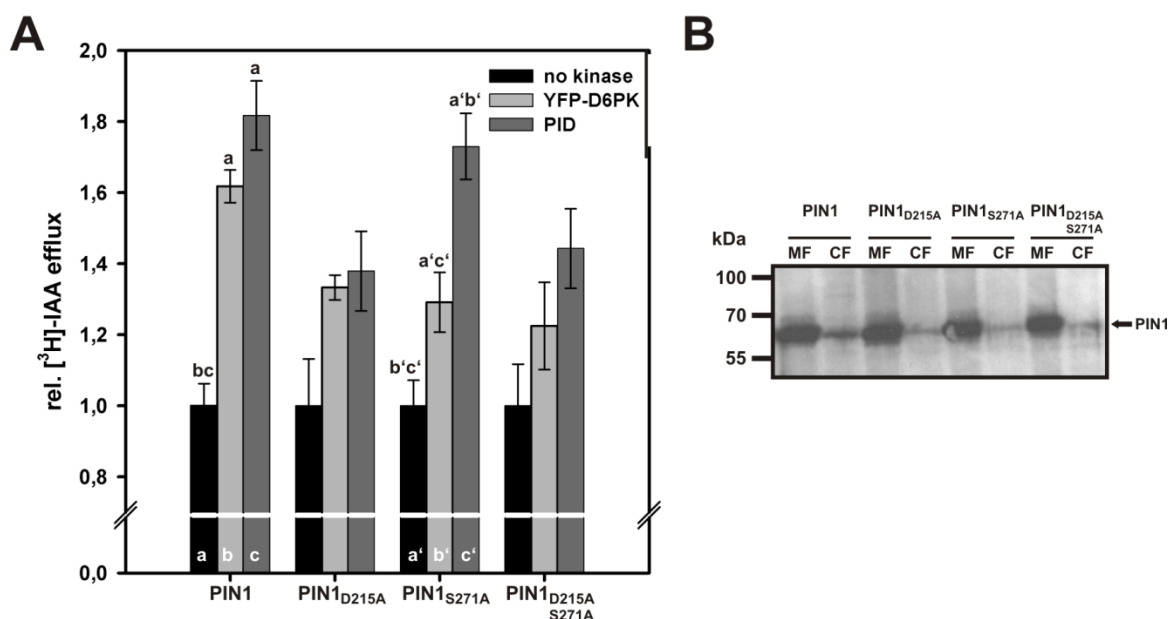
Figure 2-12 Analysis of IAA efflux mediated by PIN1$_{D215A}$, PIN1$_{S271A}$ and PIN1$_{D215A/S271A}$ upon co-expression with YFP-D6PK or PID. (A) Rel. [^{3}H]-IAA efflux from oocytes after direct injection of the substrate. Rel. efflux from oocytes expressing PIN1 or a mutant version (PIN1$_X$) without a kinase (black bars) was set to 1. All mutant versions of PIN1 are activated by YFP-D6PK (light grey bars) than wild type PIN1. PIN1$_{D215A}$ and PIN1$_{D215A/S271A}$ are activated to a lesser extent by PID (dark grey bars) than wild type PIN1 while PIN1$_{S271A}$ is activated as well as wild type PIN1. Error bars show SEM of biological replicates (n=23 for PIN1 and PIN1 + YFP-D6PK, n=14 for PIN1 + PID, n=6 for PIN1$_{S271A}$ and PIN1$_{S271A}$ + YFP-D6PK, n=4 for PIN1$_{D215A}$, PIN1$_{D215A}$ + YFP-D6PK and PIN1$_{S271A}$ + PID, n=3 for PIN1$_{D215A}$ + PID, PIN1$_{D215A/S271A}$, PIN1$_{D215A/S271A}$ + YFP-D6PK and n=2 for PIN1$_{D215A/S271A}$ + PID). Different letters indicate significant differences. Statistical analysis was performed by means of a one way ANOVA, followed by Bonferroni's post hoc test. Each PIN1 variant was tested seperately (PIN1: $p<0.001$, PIN1$_{S271A}$: $p<0.05$). (B) Western Blot analysis of mutant versions of PIN1 in protein extracts from *X. laevis* oocytes 5 days after mRNA injection. PIN1$_X$ was detected with an anti-PIN1 antibody. Like wild type PIN1, all mutant versions were found mainly in the microsomal fractions (MF), only weak signals were detected in the cytosolic fractions (CF).

variance between the biological replicates and the observed tendency can be confirmed statistically by increasing sample size.

As phosphorylation of S271 seems to be important for transport activity of PIN1, it was tested whether a phosphomimicked version of PIN1 with an S271D amino acid exchange can mediate IAA efflux from *X. laevis* oocytes without addition of a kinase. Therefore, mRNAs encoding for PIN1 or PIN1$_{S271D}$ were injected into oocytes either alone or in combination with YFP-D6PK and IAA efflux was measured 5 days later. Figure 2-13 A shows that the rel. IAA efflux from oocytes expressing PIN1$_{S271D}$ is not increased compared to oocytes

expressing the wild type PIN1 version. Expression and localization of PIN1$_{S271D}$ was confirmed by Western Blot analysis of the respective protein extracts from oocytes (Figure 2-13 B). A reason for the observed lack of activity of PIN1$_{S271D}$ can be that an aspartate at position 271 cannot replace a phosphate group functionally or that additional phosphorylations at other positions within the hydrophilic loop in combination with a negative charge at position 271 are required for activation of PIN1.
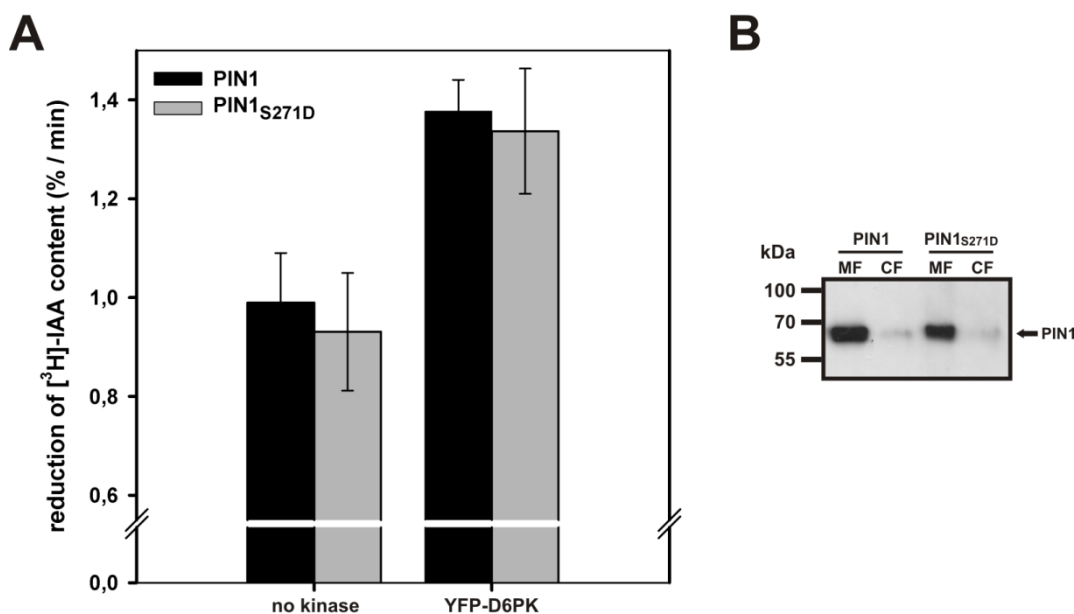
Figure 2-13 An S271D mutation in PIN1 has no effect on transport activity. (A) Rel. [^{3}H]-IAA efflux from oocytes after direct injection of the substrate. No difference was observed between oocytes expressing PIN1 or PIN1$_{S271D}$ when they were expressed without a kinase (black bars) or in combination with YFP-D6PK (grey bars). Error bars show SEM of biological replicates (n=3). (B) Western Blot analysis of PIN1 and PIN1$_{S271D}$ in protein extracts from *X. laevis* oocytes 5 days after mRNA injection. PIN1 and PIN1$_{S271D}$ were detected with an anti-PIN1 antibody. Like wild type PIN1, PIN1$_{S271D}$ was found mainly in the microsomal fraction (MF), only weak signals were detected in the cytosolic fraction (CF).

2.2.7 Described PID target sites contribute to PIN1 activity

It was demonstrated in this work that the PINOID kinase is able to stimulate IAA transport activity of PIN1 by phosphorylation in the *X. laevis* expression system (Figure 2-9 to Figure 2-11). Previous studies identified three serine residues in a conserved TPRXS(N/S) motif as the functional PID phosphorylation targets essential for proper localization of PIN proteins. In PIN1, these are the residues S231, S252 and S290 (Dhonukshe *et al.*, 2010; Huang *et al.*, 2010). *In vitro* phosphorylation assays showed that a triple mutant PIN1$_{S231A/S252A/S290A}$ was

still phosphorylated both by D6PK and by PID, whereas a quadruple mutant which carried an additional alanine also at position 271 (PIN1$_{S231A/S252A/S271A/S290A}$) could not be targeted by any of the kinases anymore (Zourelidou *et al.,* unpublished). These findings in combination with the fact that co-expression of YFP-D6PK or PID with the single mutant PIN1$_{S271A}$ still lead to enhanced IAA efflux from oocytes (Figure 2-12) suggested that phosphorylation of the three classical PID target sites might also be important for PIN1 transport activity. Therefore, the triple mutant PIN1$_{S231A/S252A/S290A}$ in which the three serines within the TPRXS(N/S) were replaced by non-phosphorylatable alanine as well as the quadruple mutant PIN1$_{S231A/S252A/S271A/S290A}$ with the additional serine to alanine exchange at position 271 were expressed in *X. laevis* oocytes and analyzed concerning their transport activity upon co-expression with YFP-D6PK or PID by measuring IAA efflux (see 7.7.4). Expression and membrane localization of the mutant versions was confirmed by Western Blot analysis of protein extracts from oocytes that were injected with the respective mRNAs (Figure 2-14 B).

Figure 2-14 A shows that the triple mutant PIN1$_{S231A/S252A/S290A}$ could still be activated by both YFP-D6PK and PID which upon co-expression caused a 1.6 fold and 1.5 fold increase in rel. IAA efflux compared to the "no-kinase" control, respectively. This means that activation of the triple mutant by D6PK is comparable to wild type PIN1 while activation achieved by PID co-expression is slightly weaker than for the wild type PIN1 (1.5 fold versus 1.8 fold increase in rel. IAA efflux compared to the "no-kinase" control). It is noteworthy that the negative effect of the triple mutation on the activatability by the two kinases seems to be stronger for PID than for YFP-D6PK while the opposite tendency was observed for the PIN1$_{S271A}$ mutant (Figure 2-12 A). This might indicate that D6PK and PID exhibit a different affinity for the respective serine residues.

In case of the quadruple mutant PIN1$_{S231A/S252A/S271A/S290A}$ only a very weak increase in IAA efflux could be achieved by co-expression of the kinases (app. 1.1 fold higher efflux compared to the "no-kinase" upon co-expression YFP-D6PK and PID, respectively). The latter increase in IAA efflux from oocytes was not significantly different from the corresponding "no-kinase" control while PIN1 and PIN1 $_{S231A/S252A/S290A}$ activation by both YFP-D6PK and PID was statistically significant ($p<0.001$ for PIN1 and $p<0.05$ for PIN1 $_{S231A/S252A/S290A}$).

In summary, the results obtained from the analysis of PIN1 mutants provide evidence that by phosphorylation of previously described PID target sites as well as of the recently identified S271, PIN1 acquires the capacity to mediated auxin efflux from oocytes. While PIN1$_{S271A}$ and

PIN1 $_{S231A/S252A/S290A}$ can still be activated to a certain degree, this trait is lost in a combined quadruple mutant, indicating that the residues crucial for PIN1 activation have been identified.
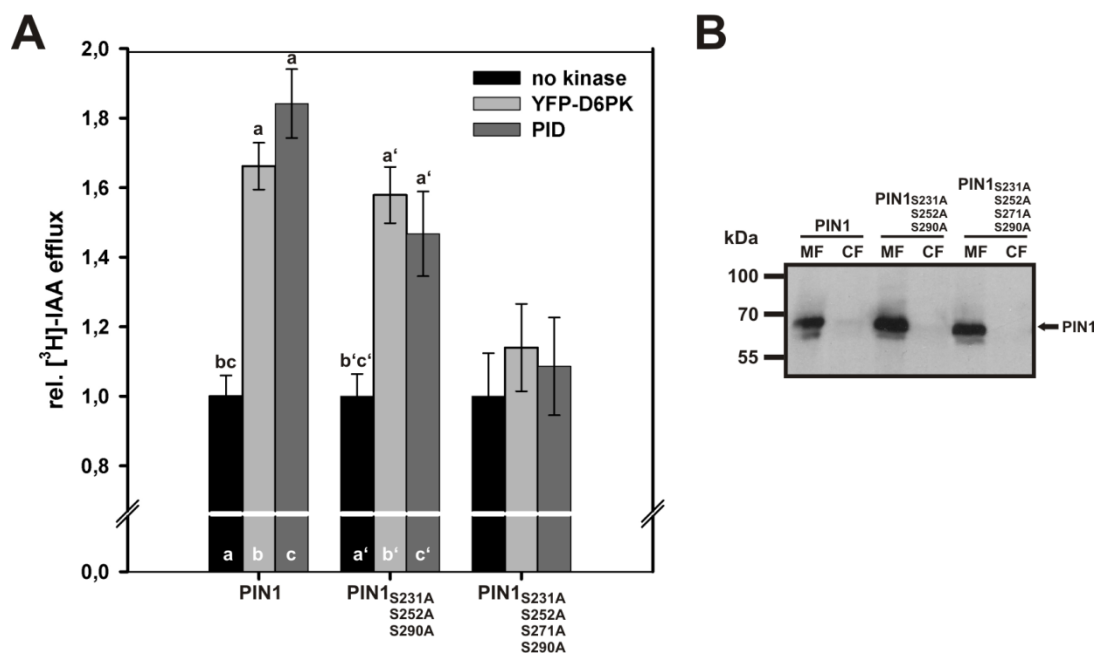
Figure 2-14 Analysis of IAA efflux mediated by PIN1$_{S231A/S252A/S290A}$ and PIN1$_{S231A/S252A/S271A/S290A}$ upon co-expression with YFP-D6PK or PID. (A) Rel. [^{3}H]-IAA efflux from oocytes after direct injection of the substrate. Rel. efflux from oocytes expressing PIN1 or a mutant version (PIN1$_X$) without a kinase (black bars) was set to 1. PIN1 and PIN1$_{S231A/S252A/S290A}$, but not PIN1$_{S231A/S252A/S271A/S290A}$ are activated by YFP-D6PK (light grey bars) or PID (dark grey bars). PIN1$_{S231A/S252A/S290A}$ is activated to a lesser extent by PID than PIN1. Error bars show SEM of biological replicates (n=23 for PIN1 and PIN1 + YFP-D6PK, n=14 for PIN1 + PID, n=4 for PIN1$_{S231A/S252A/S271A/S290A}$ without kinase / + YFP-D6PK / + PID, n=3 for PIN1$_{S231A/S252A/S290A}$ without kinase / + YFP-D6PK / + PID). Different letters indicate significant differences. Statistical analysis was performed by means of a one way ANOVA, followed by Bonferroni's post hoc test. Each PIN1 variant was tested seperately (PIN1: p<0.001, PIN1$_{S231A/S252A/S290A}$: p<0.05). (B) Western Blot analysis of mutant versions of PIN1 in protein extracts from *X. laevis* oocytes 5 days after mRNA injection. PIN1$_X$ was detected with an anti-PIN1 antibody. Like wild type PIN1, all mutant versions were found mainly in the microsomal fractions (MF), only very weak signals were detected in the cytosolic fractions (CF).

2.2.8 PIN3 is also activated by YFP-D6PK and PINOID

d6pk mutants exhibit numerous phenotypes which point towards a role of D6PK in auxin transport. The triple mutant *d6pk d6pkl1 d6pkl2* (*d6pk012)* shows an agravitropic as well as a non-phototropic phenotype (Zourelidou *et al.*, 2009; Willige *et al.*, 2013). Tropic responses are mediated by an asymmetric distribution of auxin that leads to differential growth rates and ultimately to bending of the root or the shoot. PIN3 is a central component of the lateral auxin transport system that regulates tropic growth as its relocalization in response to gravity or light stimuli triggers the redirection of auxin flows (Friml *et al.*, 2002b). Recently it was found that in the *d6pk012* mutant, PIN3 phosphorylation is reduced. This is accompanied by a reduced lateral auxin transport during the phototropic response in hypocotyls. However, the relocalization of PIN3 that is a prerequisite for the establishment of the auxin maximum at the shaded side of the hypocotyls still takes place (Willige *et al.*, 2013). It was also shown that PIN3 is phosphorylated by D6PK *in vitro* (Zourelidou *et al.*, 2009). In order to confirm the hypothesis that PIN3 is also directly activated by D6PK, PIN3 was expressed in *X. laevis* oocytes either alone or in combination with YFP-D6PK or YFP-D6PK$_{in}$ and efflux assays were performed as described in 7.7.4. In order to compare the PIN1 and PIN3 mediated IAA efflux, oocytes expressing PIN1 or PIN1 + YFP-D6PK were tested in parallel. In a first experiment, IAA content was monitored at 4 time points. Figure 2-15 shows the results of one biological replicate where 12 oocytes were tested for each sampling point. While oocytes expressing PIN3 or PIN3 in combination with the kinase-inactive YFP-D6PK$_{in}$ were basically indistinguishable from the water-injected or PIN1-expressing oocytes regarding the reduction of the IAA-content over time, PIN3 was clearly activated in the presence of YFP-D6PK. Remarkably, IAA export from oocytes expressing PIN3 + YFP-D6PK was stronger than from oocytes expressing PIN1 + YFP-D6PK. This indicates that either PIN3 is a better substrate for YFP-D6PK and is therefore activated more efficiently or that the protein in its activated state has a higher affinity for IAA which would also lead to the observed differences in the IAA export rates. A high affinity of PIN3 towards its substrate would clearly make sense as tropic responses involve a rapid redistribution of auxin that can only be achieved by an extremely efficient transport system.

PIN3 was shown to be phosphorylated by PID and to be dependent on its activity for correct localization during tropic responses (Ding *et al.*, 2011; Rakusová *et al.*, 2011). The effect of co-expression on IAA efflux in oocytes was therefore analyzed. As a negative control, PHOT1
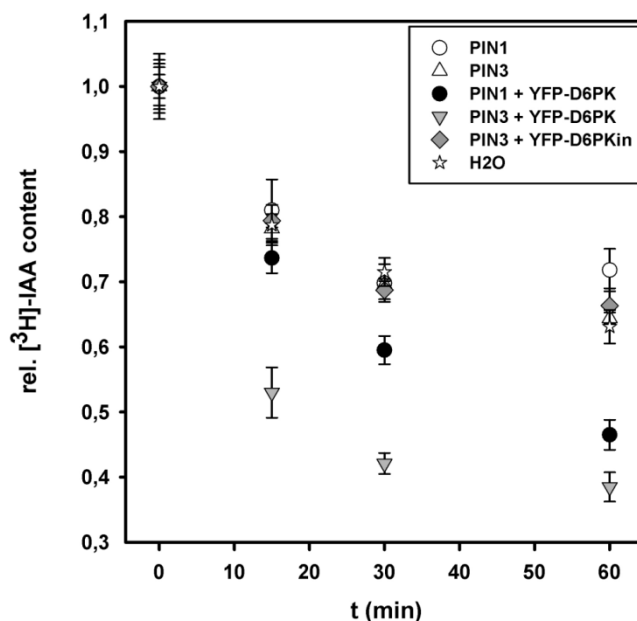
Figure 2-15 Co-expression of PIN3 and YFP-D6PK leads to strongly enhanced IAA efflux in _X. laevis_ oocytes. Reduction of [^{3}H]-IAA content in oocytes after direct injection of the substrate. CPM at time point 0 min were set to 1. Oocytes expressing PIN3 or PIN3 + YFP-D6PK$_{in}$ were undistinguishable from water-injected or PIN1-expressing oocytes. Co-expression of YFP-D6PK with PIN1 or PIN3 caused enhanced IAA export from oocytes. The effect was much stronger in case of PIN3. Error bars show SEM of technical replicates. 12 oocytes were analyzed for each time point.

was co-expressed with PIN3. An activation was not expected in this case as it was shown before that PIN3 is not a target of PHOT1 (Ding _et al._, 2011). These samples therefore served as a control to exclude the possibility that due to the overexpression of kinases and PIN proteins in the oocytes unspecific targets are phosphorylated. Efflux assays were performed as described in 7.7.4 and data were subsequently analyzed and plotted as illustrated in chapter 2.2.3. After measuring residual IAA content at the time points 0 min, 7.5 min, 15 min and 30 min, linear regressions were calculated and transport rates were determined from the negative value of the line's slopes. Subsequently, data were normalized to the values of the "no-kinase" samples. As Figure 2-16 A shows, co-expression of YFP-D6PK or PID results in app. 1.9 fold higher auxin efflux from oocytes compared to when PIN3 is expressed alone, while co-expressing PIN3 with PHOT1 does not have an effect on IAA export. The differences in the transport rates were not statistically significant which is most likely due to the relatively high variation within the three biological replicates that were tested in this set of experiments. Consistent with the observed activation of PIN3 by YFP-D6PK and PID, a smear

of lower mobility bands was observed on a Western Blot when protein extracts from the respective oocytes were labeled with a PIN3 antibody while these additional bands did not appear in samples from control oocytes that expressed only PIN3 (Figure 2-16 B).
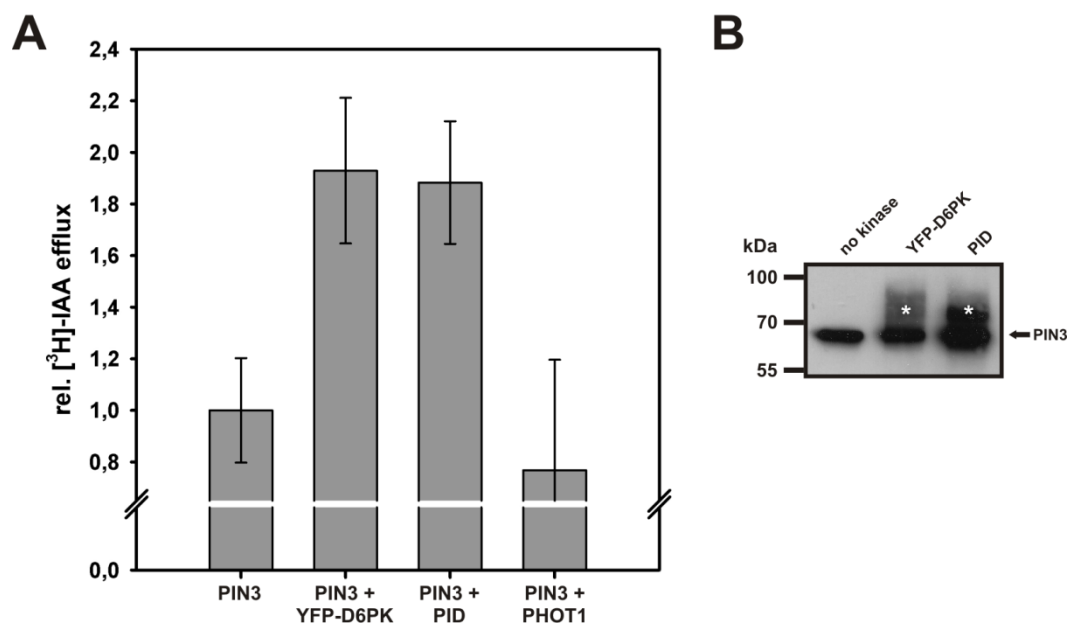
Figure 2-16 PIN3 is activated by YFP-D6PK and PID. (A) Rel. [^{3}H]-IAA efflux from oocytes after direct injection of the substrate. Rel. efflux from oocytes expressing PIN3 without a kinase was set to 1. PIN3 is activated by co-expression of YFP-D6PK or PID, but not by PHOT1. Error bars show SEM of biological replicates (n=3). (B) Western blot analysis of PIN3 in the microsomal fraction of protein extracts from *X. laevis* 5 days after mRNA injection expressing PIN3 alone, PIN3 + YFP-D6PK or PIN3 + PID. The smear of bands with lower mobility (asterisks) in protein extracts from oocytes co-expressing PIN3 + YFP-D6PK or PIN3 + PID represents phosphorylated PIN3.

For PIN1, S271 was identified as a preferential target phosphorylation site *in vitro* and *in vivo* (Zourelidou *et al.*, unpublished) which also contributes to the activatability of the protein regarding IAA efflux (Figure 2-12). In order to find out whether a similar effect could be observed for PIN3, a mutant carrying a serine to alanine exchange at the corresponding position (PIN3$_{S262A}$) was expressed in oocytes and IAA efflux was measured upon co-expression with YFP-D6PK or PID. Figure 2-17 shows that PIN3 and the mutant version PIN3$_{S262A}$ were indistinguishable in the efflux assay. The mutant induced auxin efflux to the same extent as the wild type protein when it was activated by YFP-D6PK or PID. Again, the differences were not statistically significant.
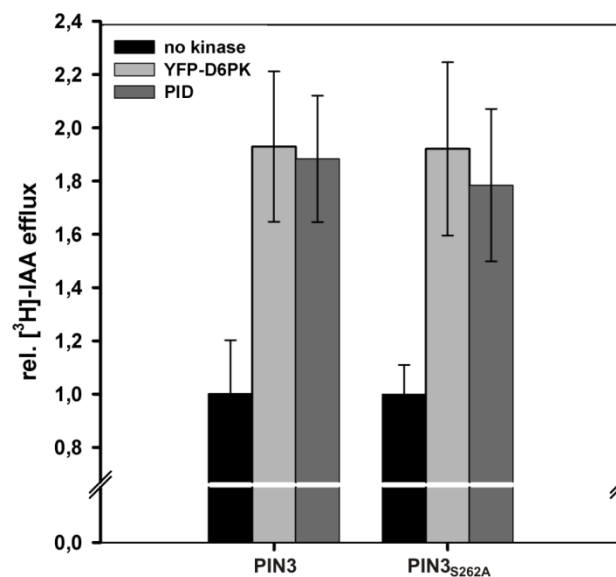
Figure 2-17 A S262A mutation in PIN3 has no effect on activation by YFP-D6PK or PID. Rel. [^{3}H]-IAA efflux from oocytes after direct injection of the substrate. Rel. efflux from oocytes expressing PIN3 or PIN3$_{S262A}$ without a kinase (black bars) was set to 1. No difference was observed between PIN3 and PIN3$_{S262A}$ upon co-expression of YFP-D6PK (light grey bars) or PID (dark grey bars). Error bars show SEM of biological replicates (n=3).

2.3 Discussion

### 2.3.1 The AGCVIII kinases D6PK and PID activate PIN1 and PIN3 by phosphorylation

PIN proteins are key players in auxin regulated development and form the backbone for polar auxin transport in the plant. A wide range of factors have been identified that are involved in the control of their trafficking and polar targeting (Grunewald and Friml, 2010). However, very little is known about regulatory processes that control the transport activity of the PINs. In this work, it could be shown that the AGCVIII kinases D6 and PID positively affect PIN-mediated auxin efflux in the *X. laevis* heterologous expression system. While expression of PIN1 and PIN3 alone did not result in any measurable auxin efflux compared to control oocytes, co-expression of an activating kinase clearly stimulated IAA efflux (Figure 2-5, Figure 2-9, Figure 2-16). An activatory effect was observed for D6PK and PID, but not for two other representative members of the AGCVIII kinases, PHOT1 and UNC, emphasizing the specificity of the interaction between the PINs and D6PK / PID (Figure 2-9 and Figure 2-16).

The transport activity of PIN1 and PIN3 upon co-expression with the D6PK was conferred by phosphorylation as demonstrated by the fact that a kinase-inactive version, D6PK$_{in}$, which differs from the wild-type protein in only one amino acid exchange in the ATP-binding domain, could not activate PIN-mediated auxin efflux anymore (Figure 2-8 and Figure 2-15). Consistently, phosphorylated protein was detected on the Western Blot only when co-expressed with an active kinase (Figure 2-4, Figure 2-8 and Figure 2-16). These results clearly indicate that phosphorylation is crucial for transport activity of PINs. However, it has to be mentioned that evidence for auxin transport activity without co-expression of any other plant proteins in non-plant derived heterologous systems has been provided for PIN1, PIN2 and PIN7. In case of PIN1, expression in *S. pombe* lead to decreased IAA accumulation, indicating enhanced auxin efflux from these cells (Yang and Murphy, 2009). Similar results were obtained for PIN2 and PIN7 in *S. cerevisiae, S. pombe* and human HeLa cells (Chen *et al.*, 1998; Luschnig *et al.*, 1998; Petrasek *et al.*, 2006; Yang and Murphy, 2009). Consequently, some PINs might have basic transport capability also in the absence of a specific activating kinase which could not be detected in *X. laevis* oocytes. Alternatively, PIN protein activity might be influenced by endogenous factors in yeast and HeLa cells that are not present in *X. laevis* oocytes. No data for heterologous expression of PIN3 were available

so far despite its important function especially in tropism (Friml *et al.*, 2002b; Ding *et al.*, 2011). When PIN3 was expressed in oocytes together with D6PK or PID, it enhanced auxin efflux even more efficiently than PIN1 (Figure 2-15 and Figure 2-16). There are several possible explanations for this observation: First, the amount of PIN3 in the oocyte plasma membrane could be increased in comparison to PIN1. This could be a result of higher expression rates, protein stability or more efficient targeting to the plasma membrane. Therefore, carrier density in the membrane should be determined by freeze-fracture electron microscopy (Boorer *et al.*, 1996). Second, the activated PIN3 might differ from PIN1 in intrinsic properties like substrate affinity, transport capacity or turnover frequency. As mentioned above, PIN3 plays an important role in tropic responses in Arabidopsis (Friml *et al.*, 2002b; Ding *et al.*, 2011). Taking into account that these processes depend on a rapid polar redistribution of auxin that can only be achieved by an extremely efficient transport system, the kinetic parameters of the carriers are of great physiological relevance. So far, nothing is known about the kinetic properties of PIN proteins, but the *X. laevis* expression system provides a suitable basis to address these questions in the future.

2.3.2 NPA interferes with auxin efflux mediated by D6PK - activated PIN1

Phenotypes of *d6pk* mutants resemble those described for *pin* mutants and can be mimicked by application of the auxin efflux inhibitor NPA, supporting the role of the D6 kinases in the regulation of auxin transport (Zourelidou *et al.*, 2009). Consistently, auxin efflux in oocytes co-expressing PIN1 and YFP-D6PK was strongly inhibited by NPA when it was co-injected with the substrate to a final concentration of 10 µM. On the other hand, no effect was observed when NPA was added to the incubation buffer at the same concentration (Figure 2-6). However, the latter observation is most likely due to the inability of NPA to enter the oocytes under the given experimental conditions. The pH of the incubation buffer was 7.4 which is optimal for the oocytes and prevents re-diffusion of exported auxin back into the oocytes. At the same time this pH will also inhibit passive uptake of NPA which has a pKa of 4.6 and is therefore – like IAA – mainly present in the deprotonated form that cannot pass the plasma membrane by diffusion. The observed inhibitory effect of NPA when present inside the cells is in accordance with its described site of action at the cytoplasmatic face of the plasma membrane. It was proposed that NPA interferes with auxin efflux via binding to a membrane associated protein that is distinct from the efflux carrier itself, but is essential for

its function (Cox and Muday, 1994; Dixon *et al.*, 1996; Morris, 2000). However, this putative NBP (NPA-binding protein, Sussman and Gardner, 1980; Rubery, 1990) has not been identified so far and the exact mechanism of NPA action remains illusive. The impact of NPA on PIN-mediated auxin efflux has so far mainly been studied in plant systems. However, the problem was that NPA also strongly inhibited background auxin efflux in cells not expressing recombinant PIN proteins (Petrasek *et al.*, 2006). This complicated the search for a putative target as it did not allow discrimination between an inhibitory effect of NPA on PIN proteins themselves or on other components of the efflux machinery that are present in plant cells. In the *X. laevis* system, NPA did not influence background efflux in control samples, i.e. oocytes expressing no plant protein or PIN1 alone, but it specifically inhibited auxin efflux mediated by activated PIN1 in the presence of YFP-D6PK (Figure 2-6 B). This suggests that NPA directly interferes with the transport activity of phosphorylated PIN1, with the kinase function of D6PK or with a protein-protein interaction between PIN1 and D6PK independent of the kinase activity that might contribute to the effective operation of auxin efflux. It will be an interesting task to analyze NPA influence in more detail in the oocyte system in order to gain insight into the exact mechanism of its function.

2.3.3 Phosphorylation of PIN1 and PIN3 by D6PK and PID has different consequences in plants

Despite the above mentioned discrepancy concerning the activity of unphosphorylated PINs in the different heterologous systems, the importance of phosphorylation as a regulatory posttranslational modification is unquestionable. A control of auxin efflux by phosphorylation was proposed even before the detailed characterization of the involved carriers, based on the finding that efflux from tobacco suspension-cultured cells is suppressed by the protein kinase inhibitors staurosporin and K252a (Delbarre *et al.*, 1998). In the following years, detailed characterization of the PIN proteins and identification of interacting kinases revealed that they are tightly regulated by phosphorylation (Friml *et al.*, 2004; Zazimalova *et al.*, 2007). As shown in this work, both PID and D6PK have the potential to stimulate PIN transport activity by phosphorylation (Figure 2-9). The fact that no additive effect was observed when both D6PK and PID were co-expressed with PIN1 (Figure 2-11) indicated that the kinases activate PIN1 in a similar way. However, there is numerous

evidence that the two kinases have very distinct functions in plants. PID is a key determinant in the polar targeting of PIN proteins as it mediates their phosphorylation-dependent recruitment into different trafficking pathways within the cell (Kleine-Vehn *et al.*, 2009). Thereby, it acts as a binary switch that directs proteins from the basal to the apical cell face as shown for PIN1, PIN2 and PIN4 (Friml *et al.*, 2004; Michniewicz *et al.*, 2007; Dhonukshe *et al.*, 2010). It was also implicated in the regulation of lateral targeting of PIN3 during gravi- and phototropic responses (Ding *et al.*, 2011). The data presented here suggest that an additional consequence of PIN phosphorylation by PID is enhanced transport activity (Figure 2-9). This hypothesis is supported by the finding that overexpression of PID in tobacco BY2 cells and Arabidopsis root hair cells results in increased auxin efflux and decreased intracellular auxin levels. The same effect was observed when PIN3 was overexpressed in these cells (Lee and Cho, 2006), indicating that manipulation of auxin levels can be achieved likewise by increasing abundancy (overexpression of PIN3) or increasing activity (overexpression of PID) of the efflux carrier.

 In contrast to PID, the D6 kinases seem to have a more constrained function as they are mainly involved in the regulation of PIN transport activity. Consequently, *d6pk* mutants show defects in auxin transport, but not in PIN localization (Zourelidou *et al.*, 2009; Willige *et al.*, 2013). Several published findings illustrate the functional link between D6PKs and PIN1 as well as PIN3 *in vivo*. Phenotypic analysis showed that several morphological phenotypes of the *d6pk* mutants resemble those observed in *pin* mutants and a synergistic genetic interaction between *PIN1* and the *D6PK* genes has been shown (Zourelidou *et al.*, 2009). A function of D6PK together with PIN3 and possibly also other PINs in control of auxin transport during phototropic hypocotyl bending was recently demonstrated (Willige *et al.*, 2013). The results strongly suggest that reduced PIN transport activity due to a lack of D6PK-mediated phosphorylation is the primary cause for phototropic growth defects in *d6pk* mutants. The data obtained in this work further validate the described observations and provide evidence that PIN activity can be tightly regulated by D6PK.

2.3.4 D6PK and PID activate PIN1 by preferential phosphorylation of different serine residues

An evident explanation for the different functions of D6PK and PID in plants is that there are distinct target sites in the PIN hydrophilic loop which are important for transport activity and for polar localization, respectively. The amino acids that are essential for PID-mediated phosphorylation-dependent polar targeting are well described and lie within three conserved TPRXS(N/S) motifs (Dhonukshe *et al.*, 2010; Huang *et al.*, 2010). The residue S271 on the other hand was identified as a preferential target site for D6PK in PIN1. In an *in vitro* assay, peptides containing this residue were strongly phosphorylated by D6PK. Mass spectrometry analysis of protein extracts confirmed that the phosphorylated version of PIN1, PIN1-pSer271, was present in wild type plants but was absent in the *d6pk012* triple mutant. This demonstrates that the S271 amino acid residue is specifically targeted by the D6 kinases *in vivo* (Zourelidou *et al.*, unpublished). In this work, different mutants that carried serine to alanine substitutions at the respective positions were analyzed with regard to their effects on PIN1 transport activity.

Auxin efflux assays revealed that transport activity of PIN1$_{S271A}$ was reduced compared to wild type when D6PK was co-expressed. Intriguingly, activation of this mutant by PID was basically indistinguishable from wild type PIN1 (Figure 2-12). This observation suggests that S271 is important for D6PK function, while PID activates independently of S271, i.e. *via* phosphorylation of different residues. The fact that PIN1$_{S271A}$ can still be activated by both kinases - although to a different extent - is also in agreement with the finding that PIN1$_{S2712A}$ can still complement the *pin1* mutant phenotype (Zourelidou *et al.,* unpublished).

Analysis of PIN1$_{S231A/S252A/S290A}$ in which the three central serines of the TPRXS(N/S) motifs are exchanged for alanines revealed that also this mutant can mediate auxin efflux upon co-expression of D6PK or PID and that the transport efficiency was only weakly impaired compared to wild type PIN1 (Figure 2-14). Interestingly, whereas the S271A mutation interfered stronger with D6PK function, the opposite effect was observed in case of the triple mutant PIN1$_{S231A/S252A/S290A}$, i.e. activation by PID was impaired more than activation by D6PK suggesting that the serines S231/S252/S290 are more important for PIN1-PID interaction than for PIN1-D6PK interaction.

While both PIN1$_{S271A}$ as well as the triple mutant PIN1$_{S231A/S252A/S290A}$ could still mediate enhanced auxin efflux from oocytes when co-expressed with D6PK or PID, this feature was

almost completely lost in a quadruple mutant where all these four serines were replaced by alanine (Figure 2-14). In agreement with that, it was shown that the quadruple mutant cannot be phosphorylated anymore *in vitro* either by D6PK or by PID (Zourelidou *et al.*, unpublished). Taken together, these results strongly suggest that the main phosphorylation sites that contribute to PIN1 activatability by D6PK and PID have been identified and include S271 as well as S231/S252/S290. However, analysis of the respective mutants clearly demonstrated that not all of the sites have to be phosphorylated at the same time to confer transport activity to PIN1. In fact, phosphorylation of either S271 or one or more of the S231/S252/S290 sites is sufficient for transport activity.

Initial experiments on the regulation of PIN3 activity revealed that a serine to alanine exchange at position 262 of PIN3 which corresponds to S271 in PIN1 did not affect the activation by either D6PK or PID when compared to wild type PIN3 (Figure 7-15). This could of course indicate that S262 is not important for PIN3 activation and that different residues are targeted by the kinases in PIN3. However, it is also possible that subtle differences in the affinities of the kinases towards the mutant could not be detected under the given experimental conditions. Therefore, a more detailed analysis including the variation of protein and substrate concentrations in the oocytes as well as the analysis of further mutants will be required in the future.

The different impacts of the S271A and the S231A/S252A/S290A mutations in PIN1 on D6PK and PID could suggest that activation by D6PK is mediated preferentially via phosphorylation of S271A whereas PID favors the serines in the TPRXS(N/S) motifs, thereby regulating polarity as well as activity. Additional factors that are not present in the heterologous system could further increase this specificity in plants. Such flexibility in the activation would provide a basis for a dynamic regulation of PIN1 mediated auxin transport. Considering the co-localization of D6PK and PINs at basal cell faces in the plant, it is tempting to speculate that D6PK-mediated phosphorylation plays a role in the activation of basally localized PINs while phosphorylation by PID is more important for apical targeting and activation of apically localized carriers. However, if D6PK phosphorylates the PID target sites that determine apical targeting also in plants, protein-protein interactions between PINs and the D6PK or other proteins might contribute to the retention of the phosphorylated activated PIN at the basal cell face.

3 Phytohormone responses during vascular development in nematode induced feeding sites

The majority of the data included in this chapter are presented in the following publication: Absmanner, B., Stadler, R. and Hammes, U.Z. (2013): Phloem development in nematode-induced feeding sites: The implications of auxin and cytokinin. Front. Plant Sci. 4:241.

3.1 Introduction

3.1.1 Plant parasitic nematodes

Plant parasitic nematodes are among the most destructive plant pathogens and represent a devastating pest worldwide. More than 4000 species have been described so far (Decraemer and Hunt, 2006). As they affect a wide range of economically relevant crops, among them soybean, potato and cotton, nematodes are held responsible for enormous yield losses in agriculture each year (Sasser, 1980; Barker and Koenning, 1998).

All plant parasitic nematodes are obligate biotrophic pathogens, which means that they rely on living cells as an exclusive nutrient source. Depending on the feeding strategy they use, the nematodes are divided into migratory and sedentary as well as ecto- and endoparasitic species (Wyss, 1997; Hussey and Grundler, 1998). Most of the damage in agriculture is caused by sendentary endoparasitic species that feed within roots, thereby establishing an intimate and complex relation with their host. By manipulating its developmental program, they induce the redifferentiation of root cells into specialized feeding sites from which they withdraw all the nutrients required for the completion of their life cycle (Bird, 1996). These feeding sites, albeit differing in genesis and structure depending on the nematode species that induces them, have the common feature that they represent induced terminal sink tissues from which the plant loses photoassimiates (Jones and Northcote, 1972; McClure, 1977).

Two major groups of sedentary endoparasitic nematodes can be distinguished based on characteristic differences in their parasitic cycles and in the type of feeding site they induce: Cyst nematodes which include the genera *Heterodera* and *Globodera* and root knot nematodes represented by the genus *Meloidogyne*.

The beet cyst nematode *Heterodera schachtii* and the southern root knot nematode *Meloidogyne incognita* belong to the best studied representatives within these two groups. One reason for this is of course their enormous economical relevance. *M. incognita* is even considered the most damaging of all crop pathogens (Trudgill and Blok, 2001). Beyond that, the popularity of *H. schachtii* and *M. incognita* as research objects is also due to the fact that both of them can infest *Arabidopsis thaliana* which makes them very suitable model organisms to study host-nematode interactions on a molecular level (Sijmons *et al.*, 1991).

3.1.2 Life cycles of cyst and root knot nematodes

Schematic overviews of the life cycles of cyst nematodes and root knot nematodes are depicted in Figure 3-1 A and C, respectively. In both cases, non-feeding second-stage juveniles (J2) hatch in the soil following a first molt inside the egg. The J2 then penetrate their host's root at the tip, preferentially in the elongation zone and migrate intracellularly (cyst nematodes) or intercellularly (root knot nematodes) towards the vascular cylinder (Wyss *et al.*, 1992; Golinowski *et al.*, 1996). Here, they induce the formation of feeding sites, so called syncytia in the case of cyst nematodes and giant cells in the case of root knot nematodes. With the onset of feeding, the nematodes become sedentary and undergo three more molts before they reach maturity. Males of cyst nematodes leave the root after the last molt and fertilze females which then start to produce hundreds of eggs. After egg production is finished, the female dies and its body forms the robust protective cyst that gave this group of nematodes its name (see Figure 3-1 B). Most of the root knot nematode species - among them *M. incognita* - are parthenogenic and males only develop under unfavorable environmental conditions (Trudgill, 1972). When females start to produce eggs, they are deposited in a proteinacous mass, the so called egg sac, at the surface of the root (see Figure 3-1 D).
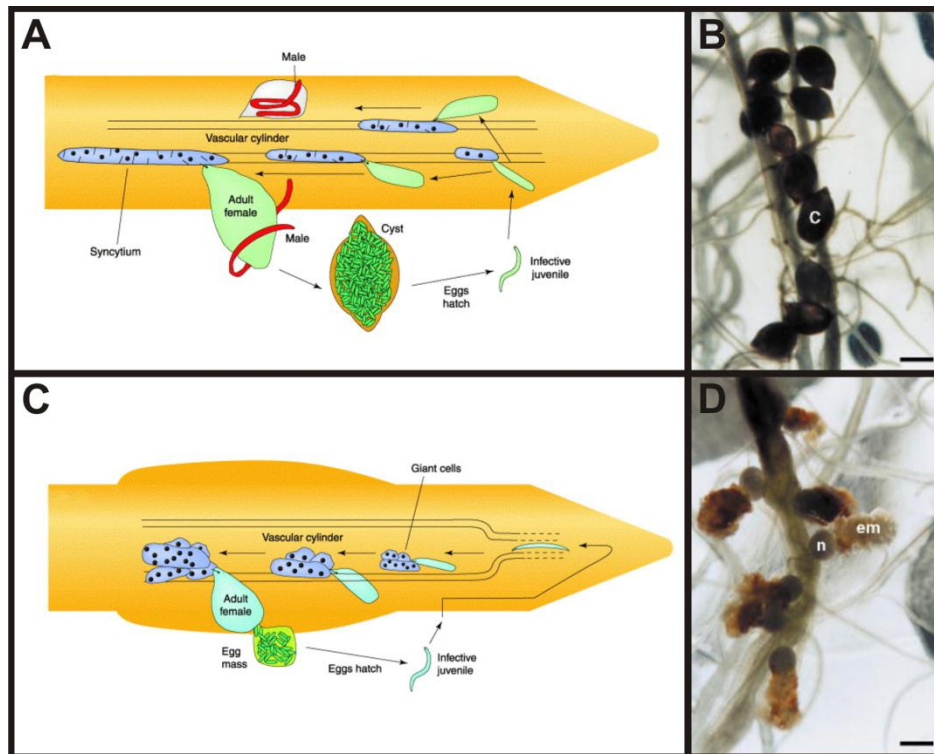
Figure 3-1 Infection of plant roots by sedentary endoparasitic cyst nematodes (A,B) and root knot nematodes (B,C). (A) Schematic overview of the life cycle of a cyst nematode. (B) *A. thaliana* roots infected by the cyst nematode *H. schachtii*. Mature females develop into brown cysts. (C) Schematic overview of the life cycle of a root knot nematode. (D) *A. thaliana* roots infected by the root knot nematode *M. incognita*. Mature females produce egg masses. Scale bars in (B) and (D) represent 500 μm. Pictures taken from Gheysen and Fenoll (2002), Williamson and Gleason (2003).

3.1.3 Sedentary nematodes induce the formation of specialized feeding sites

In order to complete their life cycle, successful establishment and maintainance of the feeding site is essential. The initial trigger for feeding site development most likely comes from effector molecules that are secreted by the nematode from specialized esophageal glands via their stylet (Davis *et al.*, 2000). In case of *H. schachtii*, one initial cell, usually a procambial or pericycle cell, is selected and serves as a starting point for the development of the syncytium which in turn is formed by cell wall breakdowns and subsequent fusion of up to 200 neighboring cells within the vascular cylinder (Figure 3-2 A, Golinowski *et al.*, 1996; Golinowski *et al.*, 1997). *M. incogntia* on the other hand selects a couple of procambial cells - usually 4 to 8 - in the differentiation zone of the root. These cells then develop into giant cells from which the nematode alternately feeds. In contrast to the cyst nematode induced

syncytia, no fusion of neighbouring cells occurs, instead the cells determined to become giant cells retain their single cell identity throughout their lifetime. The developing giant cells increase enormously in size and undergo dramatic morphological changes. They reenter the cell cycle and go through multiple rounds of mitosis without cytokinesis, resulting in more than 100 nuclei per giant cell. Also cells surrounding the developing giant cells start to proliferate extensively, leading to swelling of the root and thereby to the formation of the characteristic gall (Figure 3-2 B, Jones and Payne, 1978; Bleve-Zacheo and Melillo, 1997). Dense cytoplasm that is packed with organelles and nuclei which are enlarged after undergoing endoreduplication as well as the lack of a central vacuole are further characteristics of mature giant cells as well as of syncytia and reflect the high metabolic acticivity that is observed within the feeding cells.
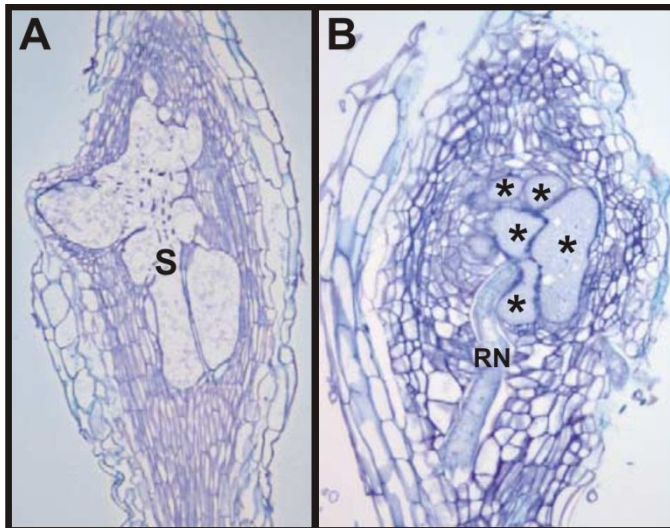
Figure 3-2 Longitudinal sections through *A. thaliana* roots infected with (A) *H. schachtii* or (B) *M. incognita* 5 dai. S: Syncytium. RN: root knot nematode. Asterisks in (B) indicate giant cells. Pictures taken from de Almeida Engler *et al.* (2005)

3.1.4 The role of phytohormones in early events of feeding site establishment and development

The initial steps of feeding site establishment and the role of phytohormones in this process have received a lot of attention. As early as in the 1960s auxin-like compounds were detected in feeding sites induced by *Meloidogyne javanica* (Balasubramanian and Rangaswami, 1962; Bird, 1962) and in a number of publications it was even claimed that the nematodes themselves can produce and secrete auxin or at least precursor molecules (Bird, 1962; Yu and Viglierchio, 1964; Johnson and Viglierchio, 1969). Nonetheless, later studies

mainly argue that the manipulation of the host's auxin transport machinery plays an important role in feeding site initiation (Goverse *et al.*, 2000; Mazarei *et al.*, 2003; Grunewald *et al.*, 2009a). Auxin is known to have crucial functions in organogenesis, for example in the formation of lateral roots where the establishment of an auxin maximum in a pericycle founder cell leads to the first asymmetric cell division that finally results in the outgrowth of the new organ (Peret *et al.*, 2009). Sedentary endoparasitic nematodes *de facto* induce the formation of a new organ – the feeding site – and it is therefore not surprising that auxin is crucial for its development. The auxin influx carrier AUX1 is strongly expressed in feeding sites (Mazarei *et al.*, 2003) and also PIN proteins show altered expression patterns in *H. schachtii* infected roots compared to control roots (Grunewald *et al.*, 2009b). Accordingly, mutants with defects in auxin signaling and transport were shown to be poor hosts for nematodes. The tomato mutant *dgt* which is characterized by strongly reduced sensitivity to auxin is almost completely resistant against cyst nematodes and also in a number of *A. thaliana* mutants a reduction in infection or developmental defects of the nematodes were observed (Goverse *et al.*, 2000; Grunewald *et al.*, 2009a). Enhanced auxin response in early feeding sites of *M. incognita, M. javanica* and *H. schachtii* has been visualized using reporter constructs. The first elevation in the auxin response was observed in the very young giant cells and syncytia themselves, but this response was transient and faded after the first days of infection. Auxin response in these early stages was linked to initial steps of feeding site formation like cell cycle activation (see 3.1.3). In case of *H. schachtii* it was described that the response was shifted towards the periphery of the syncytium about 5 dai (Hutangura *et al.*, 1999; Karczmarek *et al.*, 2004; Grunewald *et al.*, 2009a). It was speculated that the auxin response in these cells primes them for the following integration into the syncytium (Grunewald *et al.*, 2009a). However, not all of the cells surrounding the developing syncytium are really incorporated into the feeding site. Rather, they fulfill functions in the nutrient transports towards and into the feeding site as will be described in chapter 3.1.5. Therefore, other functions of the auxin response in the periphery of the feeding sites are very well possible.

Although auxin has received most of the attention, other phytohormones were implicated in feeding site development as well, among them ethylene and cytokinins.

Ethlyene overproducing *A. thaliana* mutants show hyperinfection and enhanced female development when exposed to *H. schachtii*. Presumably, increased ethylene production

leads to activation of cell wall degrading enzymes – comparable to what is happening during fruit ripening – and thereby to a more effective expansion of the syncytium (Goverse *et al.*, 2000). No convincing evidence for ethylene dependency of root knot development was found so far, highlighting the fact that syncytia and giant cells differ in their ontogenesis and that therefore the impact of different phytohormones may vary.

Cytokinins are generally considered to be essential for plant cell division, most likely through their influence on the cell cycle (Redig *et al.*, 1996; Zhang *et al.*, 1996). As activation of cell cycle genes is a crucial step in feeding site establishment (reviewed in Goverse *et al*., 2000a), a function of cytokinins in the early events is very likely. Consequently, enhanced cytokinin response upon infection with *M. incognita* was found in *L. japonicus* and in tomato using promoter activity of an A-type cytokinin response regulator as a reporter. Additionally, it was described in this study that plants with reduced cytokinin levels exhibit enhanced resistance to *M. incognita* (Lohar *et al.*, 2004). As in the case of auxin it was also shown that both cyst and root knot nematode exsudates contain cytokinins (Bird and Loveys, 1980; De Meutter *et al.*, 2003), although it is not known wether this is of relevance for the host-parasite interaction.

Taken together, it is very well accepted that during the initiation of both cyst and root knot induced feeding sites developmental programs of the host are manipulated and that phytohormones play a crucial role in this process.

3.1.5 Nutrient supply and vascularization of feeding sites

Once the feeding site is initiated, it develops into a strong sink tissue from which nutrients are lost to the parasite. However, the way how the nutrients are transported towards and into the feeding sites differ considerabely. Giant cells were shown to be symplastically isolated from the surrounding tissue (Hoth *et al.*, 2008). This means that nutrients have to be transported into the giant cells via the plasma membrane. Remodeled cell walls that form extensive ingrowths, consequently leading to a considerably increased cell surface have been described in giant cells long time ago (Jones and Northcote, 1972; Jones, 1981). Such cell wall ingrowths are a feature typically found in transfer cells where the enlarged cell surface is associated with the distribution of nutrients over the plasma membrane (Offler *et al.*, 2002). Additionally, transport proteins were shown to be highly regulated in giant cells and mutations in certain transporters cause severe phenotypes in nematode development

(Hammes *et al.*, 2005; Marella *et al.*, 2013). When for example mutants lacking the amino acid transporters AAP3 or AAP6 were infected with *M. incognita*, significantly more males than females developed (Marella *et al.*, 2013). This reflects the poor nutritional status that the nematodes have to cope with in these plants and shows that transporter-mediated loading of nutrients into the giant cells is an important process during feeding of the nematode. Assimilates have to be transported from photosynthesizing sources towards the feeding sites and this transport is mediated by the vascular tissue. Consequently, also the vasculature surrounding the giant cells undergoes tremendous changes. Giant cell development goes along with the formation of new xylem vessels which appear distorted and are often not connected to each other (Fester *et al.*, 2008). The most remarkable changes however are observed in the phloem. New phloem tissue is formed *de novo* around the giant cells and this phloem exhibits unique properties. Using the *AtSUC2* promoter as a marker for companion cells, Hoth *et al.* (2008) could show that companion cells are still present in the early stages of giant cell development but are absent in mature root knots. It is not known whether the companion cells are consumed or lose their identity and dedifferentiate. Lacking companion cells, the phloem in the root knots consists exclusively of cells that clearly possess sieve element characteristics. Strikingly, these cells often remain nucleate. They are also heavily interconnected by plasmodesmata to ensure nutrient flow from cell to cell in this phloem network that surrounds the giant cells (Hoth *et al.*, 2008). How the unloading of assimilates into the apoplast is facilitated remains elusive. Possible mechanisms include exocytosis or yet to be identified transporters.

In cyst nematodes, the situation is completely different. It was long thought that syncytia – like giant cells – are symplastically isolated (Bockenhoff *et al.*, 1996; Golinowski *et al.*, 1996; Juergensen *et al.*, 2003). Yet, this concept was clearly disproved in recent studies where it was shown that soluble GFP can diffuse from the surrounding phloem into the syncytium and that a symplastic connection between syncytia and phloem is established by the formation of functional secondary plasmodesmata (Hoth *et al.*, 2005; Hoth *et al.*, 2008). The fact that to date there is no evidence for elevated accumulation of transporters in syncytial membranes also points towards symplastic diffusion as the dominant way of assimilate flow into syncytia. As it is the case in root knots, new phloem tissue is formed also around syncytia. In contrast to the phloem found around giant cells, companion cells are present and induced in cyst nematode induced feeding sites throughout the lifetime of the

syncytium. However, compared to uninfected roots the ratio of companion cells to sieve elements is strongly shifted towards sieve elements (Hoth *et al.*, 2005). This is characteristic for unloading phloem, emphasizing the status of the syncytium as a sink tissue that is supplied with nutrients via the vasculature.

3.1.6 Aims of the project

Auxin has been implicated in the successful establishment of nematode induced feeding sites. One aim of this work was to monitor auxin response during the infection cycle of both root knot nematodes and cyst nematodes and to identify and compare the cell types that respond to the phytohormone, especially in those developmental stages where the vascularization of the feeding site occurs. Therefore, the synthetic auxin responsive DR5 promoter was used. P_{DR5}:ER-GFP (Ottenschläger *et al.*, 2003) Arabidopsis plants should be infected with nematodes and GFP fluorescence should be monitored. Auxin responsive tissues in and around the feeding sites should be identified by immunohistochemistry. More insight into the role of auxin in feeding site vascularization should be gained by comparing auxin response in nematode induced feeding sites in the wild type background to the situation in mutants with defects in auxin transport and signaling. Both auxin and cytokinin are important determinants of vascular tissue specification. Therefore, monitoring cytokinin response using a comparable approach as for auxin was a further goal of this work. Hence, plants expressing ER-GFP under the control of the synthetic cytokinin responsive TCS promoter (P_{TCS}:ER-GFP, Müller and Sheen, 2008) should be used to identify cytokinin responsive cells in nematode infected roots. Detailed analysis and comparison of auxin and cytokinin response will allow conclusions about a possible function of the two phytohormones in the specification of the vascular tissues around the feeding sites.

The phloem around giant cells exhibits unique properties and is clearly different from the phloem around syncytia or the phloem that is typically found in roots. More insight about the identity of this phloem should be gained by checking for the expression of APL, a regulator of phloem identity (Bonke *et al.*, 2003), in *M. incognita* induced root knots.

3.2 Results

3.2.1 Identification of auxin responsive cells in nematode infected roots

In order to investigate the role of auxin during vascularization of nematode induced feeding sites, auxin response in infected tissues was monitored and responsive cells were identified. For visualization of auxin response, the synthetic promoter element DR5 was used. DR5 consists of 9 inverted repeats of an 11 bp sequence which includes the auxin responsive element TGTCTC and a 46 bp CaMV35S minimal promoter element. This promoter sequence is recognized and activated by auxin response factors (ARFs) and allows the detection of early auxin response when driving the expression of a reporter gene. In this work, a well documented line in which the DR5 promoter drives the expression of ER-localized GFP (P_{DR5}:ER-GFP, Ottenschläger *et al.*, 2003) was used. Additional data were obtained using a P_{DR5}:GUS line (Ulmasov *et al.*, 1997).

3.2.1.1 Auxin response in uninfected roots

P_{DR5}:ER-GFP plants that were to be used for infection with nematodes were grown for two weeks on petri dishes containing Gamborg medium (see 7.3.2). Before infection, GFP fluorescence was examined in uninfected roots of this age (Figure 3-3). Most of the previous studies in which the DR5 promoter was used in the root context were carried out using very young seedlings. Therefore, it was essential to check the expression pattern of GFP also in older roots as this allows better comparison of auxin response in uninfected roots and in nematode induced feeding sites. In agreement with previous data, fluorescence maxima were observed in the distal cells of the root tip (Figure 3-3 A and B) and in lateral root primordia (Figure 3-3 C and D, Sabatini *et al.*, 1999; Benkova *et al.*, 2003; Ottenschläger *et al.*, 2003). Additionally, in the differentiated parts of the root, fluorescence was always detectable in two distinct cell files within the stele (Figure 3-3 D and E).

In order to identify the cell type that displayed the auxin response in the stele, immunolocalizations on roots sections of different distances from the root tip were performed (Figure 3-4). For this purpose, the roots were embedded, sectioned and decorated with antibodies as described in 7.6.3. Sieve elements were labeled using the previously described monoclonal RS6 antiserum (Khan *et al.*, 2007). Auxin responsive cells
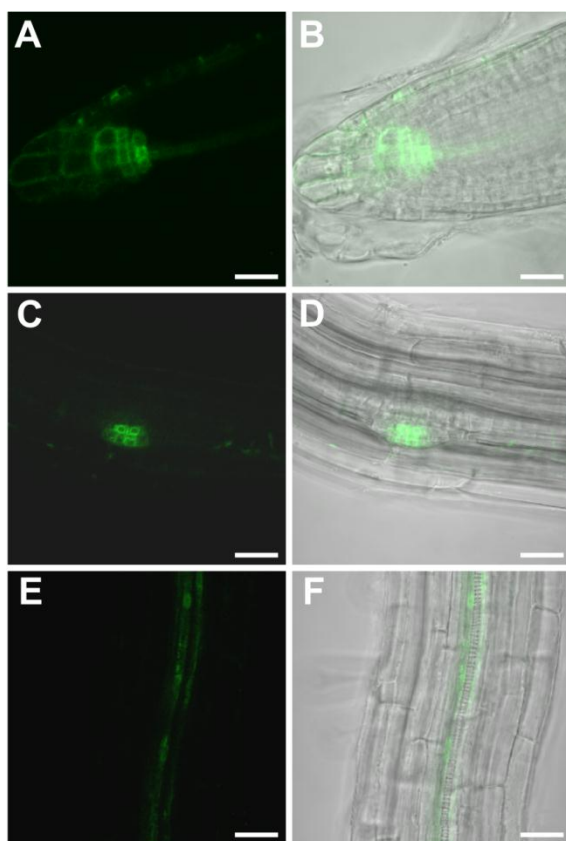
Figure 3-3 GFP fluorescence in uninfected roots of two-week old P_{DR5}:ER-GFP Arabidopsis plants. Fluorescence is observed in auxin responsive tissues. (A) and (B) Root tip (A) GFP fluorescence (B) Overlay of GFP fluorescence and bright field image. (C) and (D) Lateral root primordium (C) GFP fluorescence (D) Overlay of GFP fluorescence and bright field image. Within the vasculature (E) and (F) fluorescence is observed in two cell files. (E) GFP fluorescence (F) Overlay of GFP fluorescence and bright field image. Scale bars represent 20 µm.

were identified using a polyclonal GFP antiserum. Figure 3-4 A-D shows an immunolocalization of the RS6 epitope and GFP on a root section localized about 2.5 cm proximal of the root tip. In this part of the root, primary phloem and xylem elements are already fully differentiated. Auxin response, shown in green, occurred in cells directly adjacent to a sieve element which is labeled in red (Figure 3-4 B-D shows one of the two phloem poles). In older parts of the root the pattern observed was very similar (Figure 3-4 E-H). Auxin responsive cells were found in direct vicinity to the sieve elements labeled by the RS6 antiserum. The position of the auxin responsive cells with respect to the sieve elements as well as to the xylem clearly identifies them as companion cells. Taken together, these data show that a constitutive auxin response takes place in the fully differentiated parts of a two week old Arabidopsis root. The auxin response occurs within the phloem in cells directly adjacent to sieve elements which are companion cells.
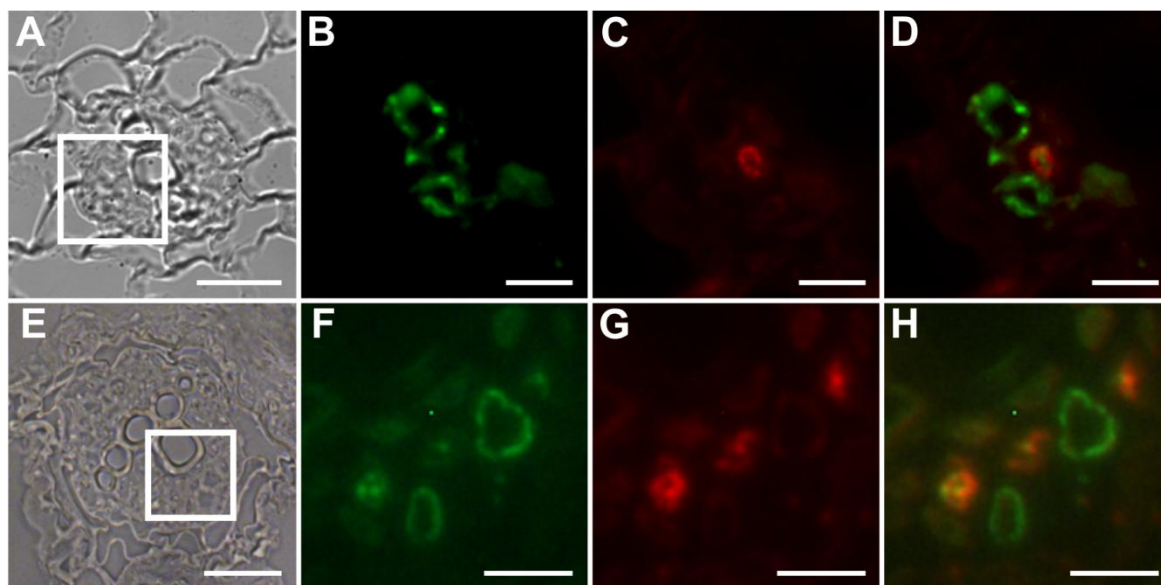
Figure 3-4 Identification of auxin responsive cells by immunohistochemistry in sections through two-week old roots of *P_DR5:ER-GFP* Arabidopsis plants. (A-D) Section through a young part of the root approximately 2.5 cm above the root tip. (E-H) Section through an older part of the root. (A) and (E) Brightfield images. (B-D) and (F-H) are details of (A) and (E), respectively, indicated by the square. (B) and (F) Auxin responsive cells decorated by a GFP antibody. Size and position is consistent with a companion cell identity. Green color results from a Cy2-conjugated secondary antibody. (C) and (G) Cells decorated with the sieve element marker antiserum RS6. Red color results from a Cy3-conjugated secondary antibody. (D) and (H) are overlays of (B) and (C) and of (F) and (G), respectively. Scale bars represent 20 μm in (A) and (E) and 5 μm in (B-D) and (F-H).

3.2.1.2   Auxin response in *M. incognita* infected roots

To identify auxin responsive cells within *M. incognita* induced tissues, GFP fluorescence in infected *P_DR5:ER-GFP* plants was monitored throughout the development of the root knots (Figure 3-5). Therefore, plants were infected with freshly hatched second-stage juveniles as described in 7.4.4. In noninfected parts of the root, above and below galls, the fluorescence was seen in two cell files in the vasculature as described above (3.2.1.1). At the beginning of the observation at 7 dai fluorescence was detected surrounding an area which displayed no fluorescence (asterisk in Figure 3-5 A). Approximately 14 dai (Figure 3-5 C and D) and 17 dai (Figure 3-5 E and F) fluorescence was observed in a net-like pattern around fluorescence-free areas (asterisks in Figure 3-5 C and E). These areas without a GFP signal are located in the position of giant cells. In fully mature and differentiated root knots the fluorescence pattern was still similar with no detectable signal at giant cell position.
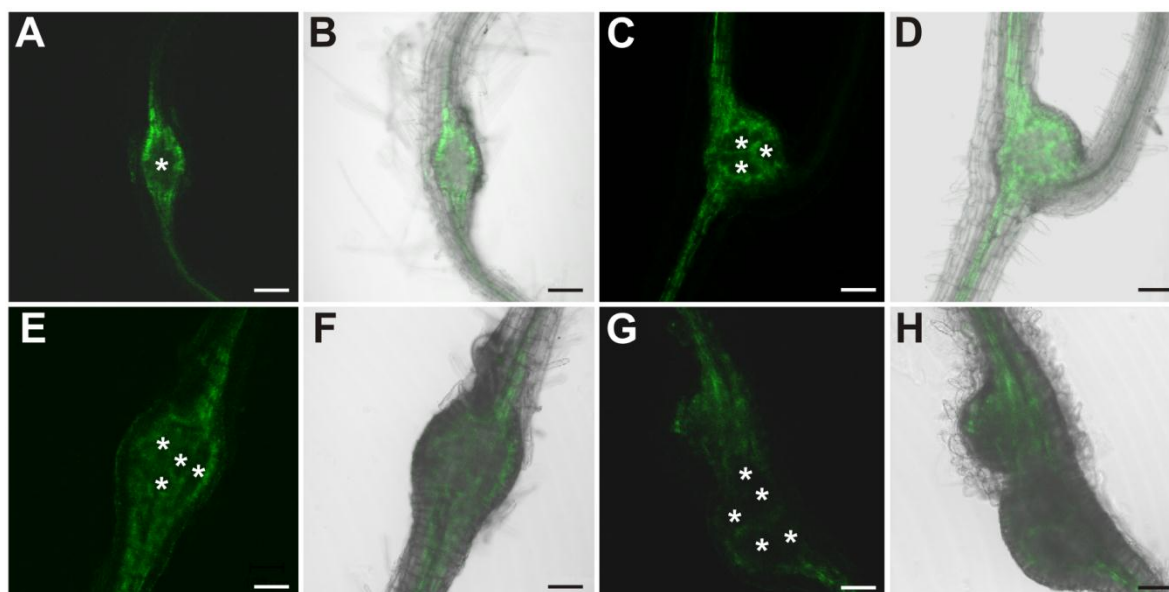
Figure 3-5 GFP fluorescence in roots of *P_DR5:ER-GFP* Arabidopsis plants infected with *M. incognita*. Fluorescence is observed in auxin responsive tissues. Note the net-like structure of the tissue consisting of cells displaying GFP fluorescence. (A), (C), (E) and (G) GFP fluorescence. (B), (D), (F) and (H) Overlay of GFP fluorescence and bright field image. (A) and (B) 7 dai, (C) and (D) 14 dai (E) and (F) 17 dai, (G) and (H) 21 dai. Scale bars represent 100 μm.

However, fluorescence was generally weaker (Figure 3-5 G and H).

To confirm these results and also to increase sensitivity, plants which contained the DR5 promoter fused to the GUS gene (*P_DR5::GUS*, Ulmasov *et al.*, 1997) were infected and stained for GUS activity as described in 7.6.1. The data obtained from this experiment were in accordance with the observations made in *P_DR5:ER-GFP* plants (Figure 3-5). In uninfected parts of the plants, the typical auxin maxima at the root tip and in lateral root primordia were observed (Figure 3-6 A). If staining time was extended, staining in the vasculature of the mature root was also visible (data not shown). Strong GUS staining was found in root knots 7 dai (Figure 3-6 B) and 17 dai (Figure 3-6 C). At the later stage, giant cells could be clearly identified visually and did not show GUS staining (asterisks in Figure 3-6 C).

Taken together, these data suggest that auxin response in root knots takes place in cells surrounding the giant cells and persists throughout the development of the nematode within the root. No signal was detected in the giant cells, although it has to be pointed out that the very early events of feeding site establishment for whom auxin response in giant cells was reported (Karczmarek *et al.*, 2004; Grunewald *et al.*, 2009a) were not considered in this work.
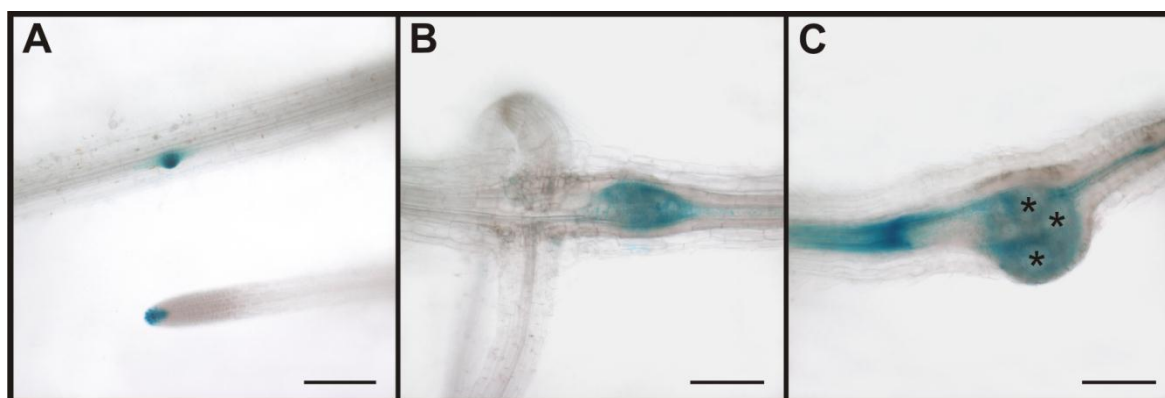
Figure 3-6 Auxin response visualized by GUS-staining in *M. incognita* infected P*DR5*:GUS plant roots. (A) Uninfected parts of the root displayed the typical staining pattern with auxin maxima in the root tip and in lateral root primordia. The tissue within the root-knot 7 dai (B) and 17 dai (C) displayed an auxin response. Giant cells (asterisks in C) were not stained. Scale bars represent 200 µm.

The expression pattern of ER-GFP and GUS under the control of the DR5 promoter was strongly similar to the pattern of GFP fluorescence that was found by (Hoth *et al.*, 2008) in root knots when soluble GFP was expressed under the control of the companion cell specific SUC2 promoter. In infected P*SUC2*:GFP plants, GFP diffused from the companion cells, which themselves are absent in mature root knots, into the protophloem-like cells surrounding the giant cells. In order to determine the earliest time point at which the net-like pattern resulting from GFP diffusion becomes apparent first in P*SUC2*:GPF and to directly compare it to the expression pattern in infected P*Dr5*:ER-GFP roots, GFP fluorescence was monitored in both lines after infection with *M. incognita (*Figure 3-7*)*. At 7 dai, fluorescence in P*SUC2*:GFP plants was still clearly limited to two strands (Figure 3-7 A and B) indicating that the plasmodesmata allowing for the diffusion of GFP had not yet been formed. In contrast, the GFP expression domain in P*DR5*:ER-GFP plants at 7 dai was already broader and spread to a network of cells within the growing root knot (Figure 3-7 E and F). At 14 dai, the plasmodesmata enabling the GFP to diffuse from the companion cells into the cells surrounding the giant cells had formed and GFP fluorescence in P*SUC2*:GFP plants was seen in the typical net like pattern (Figure 3-7 C and D). The pattern observed in P*DR5*:ER-GFP plants at 14 dai looked very similar (Figure 3-7 G and H). These data indicate that the cells that will eventually form the network of symplastically connected phloem elements surrounding the giant cells experience an auxin response before the onset of the differentiation process and also before they become connected to each other via secondary plasmodesmata.
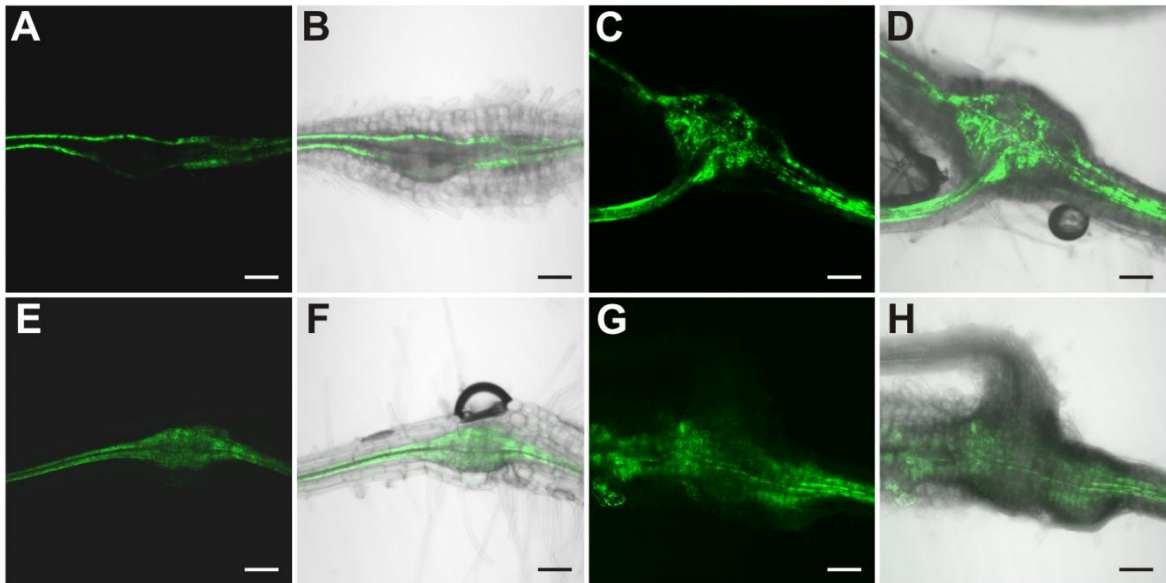
Figure 3-7 Comparison of GFP fluorescence in *M. incognita* induced root-knots in P_{SUC2}:*GFP* plants and in P_{DR5}::*ER-GFP* plants. (A-D) P_{SUC2}:*GFP* 7 dai (A and B) and 14 dai (C and D). (E-H) P_{DR5}:*ER-GFP* at 7 dai (E and F) and 14 dai (G and H). At 7 dai, GFP-fluorescence is limited to the companion cells in A and B but present in more cells in E and F. At 14 dai, GFP fluorescence is seen in a net-like pattern in both a P_{SUC2}:*GFP* (C and D) and a P_{DR5}:*ER-GFP* plant (G and H). (A,C,E,G) GFP fluorescence, (B,D,F,H) Overlay of GFP fluorescence and bright field image. Scale bars represent 100 µm.

In order to confirm these findings on a cellular level, immunohistochemical experiments were performed (Figure 3-8). Root knots of P_{DR5}:*ER-GFP* were embedded, sectioned and decorated with antibodies as described in 7.6.3. Auxin responsive cells were identified using a GFP antiserum and sieve elements were labeled with the monoclonal RS6 antiserum. Figure 3-8 A-D shows a section through a root knot 10 dai which corresponds to a time point where symplastic connection of the cells around the giant cells did not yet take place. Giant cells, marked by asterisks, can easily be identified. A ring of cells around the giant cells was labeled by the GFP antibody (Figure 3-8 B). At two opposite poles of the root knot, most likely at the position of the original phloem poles of the root, populations with elevated numbers of RS6 positive cells were detected (Figure 3-8 C). Most, but not all of these RS6 positive cells were also recognized by the GFP antibody (Figure 3-8 D). At later stages of root knot development, a different situation was observed. Figure 3-8 E-L show sections through a root knot 17 dai. At this time point, the giant cells are surrounded by a high number of sieve elements, labeled by the RS6 antiserum (Figure 3-8 G and K). This is also consistent with previous findings (Hoth *et al.*, 2008). Surprisingly, almost all of the RS6 positive cells
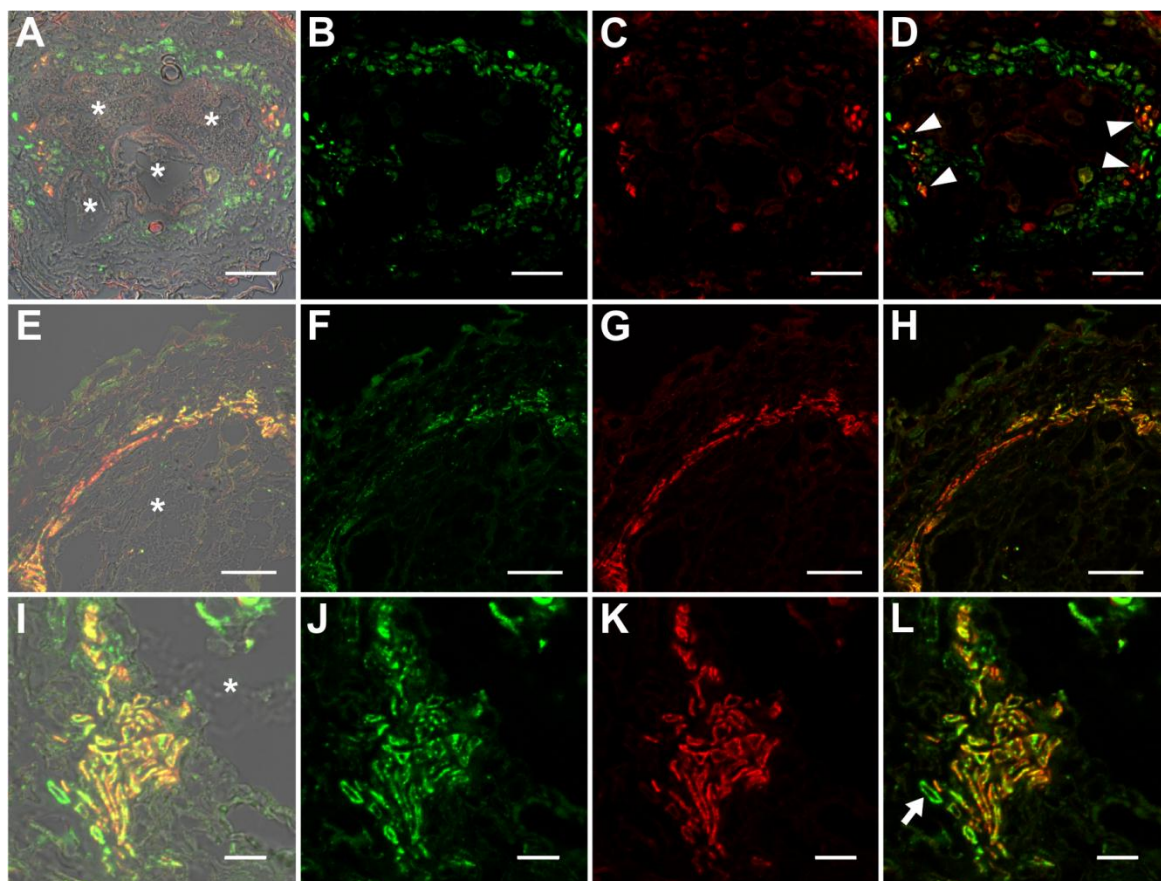
Figure 3-8 Identification of auxin responsive cells by immunohistochemistry in sections through root knots of P_{DR5}:ER-GFP Arabidopsis plants infected with *M. incognita*. (A-D) Section through a root knot 10 dai. (E-H) Section through a root knot 17 dai. (I-L) Detail of a section through a root-knot 17 dai. (A), (E) and (I) Bright field images. (B), (F) and (J) Auxin responsive cells decorated by a GFP antibody. Green color results from a Cy2-conjugated secondary antibody. (C), (G) and (K) Cells decorated with the sieve element marker antiserum RS6. Red color results from a Cy3-conjugated secondary antibody. (D), (H) and (L) are overlays of (B) and (C), (F) and (G) and (J) and (K), respectively. Asterisks in (A), (E) and (I) mark giant cells. Arrow heads in (D) point to RS6-positive cells located at two poles within the stele, probably the location of the initial phloem poles. Arrow in (L) points to the rarely observed cells that are exclusively labeled by the GFP antiserum. Scale bars represent 20 µm in (A-H) and 10 µm in (I-L).

were also labeled by the GFP antibody (Figure 3-8 F, J and H,L), indicating that all cells that differentiate into sieve elements in the root knot display an auxin response.

The described observations suggest that cells surrounding the root knot experience an auxin response and subsequently differentiate into sieve elements. The auxin response also persists after the cells start to express the sieve element marker. Cells that were exclusively labeled by the GFP antiserum were only rarely observed in root knots at 17 dai. One example is shown in Figure 3-8 L (arrow). This indicates that at this time point the formation of the

sieve element network is completed. A GFP signal was never detected in the giant cells themselves.

To confirm that the RS6 promotor is active throughout the development of the root knot, a P_{RS6}:*GUS* transgenic Arabidopsis line was infected with *M. incognita* second-stage juveniles. Uninfected roots and root knots were collected and stained for GUS activity as described in 7.6.1 (Figure 3-9). In the developing root knot, the promoter activity of RS6 mirrors the formation of the symplastic domain specified by the diffusion of GFP. Figure 3-9 A and B show the activity of the RS6 promoter in the vasculature of uninfected roots as has been described before by Werner (2011). In a very young developing root knot at 5 dai, this staining pattern was still conserved (Figure 3-9 C). At 10 dai the staining appeared diffuse and extended from the phloem poles (Figure 3-9 D). This observation is in accordance with immunolocalizations performed on a root knot of the same age where rising populations of RS6 positive cells were observed near the original phloem poles (Figure 3-8 A-D). Finally, at 17 dai, the GUS staining pattern in the P_{RS6}:*GUS* plants displayed the typical net-like pattern surrounding the giant cells (Figure 3-9 D). This is one more indication that cells around the giant cells – after experiencing an auxin response – start to express the RS6 gene.
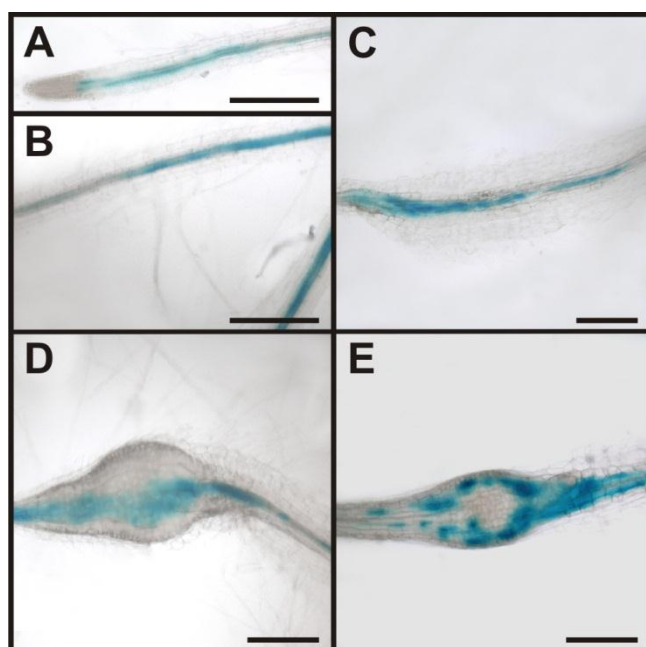
Figure 3-9 Activity of the RS6 promoter vuisualized by GUS staining in P_{RS6}:*GUS* plants. (A) and (B) Control roots. Staining is observed throughout the stele. (C-D) Root knots induced by *M. incognita* infection. (C) Root knot 5 dai. Staining is still limited to the stele. (D) Root knot 10 dai. The staining is spreading out but still in the position of the original phloem pole. (E) Mature root knot 17 dai. Staining is observed around the giant cells. Scale bars represent 200 µm

3.2.1.3 Auxin response in mutants with defects in auxin transport and signaling was not affected in root knots

In order to get more insights into the function of auxin in the development of new phloem in root knots, auxin response in mutants with defects in transport and signaling was examined. Mutants with very strong defects in this processes display severely disturbed root development and drastically impaired lateral root formation. The auxin insensitive tomato mutant *dgt* was even reported to be totally resistant against cyst nematode infection. Therefore, mutants were used for which it was shown that they can still be infected at least with cyst nematodes (Goverse *et al.*, 2000). Figure 3-10 shows the tested mutants two weeks after germination. The homozygous T-DNA insertion line *aux1* is a knock out mutant for the auxin influx carrier AUX1 (Yang *et al.*, 2006). *aux1* seedlings show a strong agravitropic phenotype as well as reduced lateral root formation compared to the wild type (Figure 3-10 A and B and Marchant *et al.*, 1999) . It has been shown that the AUX1 promotor is active in nematode induces feeding sites (Mazarei *et al.*, 2003). The double mutant *axr1-3/axr4-2* (Hobbie and Estelle, 1995) shows similar defects in root growth as the *aux1* mutant (Figure 3-10 C). In order to monitor auxin response in the mutants during infection with *M. incognita*, the P_{DR5}:ER-GFP line was introgressed into the mutant backgrounds. Figure 3-11 shows auxin response in roots knot in the *aux1* mutant background (Figure 3-11 A-H) and in the *axr1-3/axr4-2* double mutant background, respectively (Figure 3-11 I-P).
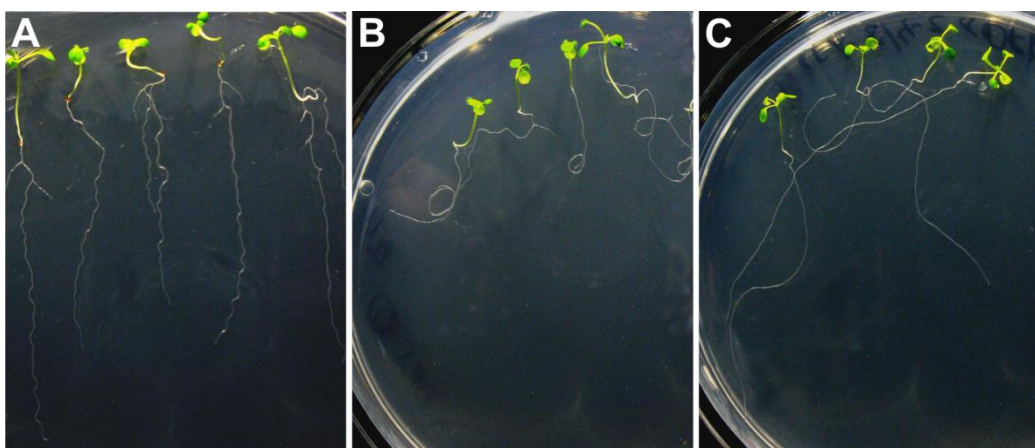
Figure 3-10 Mutants with defects in auxin transport and signaling show severe root phenotypes. Plants were grown on Ganborg medium for 2 weeks. (A) Col-0. The *aux1* mutant (B) and the *axr1-3/axr4-2* double mutant (C) show agravitropic root growth and reduced lateral root formation.

The fluorescence pattern observed was essentially indistinguishable from that of wild type plants. This was not only true for the pattern in the root knots, but also in root tips, lateral root primordia and the vasculature of two week old uninfected plants (data not shown). Furthermore, the females on these plants seemed to develop properly. Thus, the auxin response leading to phloem differentiation obviously occurred normally in the mutants studied here. However, it is noteworthy that – like in wild type - numerous lateral roots were
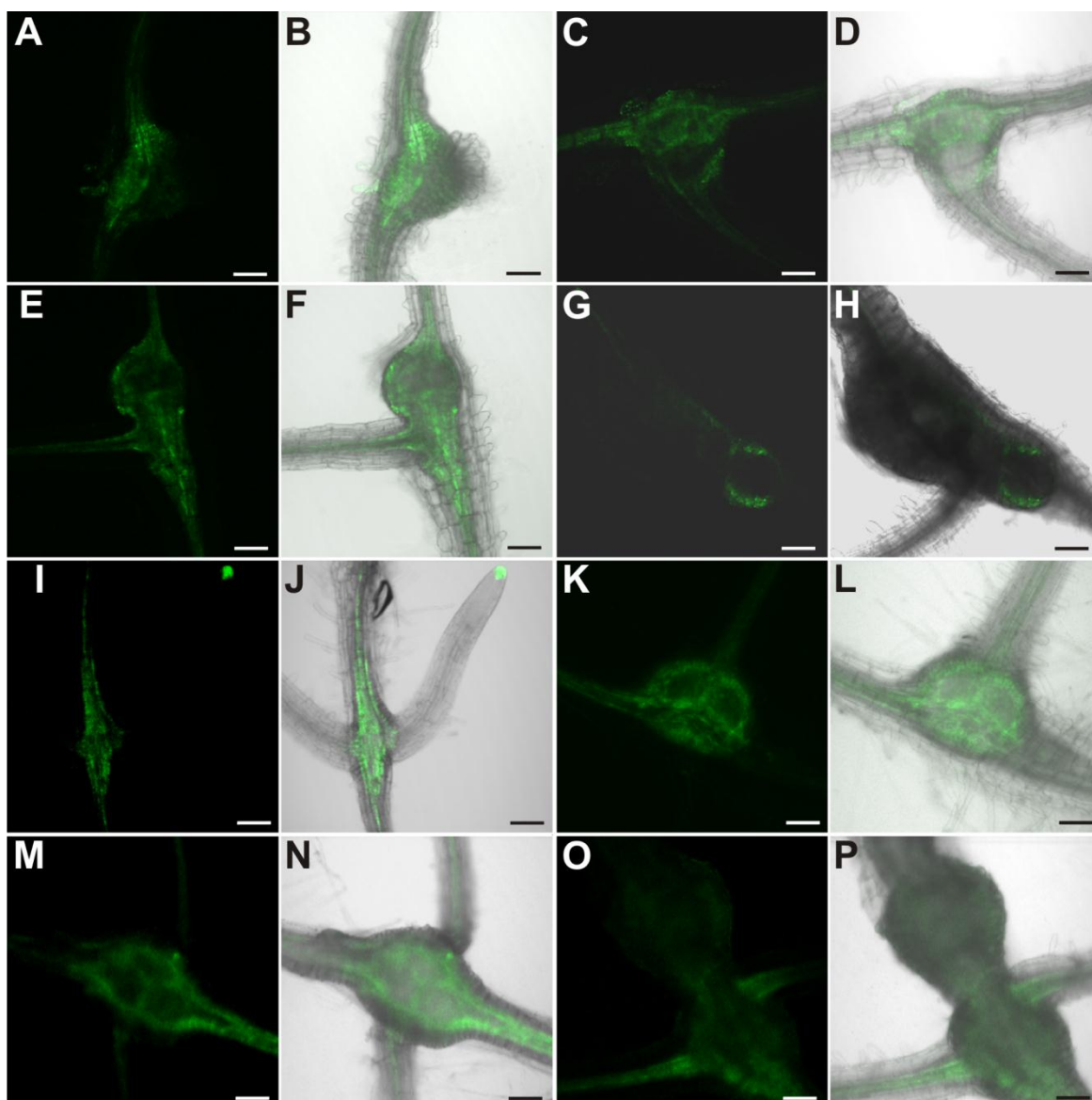
Figure 3-11 GFP fluorescence in *M. incognita*-induced root knots of plants expressing ER-GFP under control of the DR5 promoter in a mutant background. (A-H) *aux1* background, (I-P) *axr1-3/axr4-2* background. Fluorescence is observed in auxin responsive tissues in a seemingly unaltered pattern. (A), (C), (E), (G), (I), (K), (M) and (O) GFP fluorescence. (B), (D), (F), (H), (J), (L), (N) and (P) Overlay of GFP fluorescence and bright field image. (A), (B), (I) and (J) 7 dai. (C), (D), (K) and (L) 14 dai. (E), (F), (M) and (N) 17 dai. (G), (H), (O) and (P) 21 dai. Scale bars represent 100 µm.

observed associated with the root knots (Figure 3-11 D,F,H,J,L,N and P) despite the fact that the mutants show strongly reduced lateral root formation in general. This is also somewhat in contrast to the observation of (Goverse *et al.*, 2000) who described that upon infection of the *axr1-3/axr4-2* mutant with *H. schachtii*, no lateral roots at all were found associated with feeding sites.

3.2.1.4 Auxin response in *H. schachtii* infected roots

The phloem that is induced around syncytia displays completely different properties compared to the phloem that is formed around giant cells (see 3.1.5). Therefore, auxin response was also examined in *H. schachtii* infected roots in order to gain more insight into the specific role of auxin in the process of feeding site vascularization. For this purpose, two week old P_{DR5}:ER-GFP plants were infected with second-stage juveniles of *H. schachtii* as described in 7.5.2. Figure 3-12 A and B shows the fluorescence pattern in an infected root 14 dai. GFP signal was detected in the infected part of the root. Again, the pattern resembled that of infected P_{SUC2}:GFP plants (Hoth *et al.*, 2005; Hoth *et al.*, 2008). However, the syncytium itself appeared to be free of fluorescence. In order to ultimately identify the cells that responded to auxin, immunohistochemistry (7.6.3) using the GFP antiserum for identification of auxin responsive cells and the RS6 antiserum for labeling sieve elements was performed (Figure 3-12 C-F). Around the syncytium, sieve elements labeled by the RS6 antiserum were detected at an elevated number (Figure 3-12 E). Surprisingly, most of these RS6 positive cells were also recognized by the GFP antibody (Figure 3-12 D). This indicates that the sieve elements themselves or the cells that they were derived from responded to auxin. In addition and in contrast to what was observed in *M. incognita* induced root knots, there were always numerous cells in the vicinity of the sieve elements that were exclusively labeled by the GFP antibody (Figure 3-12 F). The position of these GFP-positive cells in respect to sieve elements as well as to the syncytium strongly suggests that these cells are companion cells. Previously, companion cells were clearly identified in the phloem surrounding syncytia (Hoth *et al.*, 2005). As was found for giant cells (Figure 3-5 and Figure 3-8), no GFP signal was detected inside the syncytium itself.

Taken together, the data obtained from *M. incognita* and *H. schachtii* infected roots show that in the vicinity of both types of feedings sites cells are found that respond to auxin. In root knots, obviously all of these cells develop into the RS6 expressing sieve elements as cells

that were labeld exclusively by the GFP antibody were only rarely observed in fully mature root knots. In syncytia on the other hand, sieve elements as well as companion cells develop from the proliferating cells around the syncytium. Obviously, this differential response in the developing vascular tissue around the feeding sites cannot be explained by auxin responsiveness alone. Therefore, additional signals have to play a role in this differentiation process.
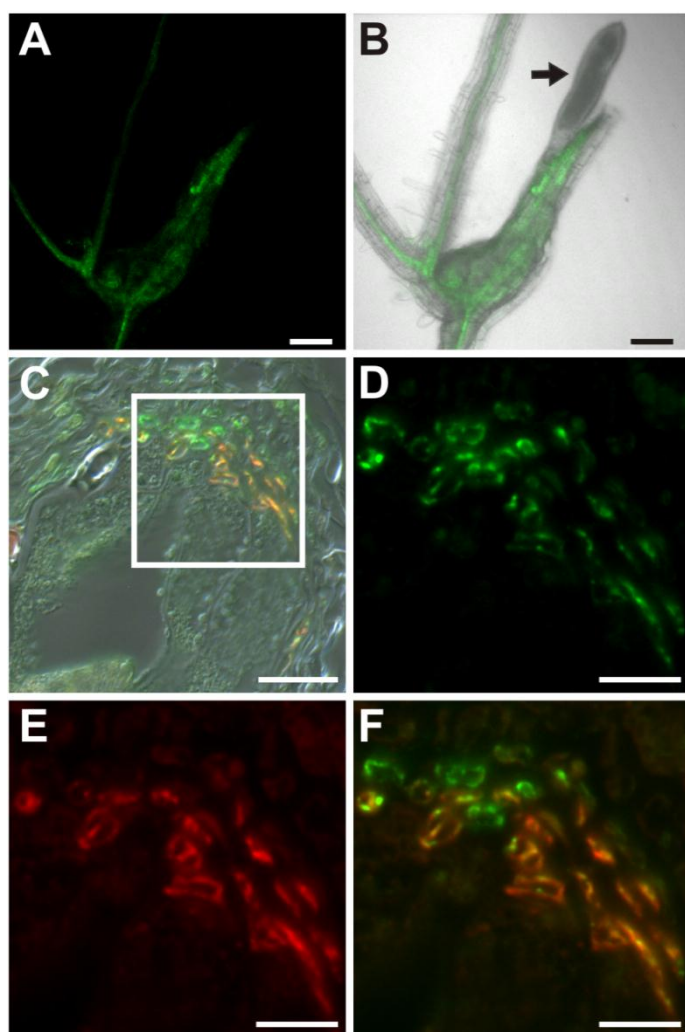
Figure 3-12 Auxin response in roots of *H. schachtii*-infected *P_{DR5}:ER-GFP* Arabidopsis plants 14 dai. (A) and (B) GFP fluorescence in an intact syncytium. (A) GFP fluorescence, (B) Overlay of GFP fluorescence and bright field image, arrow points to the nematode. (C-F) Section through a syncytium 14 dai. (D-F) is a detail of the indicated position in (C). (D) Auxin responsive cells decorated by a GFP antibody. Green color results from a Cy2-conjugated secondary antibody. (E) Cells decorated with the sieve element marker antiserum RS6. Red color results from a Cy3-conjugated secondary antibody. (F) is an overlay of (D) and (E). Scale bars represent 100 μm in (A) and (B), 20 μm in (C) and 10 μm in (D-F).

3.2.2 Identification of cytokinin responsive cells in nematode infected roots

As the differential vascularization of root knot nematode and cyst nematode induced feeding sites cannot be explained by auxin signaling alone, cytokinin response in infected tissues was examined additionally. It is a well described phenomenon that auxin acts together with other phytohormones in order to regulate developmental processes. Also, various studies have proposed a role for cytokinin in feeding site establishment or development (Bird and Loveys, 1980; De Meutter *et al.*, 2003; Lohar *et al.*, 2004). In order to study cytokinin response, the P_{TCS}*:ER-GFP* transgenic Arabidopsis line was used (Müller and Sheen, 2008). The TCS promoter is a synthetic cytokinin responsive promoter that works in a similar fashion as the DR5 promoter. It contains the concatemerized binding motifs of B-type response regulators which in Arabidopsis mediate the transcriptional activation of early cytokinin target genes (reviewed in Müller and Sheen, 2007a). These binding motifs are fused to a minimal CamV35S promoter element and together drive the expression of ER-GFP upon activation.

3.2.2.1 Cytokinin response in uninfected roots

Figure 3-13 A-D shows the fluorescence pattern that was observed in two week old uninfected P_{TCS}*:ER-GFP* plants. Cytokinin response, visualized by GFP fluorescence, was seen in the root tip (Figure 3-13 A and B) and in emerging lateral roots (Figure 3-13 C and D), but not in lateral root primordia (data not shown). This is consistent with published data (Müller and Sheen, 2008). In contrast to P_{DR5}*:ER-GFP* plants, no signal was detected in the stele of the differentiated root indicating that the companion cells do not display a marked cytokinin response.

3.2.2.2 Cytokinin response in *M. incognita* infected roots

In root knots, no cytokinin response could be observed, neither in giant cells themselves nor in the surrounding tissues. This held true throughout the development of the root knot. Figure 3-13 E-H shows root knots at 7 dai and 14 dai. Only a very faint and diffuse staing in the periphery of the root knots is visible. Therefore, cytokinin response mediated by B-type RRs does not occur in root knots at a level that can be detected using the described

approach. Obviously, in root knot development auxin signaling plays a more crucial role.
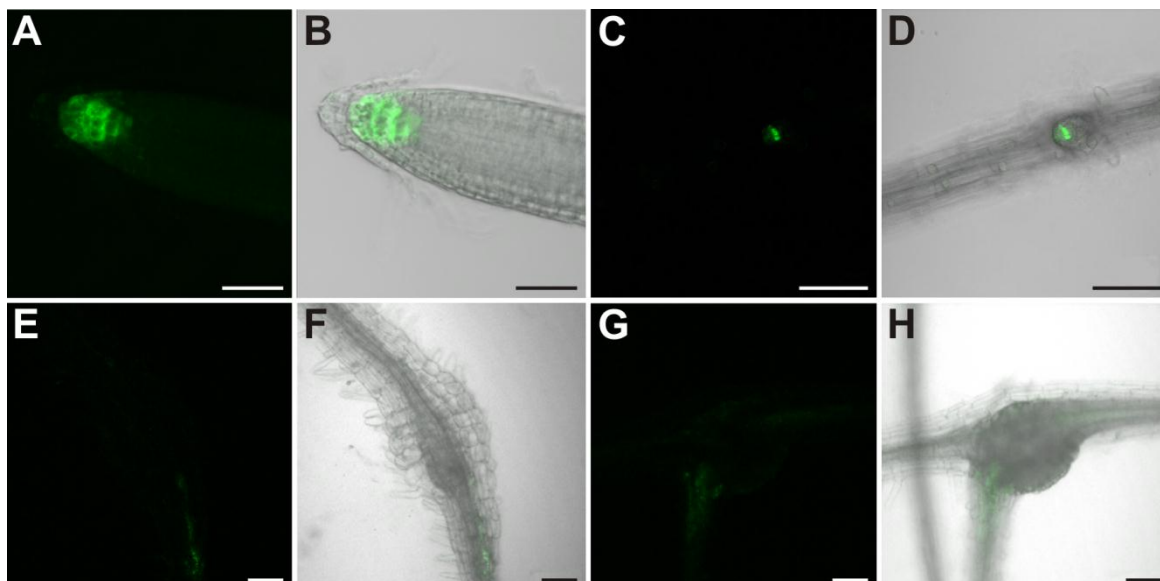
Figure 3-13 GFP fluorescence in Arabidopsis plants expressing ER-GFP under the control of the TCS-promoter. Fluorescence is observed in cytokinin responsive tissues. (A-D) GFP fluorescence in the root of a two week old P_{TCS}:ER-GFP plant. (A) and (B) Root tip. (C) and (D) Emerging lateral root. (A) and (C) GFP fluorescence. (B) and (D) Overlay of GFP fluorescence and bright field image. (E-H) GFP fluorescence in M. incognita–induced root knots in P_{TCS}:ER-GFP plants at 7 dai (E) and (F) and 14 dai (G) and (H). Throughout development staining was diffuse and virtually absent from root knots. (E) and (G) GFP fluorescence. (F) and (H) Overlay of GFP fluorescence and bright field image. Scale bars represent 50 µm in (A) and (B) and 100 µm in (C-H).

3.2.2.3 Cytokinin response in *H. schachtii* infected roots

Like in the case of auxin response, it was interesting to find out whether in *H. schachtii* induced tissues a different cytokinin response would occur. Therefore, two week old P_{TCS}:ER-GFP plants were infected with *H. schachtii* second stage juveniles as described in 7.5.2. Indeed, in contrast to the situation in root knots, a cytokinin response associated with syncytia was observed as shown in Figure 3-14 A and B in a root 14 dai. To gain insights at a cellular level, immunohistochemistry (see 7.6.3) was performed. GFP was detected with a GFP antiserum and sieve elements were identified with the RS6 antiserum. Figure 3-14 C-D shows an immunolocalization of GFP and RS6 on a section through an infected root 14 dai. GFP signal was detected in cells adjacent to the syncytium (Figure 3-14 D). These GFP-positive cells were also recognized by the RS6 antiserum, identifying them as sieve elements (Figure 3-14 E and F). Interestingy, no cells were seen in the immunolocalizations

that responded exclusively to GFP. This means that the companion cells in the phloem around the syncytia did not respond to cytokinin and stands in contrast to the pattern that was observed for auxin response in *H. schachtii* infected roots (see 3.2.1.4). In summary, this shows that the phloem around syncytia contains companion cells which respond to auxin but not to cytokinin, hence showing the same hormone response as the companion cells in the uninfected root. The sieve elements in the infected part of the root on the other hand respond both to auxin and to cytokinin. This definitely gives a hint that these sieve elements were formed *de novo* and either still contain nuclei or had lost them very recently.
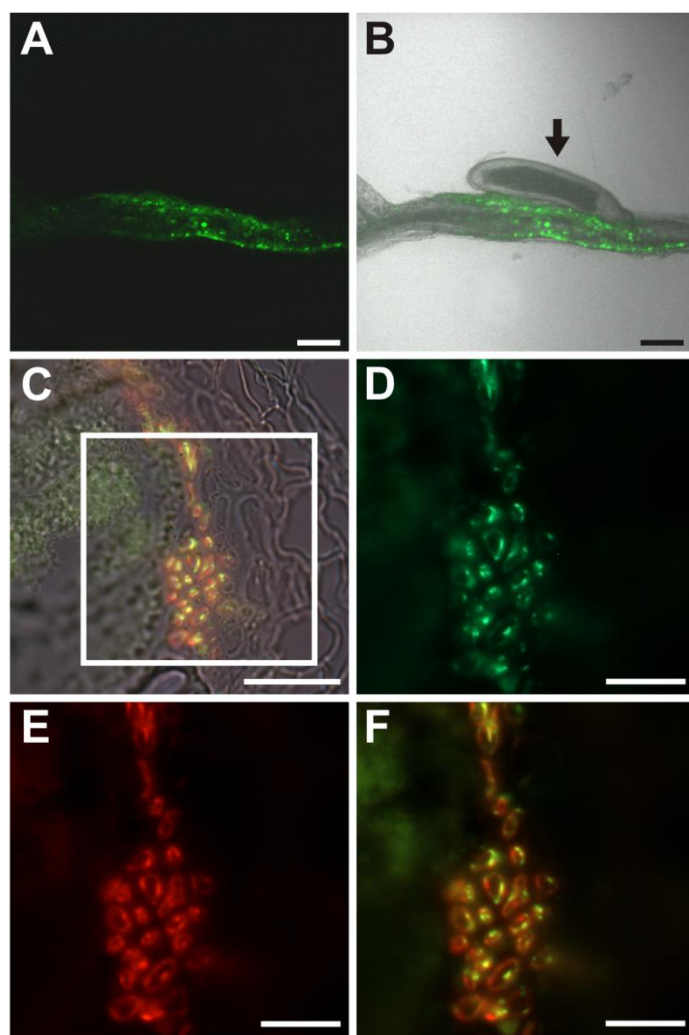
Figure 3-14 Cytokinin response in roots of *H. schachtii*-infected *P$_{TCS}$:ER-GFP* Arabidopsis plants 14 dai. (A) and (B) GFP fluorescence in an intact syncytium. (A) GFP fluorescence, (B) Overlay of GFP fluorescence and bright field image. Arrow points to the nematode. (C-F) Section through a syncytium 14 dai. (D-F) is a detail of the indicated position in (C). (D) Auxin responsive cells decorated by a GFP antibody. Green color results from a Cy2-conjugated secondary antibody. (E) Cells decorated with the sieve element marker antiserum RS6. Red color results from a Cy3-conjugated secondary antibody. (F) is an overlay of (D) and (E). Scale bars represent 100 μm in (A) and (B), 20 μm in (C) and 10 μm in (D-F).

3.2.3 Expression of a phloem identity marker in root knots

The phloem around *M. incognita* induced giant cells exhibits some unique properties, which distinguish it from the phloem around syncytia or the phloem typically found in the root of Arabidopsis. First of all, no companion cells are present in this phloem type. Furthermore, the sieve elements that surround the giant cells were shown to contain nuclei (Hoth *et al.*, 2008). Also, these nucleate sieve elements do not show the typical elongated shape and the longitudinal orientation of a mature sieve element, but they rather form a net of randomly arranged cells within the root knot. It was speculated before that these cells represent a novel type of unloading phloem and that they display protophloem character (Hoth *et al.*, 2008). To get further evidence about the identity of the phloem, plants carrying the GUS gene under the control of the APL promoter (Bonke *et al.*, 2003) were infected with *M. incognita*. APL is a MYB-type transcription factor which was shown to be required for the specification of phloem identity in Arabidopsis. It seems to play a role both in phloem-related cell divisions and cell differentiation. In parallel, it probably also suppresses xylem differentiation. The *APL* gene is expressed in the nucleated protophloem sieve elements of developing roots and in metaphloem companion cells (Bonke *et al.*, 2003).

Figure 3-15 shows the activity of the APL promoter visualized by GUS staining (see 7.6.1) in a control root and in *M. incognita* infected roots. In accordance with the published data (Bonke *et al.*, 2003), GUS staining in the control root was visible in two cell files in the vasculature (Figure 3-15 A). In a root knot 7 dai staining was observed throughout the knot, excluding the giant cells (Figure 3-15 B). Also in a mature root knot at 17 dai the staining was visible as a network around the giant cells (Figure 3-15 C). To confirm this finding, a GUS stained root knot 17 dai was embedded in low melting point agarose and sectioned to 60 μm using a vibratome (see 7.6.2). Figure 3-15 D shows a section directly above the root knot, indicated by the separation of the xylem elements (arrow). The staining is clearly seen in the companion cells. Within the root knot, the staining domain is much broader and is found in populations of cells adjacent to the giant cells (Figure 3-15 E). As companion cells are absent from the root knot, these cells most likely represent the nucleate sieve elements of the root knot phloem. The presented results indicate that the phloem around the giant cells has protophloem identity.
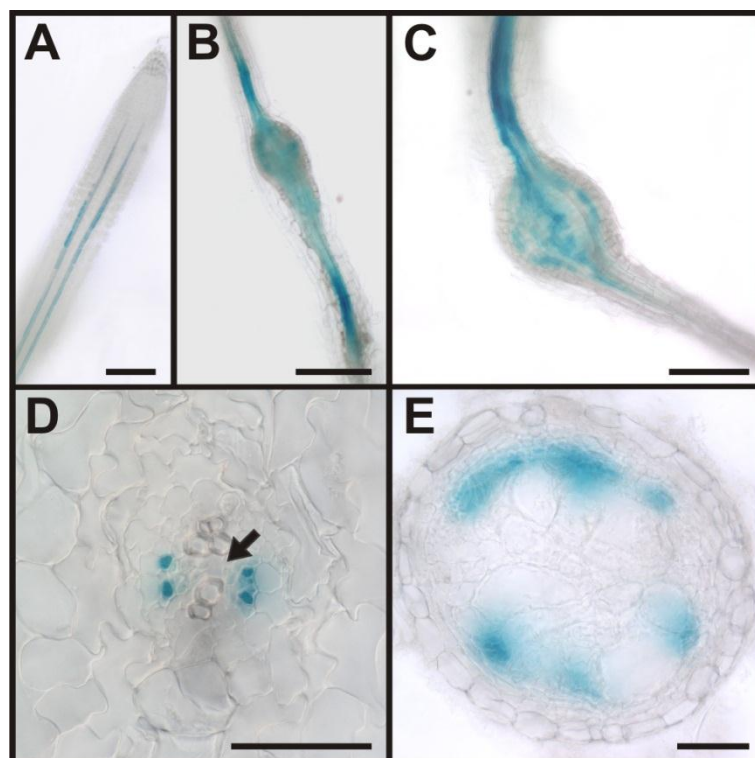
Figure 3-15 Activity of the APL promoter in *M. incognita* infected *P_APL:GUS* plants vuisualized by GUS staining. (A) In control roots staining is observed in two cell files within the stele. (B) Root knot 7 dai. The staining is limited to the stele but also observed in patches within the root knot. (C) In a mature root knot 17 dai staining is observed in a net-like pattern in cells surrounding the giant cells. (D) Cross section through the very beginning of a root knot indicated by the separation of the xylem elements (arrow). GUS staining is limited to four cells, most likely companion cells. (E) Cross section through a mature root knot 17 dai. Promoter activity indicated by GUS staining is observed in cells surrounding the giant cells. Scale bars represent 100 μm in (A), 200 μm in (B) and (C) and 50 μm in (D) and (E).

3.3 Discussion

3.3.1 Hormone response in the differentiated root of *A. thaliana*

Auxin and cytokinin are implicated in numerous aspects of plant development. In the root, it is the sophisticated crosstalk between the two hormonal pathways that allows the control of processes like the formation of the embryonic root, control of the meristem size, lateral root formation and vascular patterning. The specific effects of the two hormones hereby often depend on the developmental context and the tissue that is analyzed (Bishopp *et al.*, 2011a). Maxima of hormone response can be visualized using synthetic promoters that are activated upon binding through early targets of the signaling pathways. In case of auxin, the DR5 promoter (Ulmasov *et al.*, 1997) has been used extensively to monitor auxin response in a multitude of tissues. In the postembryonic Arabidopsis root, several maxima of auxin response are found which are established by polar auxin transport. In the root tip, auxin plays a critical role in the specification of the stem cell niche (Sabatini *et al.*, 1999; Aida *et al.*, 2004). Furthermore, lateral root formation depends on the establishment of an auxin maximum originating from pericycle cells at the xylem pole of the vascular cylinder (Benkova *et al.*, 2003). Recently, an additional maximum of auxin response at the xylem pole of the proximal root meristem was described. Here, auxin – in a mutually inhibitory interaction with cytokinin - specifies vascular tissue patterns (Bishopp *et al.*, 2011b).

Cytokinin response was traditionally visualized using promoter-GUS fusions of ARR genes. There are two different types of ARRs involved in the cytokinin signaling pathway: B-type ARRs bind to DNA and activate transcription. Among the targets of the B-type ARRs are the A-type ARRs which themselves inhibit cytokinin signaling in a negative feedback loop (Müller and Sheen, 2007b). In many publications, the A-type response regulator ARR5 was used to monitor cytokinin response. However, following A-type ARR expression might not always be the best approach for monitoring cytokinin response as these genes can also be regulated by other pathways. For example, WUSCHEL (WUS) directly represses A-type ARR transcription in order to increase sensitivity towards cytokinin in cells of the shoot apical meristem (Leibfried *et al.*, 2005). The synthetic TCS promoter contains a binding motiv that is recognized by all B-type ARRs and therefore seems to be more suitable as a universal cytokinin response reporter (Müller and Sheen, 2008). Still, it cannot give information about a possible specific regulation of A-type ARRs in a given context.

Most of the studies in which the DR5 or the TCS promoters have been used in the postembryonic roots were performed with seedlings 2-5 days after germination while clearly differentiated parts of the root two or more weeks after germination have not been examined. It was therefore important to gain insights about hormone response in those parts of the root as this is the context in which feeding site vascularization was analyzed lateron. The expression of ER-GFP under the control of both the DR5 and the TCS promoters in root tips and lateral root primordia in roots two weeks after germination was consistent with published data for seedlings (Ottenschläger *et al.*, 2003; Müller and Sheen, 2008, Figure 3-3 and Figure 3-13). In addition to these well known results, it was found that companion cells in the differentiated root constitutively respond to auxin (Figure 3-4). The companion cells are clearly identified by their position directly adjacent to the sieve elements. While there is no published support for the described observation, there are several arguments in favor of companion cells exhibiting a permanent auxin response. The proto- and metaxylem cells that respond to auxin in the differentiation zone directly proximal of the root meristem have developed into dead water conducting vessels in the differentiated parts of the root. Also the xylem axis is now clearly specified and auxin response is no longer needed in this position. Furthermore, it is by now commonly accepted that auxin as well as cytokinin are transported in the stele, particularly in the phloem (Bishopp *et al.*, 2011c). The phloem in the differentiated parts of the plant consists of sieve elements and companion cells. Sieve elements undergoe a maturation process during which they lose their nucleus and thereby the ability for gene transcription. The associated companion cells on the other hand keep their nucleus throughout their lifetime and are able to respond to stimuli by transcriptional changes. Consequently, a number of developmental processes are regulated in the companion cells. For example, CONSTANS, a nuclear zinc-finger protein that plays a central role in the photoperiod-response pathway acts in the companion cells to trigger flower development in the apex (An *et al.*, 2004), showing that in companion cells environmental stimuli are being processed. Taken together, it makes a lot of sense that companion cells in the conducting phloem exhibit a constitutive auxin response in order to monitor auxin concentration along the transport pathway to integrate hormonal information.

No GFP fluorescence reflecting a positive transcriptional output in response to cytokinin signaling was detected in the stele of P_{TCS}:ER-GFP plants. A reason for this can be low concentrations of cytokinins in the phloem or reduced sensitivity of the cells towards the

hormone. Still, it cannot be excluded that a cytokinin response which could not be detected with the approach applied in this work occurs. Very recently, an improved version of the TCS promotor with a higher sensitivity has been introduced (Zürcher *et al*., 2013) and might give better insights into the cytokinin responses in phloem tissues in the future.

3.3.2 Differentiated giant cells and syncytia do not respond to auxin and cytokinin

As the focus of this work was the analysis of the vascularization of the feeding sites, phytohormone response was monitored starting from 7 dai which is just before the vasculature begins to undergo changes. The feeding sites themselves, i.e. giant cells and syncytia have already acquired their identity at that time point although they still increase in size. It is noteworthy that neither auxin nor cytokinin response was detected in giant cells or in syncytia at any of the time points that were addressed. In case of auxin this is in accordance with earlier studies where a transient DR5 driven reporter gene activity was described in early developing feeding sites (Hutangura *et al.*, 1999; Karczmarek *et al.*, 2004; Grunewald *et al.*, 2009a). In one of these publications a model was presented where the feeding site acts as a source of auxin which is then transported to the surrounding cells (Grunewald *et al.*, 2009b). Although it was speculated that the auxin stimulus primes the cells in the periphery for their subsequent incorporation into the syncytium, the data presented in this work suggest that the auxin response is linked to vascular proliferation that occurs around the feeding site. Despite the fact that auxin response in the feeding sites is limited to the very early stages, it cannot be excluded that the feeding sites act as a source of auxin also in later stages to trigger the developmental effects in the surrounding vasculature. DR5 provides information only about auxin response, not about the sensitivity of a certain tissue towards auxin or about auxin concentration. These features might very well change during the development of the feeding site. Unfortunately, nothing is known about the auxin concentrations in the feeding sites or in the surrounding tissue.

The same drawbacks as mentioned for the DR5 promoter also hold true for TCS. Again, it is possible that the feeding sites serve as a source of cytokinin but do not respond themselves as was shown by the lack of GFP signal in the feeding sites in infected *P_{TCS}:ER-GFP* plants (Figure 3-13 and Figure 3-14).

Irrespective of the source of the phytohormones it could be shown in this work that the vascular tissues surrounding the feeding sites display responses to auxin in the case of *M. incognita* and to both auxin and cytokinin in the case of *H. schachtii.* The possible function of the differential hormone responses in the vascularization process will be discussed in the following chapters.

3.3.3 Auxin response and vascularization in *M. incognita* induced root knots are tightly linked

Giant cells represent a strong sink tissue that has to be supplied with assimilates *via* the vasculature. Consequently, a strong induction of phloem tissue is found around the giant cells which is unique in various aspects. First of all, it only consists of cells with sieve element identity, but no companion cells distinguishable by the expression of the SUC2 marker are present (Hoth *et al.*, 2008). Loss of companion cell identity as well as proliferation and differentiation of new sieve elements in the root knot phloem start between one and two weeks after infection. This is also the time frame when a symplastic connection between the sieve elements is formed which allows the diffusion of soluble GFP expressed under the control of the SUC2 promoter from the companion cells outside of the root knot into the sieve element network around the giant cells (Hoth *et al.*, 2008). Comparing GFP fluorescence in *M. incognita* infected P_{SUC2}:*GFP* and P_{DR5}:*ER-GFP* plants showed that an auxin response in the root knot precedes the described changes in the phloem. At 7 dai auxin response was already found in a broad domain in the developing root knot while GFP expressed under the control of the SUC2 promoter was limited to two cell files, which represent companion cells in a still regular root phloem (Figure 3-7 A,B and E,F). At 14 dai, the domains of GFP fluorescence looked very similar in P_{SUC2}:*GFP* and P_{DR5}:*ER-GFP* plants, i.e. fluorescence was found in a network of cells around the giant cells. This already gave an indication that it could be the sieve elements that respond to auxin (Figure 3-7 C,D and G,H). The immunolocalization experiments performed with root knots of different ages further suggested that cells around the giant cells receive an auxin input and subsequently differentiate into sieve elements (Figure 3-8). Surprisingly, most of the sieve elements in the root knot retained the GFP signal indicating that auxin dependent transcription took place also after they had changed their identity. This is in principle possible as it was shown that

these sieve elements are nucleate and are therefore still capable of a transcriptional response (Hoth *et al.*, 2008). However, it cannot be ruled out that some of the sieve elements developed further and their nuclei degraded which would imply that the ER-localized GFP experiences a slow protein turnover and is therefore still present. This scenario cannot be excluded as GFP is a rather stable protein and it was shown that even in rapidly dividing *E. coli* cells it has a half life time of about 24 hours (Andersen *et al.*, 1998).

In mature root knots at 17 dai cells that responded exclusively to auxin without also testing positive for the sieve element marker RS6 were only very rarely observed (Figure 3-8 E-L). This first of all indicates that the differentiation of new sieve elements has been more or less completed and no new cells received an auxin stimulus that precedes their differentiation into sieve elements. It was shown in this work that companion cells in the phloem of the mature root exhibit a constitutive auxin response (Figure 3-4). The lack of auxin responsive cells in the root knot at 17 dai which do not have sieve element identity at the same time therefore represents – in addition to the data of (Hoth *et al.*, 2008) – a further line of evidence that companion cells are absent from the root knots. So far companion cells have been identified by checking the expression of the *SUC2* gene which encodes for a companion cell specific sucrose transporter. However, the possibility that *SUC2* expression is specifically downregulated in root knot companion cells although they are still present has to be considered. Keeping in mind the nutrient flow in the root knot, this would make physiological sense. Assimilates are transported into the giant cells via the plasma membrane. Before they can be taken up, they need to be exported from the phloem into the apoplast. The presence of SUC2 in companion cells would lead to a re-import of sucrose back into the phloem and direct the nutrient flow in the wrong direction. On the other hand, downregulation of SUC2 would direct the flow towards the giant cells, provided that they have means to take up the sucrose. Indeed it was shown that another sucrose transporter, SUC1, is specifically upregulated in root knots (Hammes *et al.*, 2005).

In order to find out more about the significance of the auxin response for the vascularization process in root knots, mutants with defects in signaling and transport were infected with *M. incognita*. Although this was not quantified, the mutants seemed to be infected worse than wild type plants which is in accordance with published data from a study where the same mutants were infected with *H. schachtii* (Goverse *et al.*, 2000*)*. However, no differences in the pattern of GFP fluorescence could be detected between root knots induced in wild type

and mutant plants, respectively (Figure 3-11). It is therefore possible that once the feeding site is successfully established, vascularization occurs independently of the defects in these specific mutants, namely AUX1 mediated auxin import and AXR1 dependent auxin response. Maybe, the defects can be overcome in the root knot by bypassing the effected protein functions. In accordance with that, a strong induction of lateral roots comparable to the situation in wild type was observed associated with root knots in the mutants although these plants normally have severely reduced numbers of lateral roots (Figure 3-10 and Figure 3-11).

In contrast to auxin response, B-type ARR mediated cytokinin response does not seem to play a role in root knot development and vascularization as no GFP fluorescence could be detected in P_{TCS}:ER-GFP root knots (Figure 3-13). On the other hand the type-A ARR5 promoter was strongly active in root knots in *L. japonicus* specifically in those cells that surround the giant cells (Lohar *et al.*, 2004). Type-A ARRs were shown to be strongly upregulated by exogenous cytokinin and mediate a feedback loop by which the plant reduces its sensitivity towards cytokinin (D'Agostino *et al.*, 2000; To *et al.*, 2004). Interestingly, they play crucial roles in the antagonistic action of auxin and cytokinin for example in root stem cell specification during embryogenesis. In this context, auxin counteracts cytokinin signaling by inducing the expression of two A-type ARRs (Müller and Sheen, 2008). The lack of GFP fluorescence in infected tissue of P_{TCS}:ER-GFP plants could therefore be a consequence of a concerted repression of the cytokinin signaling pathway, possibly mediated by auxin.

3.3.4 Sieve elements and companion cells in phloem induced by *H. schachtii* respond differentially to auxin and cytokinin

As previously published, the phloem around syncytia consists of sieve elements and companion cells with the ratio shifted in favor of sieve elements. The data presented there suggest that this phloem is typical metaphloem, i.e. it consists of elongated differentiated sieve elements and companion cells (Hoth *et al.*, 2005; Hoth *et al.*, 2008).

In this work, it was shown that the vasculature surrounding the feeding site clearly exhibits an auxin response as was vizualised by GFP fluorescence derived from ER-GFP expressed under the control of the DR5 promoter. Auxin response was observed in sieve elements as

well as in companion cells (Figure 3-12). In addition and in contrast to the situation in root knots, a cytokinin response in a B-type response regulator mediated fashion occurs in *H. schachtii* infected tissues (Figure 3-14 A,B). Immunolocalization experiments showed that in contrast to the auxin response, cytokinin response was limited to the sieve elements and was absent from companion cells (Figure 3-14 C-F). Companion cells in cyst nematode induced tissue therefore respond to the two hormones in the same way as they do in the regular root phloem, i.e. they respond to auxin but not to cytokinin. The observation that the sieve elements in the *H. schachtii* induced phloem respond both to auxin and cytokinin seems somewhat surprising as typically fully differentiated sieve elements lack nuclei and therefore cannot respond to stimuli on a transcriptional level. Still, although the proliferation of phloem in *H. schachtii* induced tissue is not as pronounced as in *M. incognita* induced root knots, the tissue is of secondary origin and can therefore very well be in a differentiation state where the nuclei haven't degraded yet. However, as already mentioned earlier (3.3.3), again the possibility has to be considered that the GFP signal is retained even after the nuclei were lost.

The fact that, at a certain stage in their development, the sieve elements around the syncytia respond to auxin as well as to cytokinin raises the question whether this specific pattern of phytohormone response is connected to the structure of this phloem. It is well known that cytokinin is involved in the regulation of meristematic activity and vascular differentiation and that in different tissues the impact of this regulation varies (reviewed in Perilli *et al.*, 2010). Therefore, it is tempting to speculate that the ratio of auxin to cytokinin in the cells of the syncytia-surrounding phloem has an influence on the number of divisions that a cell undergoes after the first division of the metaphloem initial. If the ratio is in favor of auxin, the cell would assume companion cell identity and if both auxin and cytokinin signaling occurs, the sieve elements would proliferate which would eventually result in the excess number of sieve elements in the phloem tissue.

In *M. incognita* induced root knots, the situation is different, as discussed in 3.3.3. The different hormone responses in root knot nematode and cyst nematode induced tissues go hand in hand with specific characteristics of the phloem around giant cells and syncytia, respectively. Sieve elements in the root knots which respond only to auxin proliferate much stronger and seem to be in a less differentiated state than the sieve elements in *H. schachtii* induced tissues which respond to both hormones. Companion cells which respond

exclusively to auxin are sustained around syncytia, but are lost in root knots. The question whether the ratio of the phytohormones and the distinct responses to auxin and cytokinin signaling alone can lead to the observed differential vascularization remains open. In future experiments, detailed analysis of additional mutants and marker lines is indispensable.

3.3.5 Giant cells and syncytia are surrounded by different types of phloem

The distinct hormone responses in root knot nematode and cyst nematode induced vascular tissues emphasize the structural and functional differences between the phloem types that are found there. While the phloem around syncytia clearly is metaphloem, the phloem in the root knots seems to be completely different. It obviously shares certain features with protophloem, i.e. the cells are nucleate frequently and no companion cells are found associated with the sieve elements (Hoth *et al.*, 2008). Further evidence for a protophloem identity is added by the fact that the APL promoter is active in the root knot sieve elements (Figure 3-15). In the wild type root APL which is required for phloem cell specification is expressed in protophloem sieve elements and in metaphloem companion cells (Bonke *et al.*, 2003). As companion cells are absent from the root knot phloem, the cells that are expressing *APL* in the root knot very likely are protophloem sieve elements.

Nevertheless the random arrangement of the sieve elements in the root knot and the lack of the elongated shape that characterizes sieve elements in a differentiated tissue might also suggest that the sieve elements in the root knot exhibit a mixed identity. As the function of the protein that contains the RS6 sieve element marker is not known and does not tell us anything about whether a sieve element is terminally differentiated or not, it is very important to use additional markers that will allow further insight into the identity of this unique tissue.

4 Comprehensive discussion and outlook

In the presented work, different aspects of the complex network that underlies phytohormone action were studied. A special focus was placed on auxin which is involved in virtually every aspect of plant growth and development. The ability of auxin to fulfill such a wide variety of tasks is largely derived from the plant's capacity to establish temporal and spatial auxin maxima and gradients. This differential auxin distribution is then interpreted on the level of the individual cell by a dynamic and flexible signaling pathway and results in a context dependent transcriptional output (Vanneste and Friml, 2009).

Asymmetric auxin distribution is mainly achieved by PAT. The most important determinants for PAT are the PIN proteins which mediate auxin efflux from cells and - by their polar subcellular localization in the plasma membrane – define the direction of its flow. A number of factors that are involved in PIN trafficking and polar localization have been characterized, among them the AGCVIII kinase PID, which controls PIN polar targeting by phosphorylation of conserved serine residues in the hydrophilic loop of the carrier proteins (Feraru and Friml, 2008).

In this work, new insights into the biochemical mechanisms that underlie the regulation of PIN protein function were gained by studying the impact of several members of the AGCVIII kinase family on the transport activity of PIN1 and PIN3. Using a heterologous expression system, it could be shown that co-expression of PINs with D6PK or PID leads to phosphorylation and enhanced auxin efflux from *X. laevis* oocytes (Figure 2-4, Figure 2-5, Figure 2-9, Figure 2-16). The analysis of PIN1 mutants lead to the identification of amino acid residues that are essential for its activation by the two kinases (Figure 2-12, Figure 2-14). It has been shown in plants that in contrast to PID, D6PK has no impact on the subcellular localization of PINs (Zourelidou *et al.*, 2009). Therefore, D6PK and PID regulate PIN-mediated polar auxin transport in a different manner, i.e. either by modifying transport properties or by influencing both transport activity and polar localization of the proteins.

Auxin abundance which is established by metabolism and transport is interpreted by the cell and translated into a transcriptional output. Early transcriptional responses are mediated by the ARFs which activate target genes by binding to conserved sequence motifs, the AuxRes (Ulmasov *et al.*, 1995, see also chapter 1.2). These conserved response elements serve as a basis for synthetic promoters like DR5 (Ulmasov *et al.*, 1997) which – upon fusion with a

reporter gene – allow monitoring early auxin responses in plant tissues. The synthetic DR5 promoter has drawbacks because reporter gene expression does not necessarily reflect just auxin concentration. Instead, it can also depend on the sensitivity of individual cells towards the hormone. A good correlation between auxin concentration and response maxima was found in the root with the exception of columella cells where a low auxin concentration stands in contrast to high reporter gene expression (Petersson *et al.*, 2009). Furthermore, it was shown in a number of publications that a high reporter gene activity corresponds to expected auxin concentration maxima that were predicted based on the analysis of the PIN protein localization patterns (Benkova *et al.*, 2003; Friml *et al.*, 2003; Blilou *et al.*, 2005). An analogous reporter construct for monitoring cytokinin response is the TCS promoter that contains the binding motifs for B-type response regulators which mediate the activation of early cytokinin target genes (Müller and Sheen, 2008).

The reporter constructs described above were used to analyze vascularization events during infection of Arabidopsis roots with two different species of plant parasitic nematodes. With this approach, first insights into the impact of both auxin and cytokinin on the proliferation and differentiation of the unique phloem structures that are found in *M. incognita* and *H. schachtii* induced feeding sites should be gained. It could be shown that differential hormone responses take place in the nematode induced tissues depending on the attacking species. In developing root knots that are induced by *M. incognita*, an auxin response in cells around the giant cells preceded their subsequent differentiation into sieve elements (Figure 3-8). This auxin response possibly primes the cells for the differentiation process in the course of which they obtain sieve element identity. The auxin response persisted even after the cells had undergone differentiation which is possible as the sieve elements retain their nuclei (Hoth *et al.*, 2008). Cytokinin signaling could not be observed in root knots of P_{TCS}:*ER-GFP* plants which means that either cytokinin levels are low or cells are not susceptible to the signal. In contrast, the phloem around *H. schachtii* induced syncytia responded to both auxin and cytokinin. Auxin response was detected in companion cells and sieve elements while cytokinin response was limited to the sieve elements (Figure 3-12, Figure 3-14). The fact that the sieve elements in the nematode induced tissues respond to auxin seems somewhat surprising. In the primary root meristem, auxin response is found in the xylem axis (Bishopp *et al.*, 2011b) while in the differentiated part of an uninfected root, companion cells respond (Figure 3-4). This might indicate that the sieve elements around giant cells and

also around syncytia have mixed identity, taking over companion cell tasks. Taking into account the distinct characteristics of the phloem tissues around syncytia and giant cells and the differential hormone responses, the ratio of cytokinin and auxin response might contribute to the identity of the *de novo* formed phloem. It is well known that in the distal meristem, cytokinin promotes differentiation (Perilli *et al.*, 2012), but specific functions in phloem cell type specification have not been described. However, the cytokinin response found in *H. schachtii* induced tissue might influence the differentiation state of the phloem which - in contrast to the phloem in root knots - consists of the typical elongated sieve elements and associated companion cells.

The finding that phloem cells in nematode induced tissues respond to auxin and cytokinin and do so in a species-specific manner raises several questions that need to be answered in the future. First of all it would of course be important to find out which specific target genes are activated in response to the hormone inputs in the developing vascular tissues and how these target genes are involved in the phloem specification. Therefore, the corresponding cells should be isolated by fluorescence activated cell sorting and analyzed on a transcriptomic level using RNA sequencing.

Infection of a host plant with a plant parasitic nematode results in the manipulation of the plants hormone household and consequently of its developmental program. Auxin is very important for the successful establishment and development of the feeding sites and it has been discussed extensively what the source of the hormones is. Auxin-like compounds were detected in nematode secretions and might contribute to the initiation of the feeding site. (Bird, 1962; Yu and Viglierchio, 1964; Johnson and Viglierchio, 1969). In later stages of development, elevated auxin biosynthesis might play a role in the accumulation of the hormone. However, several observations indicate that it is the manipulation of the auxin transport machinery which has the greatest impact on feeding site development. During nematode infection, the root undergoes changes that resemble the formation of a new organ. Auxin transport-dependent gradients generally represent a module for organ formation (Benkova *et al.*, 2003). Consistently, the auxin influx carrier AUX1 is strongly expressed in feeding sites (Mazarei *et al.*, 2003). Additionally, *pin* mutants are infected to a lesser extent by *H. schachtii* and application of the auxin transport inhibitor NPA disturbs expansion of syncytia (Goverse *et al.*, 2000). In *H. schachtii* infected roots, PIN proteins show altered expression and localization patterns in early stages of the infection cycle compared

to control roots (Grunewald *et al.*, 2009b). It was shown that in a very early stage, *PIN1* and *PIN7* expression is downregulated in the feeding site. The absence of efflux carriers would cause reduced export and consequently accumulation of auxin in the feeding site. Furthermore, a shift from basal to lateral localization of PIN3 and PIN4 was observed. This change in PIN localization would contribute to transport of auxin from the syncytium to the surrounding tissue which is the developing vasculature. Later stages of feeding site development were not addressed in this study, therefore it's not know if and how PIN proteins are localized in the nematode-induced phloem. In order to find out whether relocalization of PINs is a common feature during feeding site development, it would be of great interest to study their expression and localization also in *M. incognita* induced tissues. When control roots were compared to *M. incognita* infected roots in a microarray analysis, *PIN7* expression was found to be upregulated (Hammes *et al.*, unpublished). PIN7 would therefore be a first candidate to study in more detail regarding a possible function in redirecting auxin fluxes in *M. incognita* induced tissues. Additionally, analysis of the expression and localization of the PIN-interacting kinases might contribute to our understanding of how auxin is redistributed during the infection cycles of the different nematode species.

5 Summary

The phytohormone auxin is a major determinant of plant growth and development. Many aspects of its action depend on the formation of local maxima or gradients within tissues. PIN-FORMED (PIN) proteins facilitate auxin efflux from cells and, by their dynamic polar localization, provide a basis for its directional transport. PIN-dependent auxin transport is regulated by several members of the plant specific AGCVIII kinase family. Phosphorylation of the central serine residues in three conserved TPRXS(N/S) motifs by PIONOID (PID) is crucial for polar targeting of PINs. The D6 protein kinases (D6PKs) were also shown to be involved in the control of polar auxin transport and are functionally linked to PIN1 and PIN3, however they do not interfere with PIN subcellular localization.

In this work, the *X. laevis* oocyte expression system was used to study the impact of D6PK and other representative members of the AGCVIII kinase family on transport activity of PIN1 and PIN3. An assay was established that allowed monitoring auxin efflux after direct injection of oocytes with radiolabeled substrate. It could be shown that co-expression of PIN1 and PIN3 proteins with D6PK or PID results in phosphorylation of PINs and in enhanced auxin efflux. Contrarily, expression of PIN proteins alone did not cause measurable auxin efflux when compared to water-injected control oocytes. Based on the observation that a kinase-inactive version of D6PK could no longer stimulate PIN-mediated auxin efflux, it was concluded that phosphorylation is essential for PIN function. Activation of PIN1 and PIN3 could be achieved by co-expression of D6PK and PID, but not two other members of the AGCVIII kinase family, PHOT1 and UNC, demonstrating the specificity of the interaction between PINs and D6PK / PID.

Analyses of different mutants lead to the identification of phosphorylation target sites that are essential for D6PK / PID – mediated PIN1 transport activity. A serine to alanine substitution at position 271 caused decreased auxin efflux from $PIN1_{S271A}$ / D6PK co-expressing oocytes, but had no effect on PID mediated activation, indicating that S271 is important for D6PK function, while PID acts independently of S271, i.e. vy phosphorylation of different residues. Consistently, an opposite effect was observed in a $PIN1_{S231A/S252A/S290A}$ triple mutant with alanines replacing the central serines in the TPRXS(N/S) motifs. The different impacts of the S271A and the S231A/S252A/S290A mutations on D6PK and PID function suggested that activation of PIN1 by D6PK is mediated preferentially *via*

phosphorylation of S271A whereas PID favors the central serines in the TPRXS(N/S) motifs, thereby regulating polarity as well as activity. While both PIN1$_{S271A}$ as well as the triple mutant PIN1 $_{S231A/S252A/S290A}$ could still mediate enhanced auxin efflux from oocytes when co-expressed with D6PK or PID, although to a varying extent, transport activity was almost completely lost in a combined quadruple mutant PIN1 $_{S231A/S252A/S271A/S290A}$. The results obtained from the analysis of PIN1 mutants suggest that the main phosphorylation sites that contribute to PIN1 activatability by D6PK and PID have been identified and include S271 as well as S231/S252/S290. However, it was clearly demonstrated that not all of the sites have to be phosphorylated at the same time to confer transport activity to PIN1. In fact, phosphorylation of either S271 or one or more of the S231/S252/S290 sites is sufficient for transport activity under the given experimental conditions.

PIN3 generally exhibited higher transport rates than PIN1 when co-expressed with an activating kinase, probably reflecting its function in processes that involve rapid polar redistribution of auxin. A serine to alanine exchange at position 262 of PIN3 which corresponds to S271 in PIN1 had no effect on the activation by either D6PK or PID when compare to wild type PIN3 indicating that different amino acid residues are important for PIN3 activity.

In summary, the results obtained in the first part of this work provide evidence that the transport activity of the auxin efflux carriers PIN1 and PIN3 is controlled by the AGCVIII kinases D6PK and PID and depends on phosphorylation of specific amino acid residues, thereby giving important insights into the biochemical mechanisms that control PIN protein function.

In the second part of the thesis, the role of phytohormone responses in plant-nematode interactions was studied. Plant parasitic nematodes are destructive pathogens with a broad host range and cause enormous yield losses each year. The sedentary endoparasitic nematodes are divided into two groups, the root knot nematodes (RKN) and the cyst nematodes (CN). The free living juveniles of RKN and CN enter their host plant's roots and induce the formation of highly specialized feeding sites termed giant cells or syncytia, respectively, in the vascular cylinder. From these feeding sites, all the nutrients required for growth and development of the nematodes are withdrawn. Giant cells and syncytia are functionally equivalent and represent strong terminal sink tissues. However they differ in their genesis and in the way how they are loaded with nutrients. While syncytia are

connected to the surrounding vasculature by plasmodesmata, giant cells are symplastically isolated and nutrient uptake occurs *via* membrane dependent processes. Both syncytia and giant cells are enclosed in vascular tissue which is formed *de novo* and is required for the transport of nutrients towards the feeding sites. The unloading phloem that is induced around syncytia consists of sieve elements and companion cells with the ratio shifted towards an excess of sieve elements. Giant cells on the other hand are surrounded by a unique phloem tissue that is built up of nucleate sieve elements whereas companion cells are absent.

It was shown before that both CN and RKN secrete auxin- and cytokinin-like compounds and that auxin plays an important role in the establishment of the feeding sites. However, nothing was known about how the vascularization of syncytia and giant cells is controlled and whether phytohormones play a role in this process. Therefore auxin and cytokinin responses were monitored in nematode infected Arabidopsis roots using the synthetic hormone responsive promoters DR5 and TCS, respectively, fused to the coding sequence for ER-localized green fluorescent protein (GFP). GFP fluorescence was recorded and immunohistochemical experiments were performed in order to identify the cell types within the nematode induced tissues that responded to the phytohormones. This provided insights into a possible function of phytohormone dependent processes in feeding site vascularization. In uninfected differentiated parts of control roots a constitutive auxin response was found in companion cells, but no response to cytokinin mediated by B-type response regulators was observed. Neither giant cells nor syncytia themselves responded to auxin or cytokinin at the timepoints of the infection cycle that were analyzed in this work but the response was limited to cells that surrounded the feeding sites. The observed hormone responses differed between RKN and CN-induced tissues.

In developing root knots, an auxin response in cells around the giant cells preceded their subsequent differentiation into sieve elements, which were identified using a well established sieve element marker. Possibly, the auxin response primes these cells for the differentiation process. GFP signal was retained even after the responding cells had assumed sieve element identity while cells that tested positive only for GFP but not for the sieve element marker were an exception in the mature root knot. The latter observation adds further evidence to the previously described finding that companion cells are absent from fully developed root knots. Cytokinin signaling could not be observed in root knots of

P$_{TCS}$:ER-GFP plants which means that either cytokinin levels are low or cells are not susceptible to the signal.

In contrast to the situation in root knots, the phloem around syncytia responded to both hormones. Auxin response was detected in companion cells and sieve elements while cytokinin response was limited to the sieve elements. Taking into account the distinct characteristics of the phloem tissues around syncytia and giant cells and the differential hormone responses, the ratio of cytokinin and auxin response might contribute to the identity of the *de novo* formed phloem, i.e. metaphloem in CN induced tissues and protophloem in RKN induced tissues.

6   Zusammenfassung

Wachstum und Entwicklung von Pflanzen werden maßgeblich durch das Phytohormon Auxin beeinflusst. Sehr häufig spielt dabei die Ausbildung von Konzentrationsgradienten oder lokalen Maxima eine wichtige Rolle. In diesen Prozessen nehmen die PIN-FORMED (PIN) Proteine eine zentrale Rolle ein, indem sie den Auxin Efflux aus den Zellen vermitteln und zusätzlich durch ihre polare subzelluläre Lokalisierung die Richtung des Transportes innerhalb der Pflanze vorgeben. PIN-basierter Auxin Transport wird durch verschiedene Mitglieder der Pflanzen-spezifischen AGCVIII Kinase Familie reguliert. In Arabidopsis ist die Phosphorylierung der zentralen Serin-Reste in drei konservierten TPRXS/(N/S) durch PINOID (PID) von entscheidender Bedeutung für die korrekte polare Lokalisierung der Proteine innerhalb der Zelle. Auch für die vier Mitglieder der D6 Protein Kinasen (D6PKs) wurde eine funktionelle Verbindung zu PIN Proteinen, insbesondere PIN1 und PIN3, gezeigt. D6PKs nehmen eine wichtige Funktion in der Kontrolle von polarem Auxin Transport ein, ohne jedoch die Lokalisation von PIN Proteinen zu beeinflussen.

In der vorliegenden Arbeit wurde der Einfluss von D6PK und weiteren repräsentativen Vertretern der AGCVIII Kinase Familie auf die Transportaktivität von PIN1 und PIN3 im Expressionssystem der *X. laevis* Oocyten untersucht. Dazu wurde ein experimentelles Verfahren etabliert, das es erlaubt, Auxin Efflux nach direkter Injektion der Oocyten mit radioaktiv markiertem Substrate zu messen. Mit Hilfe dieser Methode konnte gezeigt werden, dass die Koexpression von PIN1 und PIN3 mit den Kinasen D6PK bzw. PID in einer Phosphorylierung der PIN Proteine sowie erhöhtem Auxin Efflux resultiert. Die Expression der PIN Proteine ohne zusätzliche Kinase führte dagegen zu keinem von Wasser-injizierten Kontroll-Oocyten unterscheidbaren Auxin Efflux. Ebenso konnte durch Koexpression einer inaktiven D6PK Variante keine erhöhte Transportaktivität hervorgerufen werden. Phosphorylierung der PIN Proteine ist demnach entscheidend für ihre Transportaktivität in *X. laevis* Oocyten. Die Spezifität der Interaktion zwischen PIN Proteinen und D6PK bzw. PID wurde durch Untersuchungen bestätigt, die zeigten, dass zwei weitere Vertreter der AGCVIII Familie, PHOTOTROPIN1 (PHOT1) und UNICORN (UNC), keine Transportaktivität vermitteln können.

Durch die Analyse verschiedener PIN1 Varianten mit Punktmutationen an potentiellen Phosphorylierungsstellen konnten Aminosäurereste, die für die D6PK bzw. PIN-induzierte

Aktivierung von essentieller Bedeutung sind, identifiziert werden. Ein Austausch des konservierten Serins S271 gegen Alanin führte zu einer reduzierten Aktivierbarkeit dieser Mutante durch D6PK, wohingegen die Transportaktivität bei Koexpression von PID der von Wildtyp PIN1 entsprach. Dieses Ergebnis deutet darauf hin, dass S271 wichtig für die D6PK-vermittelte Transportaktivität von PIN1 ist, während PID unabhängig von diesem Serinrest agiert. Der entgegengesetzte Effekt, d.h. eine effektivere Aktivierung durch D6PK im Vergleich zu PID, wurde bei der Untersuchung einer Dreifach-Mutante beobachtet, in der die zentralen Serine innerhalb der konservierten TPRXS(N/X) durch Alanine ersetzt waren. Die unterschiedlichen Auswirkungen der S271A und der S231A/S252A/S290A Mutationen auf die Funktion von D6PK und PID weisen darauf hin, dass D6PK präferentiell an der Stelle S271 phosphoryliert, während die Aktivierung durch PID bevorzugt durch Modifikation der Serine in den TPRXS(N/X) Motiven, welche zusätzlich eine Rolle bei der polare Lokalisierung von PIN1 in pflanzlichen Zellen spielen, erreicht wird. Die Kombination der S271A und S231A/S252A/S290A Mutationen führte zum nahezu vollständigen Verlust der Aktivierbarkeit der Vierfach-Mutante. Es kann daher angenommen werden, dass die für die D6PK- bzw. PID-induzierte Transportfunktion essentiellen Aminosäurereste identifiziert wurden, wobei eine gleichzeitige Phosphorylierung aller vier Stellen nicht erforderlich für die Aktivität des Proteins ist. Vielmehr kann diese entweder durch S271-Phosphorylierung oder durch Phosphorylierung der Serine in den TPRXS(N/X) Motiven vermittelt werden.

Ein Vergleich der Transportraten, die durch Expression von PIN1 und PIN3 in Gegenwart von D6PK oder PID erzielt werden konnten, zeigte, dass PIN3 allgemein höheren Auxin Efflux verursacht als PIN1. Das beobachtete Ergebnis ist sehr gut mit der Funktion des Proteins in Tropismus-Prozessen, welche eine schnelle Umverteilung von Auxin erfordern, vereinbar. Ein Serin/Alanin-Austausch an Position 262 von PIN3, welche S271 in PIN1 entspricht, wirkte sich unter den gegebenen experimentellen Bedingungen nicht auf die Transportaktivität des Proteins bei Koexpression mit D6PK oder PID aus. Dieser Aminosäurerest spielt daher in PIN3 möglicherweise keine entscheidende Rolle für die Transportaktivität.

Zusammenfassend ist festzustellen, dass D6PK und PID die Transportaktivität von PIN Proteinen durch Phosphorylierung spezifischer Aminosäurereste regulieren. Durch Benutzung des heterologen *X. laevis* Expressionssystem konnten somit wichtige Einblicke in die biochemischen Mechanismen, die der Regulation des PIN-vermittelten Auxin Transportes zugrunde liegen, gewonnen werden.

Im zweiten Teil dieser Arbeit wurde die Rolle von Phytohormonantworten während der Interaktion zwischen pflanzenparasitischen Nematoden und ihrer Wirtspflanze untersucht. Pflanzenparasitische Nematoden, deren Wirtsspektrum eine Vielzahl von Nutzpflanzen umfasst, verursachen jährlich erhebliche Ernteausfälle. Die sedentären endoparasitischen Nematoden werden in zwei Gruppen unterteilt, die Wurzelgallennematoden (WGN) und die Zystennematoden (ZN). Die frei lebenden Larven dieser Nematoden dringen in die Wurzeln ihrer Wirtspflanze ein und induzieren in der Stele die Ausbildung spezialisierter Fütterungsstrukturen, sogenannter Riesenzellen bzw. Synzytien, durch die sie der Pflanze Nährstoffe entziehen. Sowohl Riesenzellen als auch Synzytien stellen starke terminale Sinkgewebe dar und sind somit funktionell äquivalent. Sie unterscheiden sich jedoch in ihrer Entstehung und in der Art der Nährstoffbeladung. Diese erfolgt symplastisch bei Synzytien und apoplastisch im Fall der Riesenzellen. Beide Arten von Fütterungsstrukturen sind in Leitgewebe eingebettet, welches im Verlauf der Infektion *de novo* gebildet wird. In der Umgebung der Syncytien findet man die Induktion von Phloem, das aus Siebelementen und Geleitzellen besteht, wobei das Verhältnis zu Gunsten der Siebelemente verschoben ist. Riesenzellen hingegen sind von einem einzigartigen Phloemgewebe umgeben, das ausschließlich aus Siebelementen, welche Kerne enthalten, aufgebaut ist, während Geleitzellen vollständig fehlen.

Es ist bekannt, dass ZN und WGN Auxin- und Cytokinin-ähnliche Substanzen sekretieren und dass Auxin eine wichtige Funktion bei der Etablierung der Fütterungsstrukturen in der Wirtspflanze einnimmt. Jedoch sind die Mechanismen, die der Vaskularisierung der Fütterungsstrukturen zu Grunde liegen sowie die Rolle, die Phytohormone in diesem Prozess einnehmen, weitgehend unverstanden. In der vorliegenden Arbeit sollten daher die Auxin- und Cytokinin-Antworten in infizierten Wurzeln von Arabidopsis mit Hilfe der synthetischen Hormon-induzierbaren Promotoren DR5 und TCS, welche jeweils mit der kodierenden Sequenz für ER-lokalisiertes Grün fluoreszierendes Protein (GFP) fusioniert waren, untersucht werden. Mit Hilfe immunohistochemischer Experimente und Fluoreszenz-mikroskopie wurden Zellen innerhalb der Nematoden-induzierten Gewebe, die eine Hormonantwort aufweisen, identifiziert. Dadurch konnten erste Einblicke in eine mögliche Funktion von Auxin- und Cytokinin-abhängigen Prozessen bei der Vaskularisierung Nematoden-induzierter Fütterungsstrukturen gewonnen werden. Zunächst konnte gezeigt werden, dass in nicht infizierten, differenzierten Bereichen von Kontrollwurzeln eine

konstitutive Auxin-Antwort in Geleitzellen stattfindet, es jedoch nicht zu einer Cytokinin-Antwort in vergleichbaren Bereichen von Kontrollwurzeln kommt. Weder in Riesenzellen noch in Synzytien konnte zu den in dieser Arbeit analysierten Zeitpunkten des Infektionszyklus eine Hormonantwort beobachtet werden. In den die Fütterungsstrukturen umgebenden Geweben, welche die Vaskulatur ausbilden, fand hingegen eine hormon-abhängige Expression von GFP statt. Dabei unterschieden sich die Hormonantworten in den durch ZN und WGN induzierten Geweben.

Im Fall der sich entwickelnden Wurzelgallen konnte gezeigt werde, dass eine Auxin-Antwort in den an die Riesenzellen angrenzenden proliferierenden Zellen stattfindet, bevor sich diese zu Siebelementen differenzieren. Möglicherweise fungiert der Auxin-Stimulus in diesen Zellen als Auslöser für den Differenzierungsprozess. Das GFP-Signal blieb auch in bereits differenzierten Siebelementen in vollständig entwickelten Wurzelgallen erhalten, jedoch wurden in diesen späten Stadien nur in Ausnahmefällen Zellen gefunden, die ausschließlich durch das GFP-Antiserum erkannt wurden, ohne gleichzeitig auch positiv für den Siebelement-Marker RS6 zu testen. Diese Beobachtung bestätigt, dass in vollständig vaskularisierten Wurzelgallen keine Geleitzellen vorhanden sind. In infizierten $P_{TCS}:ER\text{-}GFP$ Pflanzen konnte kein GFP-Signal in Wurzelgallen und somit keine Cytokinin-Antwort nachgewiesen werden, was einerseits auf niedrige Cytokinin-Konzentrationen unterhalb des Schwellenwertes für eine Aktivierung des synthetischen Promoters oder auf eine reduzierte Sensitivität der Zellen innerhalb der Wurzelgallen gegenüber Cytokinin zurückzuführen ist.

Im Gegensatz zu der in Wurzelgallen auftretenden Situation konnte in der Vaskulatur in der Umgebung der Zystennematoden-induzierten Synzytien sowohl eine Auxin- als auch eine Cytokinin-Atwort nachgewiesen werden. Die Auxin Antwort trat dabei sowohl in Geleitzellen als auch in Siebelementen auf, wohingegen die Cytokinin-Antwort auf die Siebelemente beschränkt war. Da die Induktion der verschiedenen Phloem-Typen in WGN- und ZN-induzierten Geweben mit einer differentiellen Hormonantwort einhergeht, ist es denkbar, dass das Verhältnis von Auxin zu Cytokinin bzw. die Stärke der einzelnen Antworten zur Identität des jeweiligen Phloems, also Protophloem in Wurzelgallen und Metaphloem in der Umgebung der Synzytien, beiträgt.

7 Material and Methods

7.1 Molecular biological work

Standard methods of molecular biology were performed according to (Sambrook *et al.*, 1989) using molecular grade reagents.

7.2 Confocal microscopy

Confocal laser scanning microscopy was performed at a Zeiss Axiovert 200 M microscope equipped with a confocal laser scanning unit LSM 510 META using the 488 nm line of the argon laser for excitation and a BP 505-550 filter for selective GFP detection.

7.3 Work with plants

7.3.1 Plant material

The *Arabidopisis thaliana* Columbia accession (Col-0) was used as a wildtype. Homozygous lines containing P_{DR5}:*ER-GFP* (Ottenschläger *et al.*, 2003) or P_{DR5}:*GUS* (Ulmasov *et al.*, 1997) were used to monitor auxin response. A homozygous line containing P_{TCS}:*ER-GFP* (Müller and Sheen, 2008) was used to monitor cytokinin response. APL promoter activity was monitored in a homozygous P_{APL}:*GUS* transgenic line (Bonke *et al.*, 2003). The P_{SUC2}:*sGFP* transgenic line is a companion cell marker line (Imlau *et al.*, 1999). P_{RS6}:*GUS* was described by Werner (2011). The auxin resistant double mutant *axr1-3 axr4-2* (Hobbie and Estelle, 1995) was obtained from ABRC. *aux1* was available as a homozygous T-DNA insertion line from Yang *et al.* (2006).

7.3.2 Growth conditions

For growth in soil, seeds were put on a mixture of 65 % substrate, 15 % sand and 10 % expanded clay. The seeds were stratified at 4 °C in the dark for two days and then transferred to plant growth chambers under long day conditions (16 hours light / 8 hours dark). For growth of plants on plates under sterile conditions, seeds were surface sterilized.

The desired amount of seeds was incubated with 700 µl of 70 % ethanol (v/v) in a 1.5 ml reaction tube for 3 min and repeatedly vortexed. Seeds were pelleted by 15 sec centrifugation and ethanol was replaced by an aquaeous solution of 1 % NaOCl (v/v) and 0.1 % Mucasol® ((v/v), Merz Consumer Care GmbH). Seeds were incubated for 2 min in this solution and the sample was centrifuged for 15 sec again. Afterwards, the seeds were washed 4 times with 1 ml of sterile H_2O by resuspension, vortexing and subsequent centrifugation for 15 sec and then dispersed in 0.1 % sterile agarose (w/v). For nematode infection, 5 to 10 seeds were placed in a row on solid Gamborg medium. Otherwise, seeds were sown out on ½ MS medium. Plates were sealed and after stratification for two days at 4 °C in the dark they were placed in an upright position in the plant growth chamber under short day conditions (8 hours light / 16 hours dark).

Solid Gamborg medium:

0.3 % Gamborg medium including vitamins ((w/v), Duchefa), 2 % sucrose (w/v),

1 % phytoagar ((w/v), Duchefa), pH was adjusted to 6.1 with KOH

Solid ½ MS medium:

0.25 % Murashige & Skoog medium including vitamins and MES buffer ((w/v), Duchefa),

1 % phytoagar ((w/v), Duchefa), pH was adjusted to 5.7 with KOH

7.3.3 Crossing of transgenic lines

For crossing auxin resistant mutant lines with P_{DR5}:ER-GFP plants, flowers of the auxin mutant lines were emasculated and pollinated with P_{DR5}:ER-GFP pollen two days later. Mature siliques were harvested and seeds were sown out on ½ MS plates (see 7.3.2). Plants that contained the P_{DR5}:ER-GFP reporter construct were identified by microscopy at the Axioskop FL epifluorescence microscope (Zeiss, excitation: BP 450 − 490, beam splitter FT 510, emission LP 520).

Homozygous lines for the mutant allels of *AXR1, AXR4* and *AUX1* were identified by PCR using the following primers:

axr1-3: *axr1-3*fw: 5'GAAACTTGATAGAATCTA3',   *AXR1*fw: 5'GAAACTTGATAGAATCTG3', *AXR1*rev: 5'TACCATCTTGGACTTAACCAAATCC3'.

axr4-2: AXR4fw: 5'GATTGAAACTGGAGATTTGCCTT3', *axr4-2*rev: 5'TCTGACGTAGGTGTC
GAAATCT3', *AXR4*rev: AGCTAAAGATGCTCTGCTCCTACCG3'.

aux1: AUX1-LP: 5'GGCTCCCGTAAAATAAAGCAC3', *AUX*1-RP: 5'AATTATCGTTGGTTTCA
GGTGG3', LB-SALK: 5'TGGTTCACGTAGTGGGCCATCG3'.

7.4 Work with *M. incognita*

7.4.1 Cultivation of *M. incognita* on tomato

M. incognita was constantly cultured under nonsterile conditions on roots of *L. esculentum* cv. Moneymaker in the greenhouse. Eggs were collected from galled roots using the NaOCl method (Hussey and Barker, 1973). Therefore, infected roots were cleaned from soil and cut into small pieces of a maximum of 1 cm. The chopped roots were shaken rigorously in 500 ml of 0.7 % NaOCl (v/v) for 3 min in order to dissolve eggs from the egg masses attached to the roots. The suspension was then filtered successively through a set of sieves with apertures of 250 µm, 45 µm and 20 µm. The 250 µm and the 45 µm sieves hold back root tissue and residual larger soil particles but allow the passage of single eggs. The sieves were washed with about 2 l of tab water and all the flow through was collected in a bowl. This washing step serves to separate eggs from the root tissue more efficiently as well as to immediately dilute the NaOCl solution. Extended exposure to NaOCl harms the eggs. Eggs were then collected on the 20 µm sieve and washed off with app. 200 ml of tab water. The collection step with the 20 µm sieve was repeated two more times to ensure efficient recovery of all eggs from the suspension. For infection of new tomato plants, the egg suspension was further concentrated by filtering it through the 20 µm sieve again and resuspending the eggs in a smaller volume of about 100 ml of tab water. Each tomato plant was infected with an inoculum of about 15000 - 20000 eggs.

7.4.2 Isolation of second-stage juveniles of *M. incognita*

For infection of *A. thaliana* with *M. incognita* on plates, second-stage juveniles (J2) were collected. Therefore, egg suspensions that were obtained from tomato plants (see 7.4.1) were used. These suspensions contain eggs of different developmental stages. To

synchronize hatching of the J2 as much as possible, the suspension was kept in the greenhouse for another week. For sufficient supply with oxygen, a cylindrical air stone that was connected to an aquarium air pump (Elite) was put into the flask containing the egg suspension. The flask was wrapped with aluminium foil to protect the eggs from light. After one week, the eggs were collected on a 20 μm sieve and resuspended in 100 ml of tab water. The eggs were then placed on a hatching device consisting of 3-4 cotton wool milk filters in a kitchen sieve that was placed on a beaker. The beaker was filled with tab water so as to just cover the bottom of the sieve. The concentrated egg suspension was carefully poured onto the milk filters and the whole device was protected from light and incubated in the greenhouse. After 24 hrs, freshly hatched J2 which had moved through the milk filters were harvested for the first time. The larvae were collected on a 20 μm sieve and resuspended in approximately 50 ml of tab water. The beaker was filled with fresh water and the harvesting procedure could be repeated two to three more times every second day. Harvested J2 were stored at 4 °C for a maximum of one week until used further.

7.4.3 Surface sterilization of second-stage juveniles

Second-stage juveniles were surface sterilized with $HgCl_2$. Freshly hatched J2 juveniles (7.4.2) were collected on a filter device and washed with sterile tab water. The filter with the larvae was then placed in a glass petri dish and filled with 0.02 % $HgCl_2$ (v/v). After 30 s, the filter was lifted with sterile tweezers to drain off the $HgCl_2$ solution. Sterilization was followed by three washing steps with sterile tab water, each time placing the filter in a new petri dish. The sterile J2 were then rinsed out from the filter into a glass petri dish with sterile tab water.

7.4.4 Infection of *A. thaliana* with *M. incognita* second-stage juveniles

For infection of *A. thaliana*, about 2.5 week old plants that were grown on plates as described in chapter 7.3.2 were used. Larvae were transferred with sterile thinned pasteur pipettes in order to allow better dosage of the larvae. For each plate, an inoculum of approximately 500 – 750 sterile J2 larvae was selected under the binocular and pipetted onto the roots. The plates were left open until the liquid had dried. Afterwards, they were

sealed and placed in the plant chamber under short day conditions in an upright position.

7.4.5 Infection of *A. thaliana* with *M. incognita* by egg mass transfer

Another possibility for infection is the transfer of egg masses from plate to plate. Therefore, plates with infected plants were kept in the growth chamber for at least 7 weeks until the life cycle of the nematodes was finished and new egg masses were formed. The plates were then opened under the clean bench and 3 to 4 egg masses were transferred to each new plate with sterile tweezers.

7.5 Work with *H. schachtii*

For a first infection of *A. thaliana*, plants that were grown on plates (se 7.3.2) for 2 weeks were sent to the HZPC Holland B.V. (Research & Development, Metslawier, Netherlands) where they were infected with second-stage juveniles of *H. schachtii*. Additionally, plates with sterile infected *S. tuberosum* plants were obtained that were used to isolate infectious larvae. In *in vitro* culture, *H. schachtii* completes its life cycle within 5 to 6 weeks. When cysts are fully developed, plates can be stored at 4 °C for several months until used further.

7.5.1 Isolation of second-stage juveniles of *H. schachtii*

In order to obtain second-stage juveniles of *H. schachtii*, cysts were collected from plates (see 7.5) and placed in sterile tab water on a sieve with a 200 µm aperture. After about 100 cysts were collected, the sieve was placed in a Bärmann funnel that was composed as follows: A piece of a plastic tube was connected to a funnel and the end of the tube was closed with a clamp. The funnel was placed in an Erlenmeyer flask and the flask was put into a beaker. The beaker was covered with aluminium foil and the whole device was autoclaved. For hatching, the sieve with the collected cysts was loosely placed on the funnel and the funnel was the filled with 3 mM $ZnCl_2$ (v/v) until the cysts were covered. $ZnCl_2$ stimulates hatching of the larvae. The hatching device was then incubated at 25 °C in the dark. Hatched larvae would migrate through the pores of the sieve and settle at the closed end of the tube. Every four days, larvae were harvested on a 20 µm sieve. Larvae were washed 3 times with

sterile water and then rinsed out from the sieve into a glass petri dish. The harvesting procedure could be repeated 2 – 3 times. Larvae were stored at 4 °C and were used for infection of *A. thaliana* within 5 days.

7.5.2 Infection of *A. thaliana* with *H. schachtii* second-stage juveniles

For infection of *A. thaliana*, about 2 week old plants were used that were grown on plates as described in chapter 7.3.1. An inoculum of app. 300 larvae (7.5.1) was transferred to each plate with a thinned sterile pasteur pipette. Plates were left open until the liquid had dried. They were then sealed with Leukopor tape and placed in the plant chamber under short day conditions in an upright position.

7.6 Work with nematode infected plant material

7.6.1 GUS staining

For GUS staining of nematode infected roots, root segments with infection sites were isolated from plates and transferred to GUS staining solution. The samples were then incubated at 37 °C until the staining was clearly visible. Afterwards, they were washed 3 times in $NaPO_4$ buffer (pH 7.2) and were analyzed by brightfield microscopy at the Discovery V8 Zoom Stereo Microscope (Zeiss) or at the Axioskop FL epifluorescence microscope (Zeiss).

GUS staining solution:
0.05 M $NaPO_4$ pH 7.2, 0.5 mM $K_3Fe(CN)_6$, 0.5 mM $K_4Fe(CN)_6$, 1 % Triton X-100 (v/v), 1.25 mM X-Gluc

7.6.2 Sectioning of GUS-stained tissue

In order to prepare cross sections of GUS-stained tissue, samples were emdebbed in 0,5 % low melting agarose in 0.05 mM KPO_4 buffer(pH 7.0) in a 24 well plate. Sections of 60 µm thickness were prepared at a vibratome 1500 series sectioning system (The Vibratome Company).

7.6.3 Immunohistochemistry

Immunohistochemical experiments were performed based on the description by (Stadler and Sauer, 1996)

7.6.3.1 Fixation and embedding of plant tissue in methacrylate

All steps of the fixation and embedding procedure were done at 4 °C. Fixation, dehydration and infiltration with methacrylate were performed in 1.5 ml tubes. For changing solutions, pasteur pipettes with thinned ends were used. Uninfected roots or root segments containing nematode induced feeding sites were isolated from plates and fixed in 1 ml of ethanol p.A. / acetic acid (3:1) for 1.5 hrs in total. After 30 min, the fixing solution was changed. After fixation, the samples were washed 3 times with 70 % ethanol (v/v). Before embedding, the 70 % ethanol solution was replaced by 70 % ethanol containing 1 mM DTT and the samples were incubated over night at 4 °C. The samples were then dehydrated by 3 successive 20 min incubation steps in 1 ml of 85 %, 90 % and 95 % ethanol (v/v) supplemented with 1 mM DTT followed by two final 30 min incubation steps in 100 % ethanol with 10 mM DTT. After dehydration, the samples were slowly infiltrated with methacrylate-mix. The methacrylate-mix was fumigated with nitrogen gas for 20 min before each use in order to remove dissolved oxygen. For infiltration, the samples were successively incubated for at least 6 hrs each in ethanol p.A. with 10 mM DTT / methacrylate-mix in a ratio of 2:1, 1:1 and 1:2. Afterwards, two incubation steps for at least 6 hrs in methacrylate-mix and a final 24 hrs incubation in methacrylate-mix were carried out. For polymerization, the tissue samples were transferred to ultrathin PCR tubes with cone-shaped lids (Biozym Scientific GmbH). The tubes were completely filled with methacrylate-mix and were then closed with the cut off lids upside down. Polymerization of the methacrylate was achieved by irridating the samples with UV light (302 nm) for 15 hrs at 4 °C.

Methacrylate-mix:
75 % butyl methacrylate (v/v), 25 % methyl methacrylate (v/v), 0.5 % benzoin ethyl ether (w/v), 10 mM DTT

7.6.3.2 Sectioning of embedded tissue

Plastic tubes were removed from the embedded samples and sections of 2.5 – 3 µm were prepared on a Reichert Om U2 microtome (Reichert Austria, now Leica) with glass knifes. The knifes were broken from glass stripes with a LKB 7800 B knife maker (W. Reichert Labtech). Sections were collected and transferred into a drop of H_2O bidest on adhesive polysine® microscope slides (Thermo Scientific) which were then placed on a heatable stretching desk at 50 °C until the water had evaporated.

7.6.3.3 Immunolocalization

For removal of methacrylate, the slides with the attached sections were treated for 2 min with 100 % acetone (p.A) in a glass staining box. Afterwards, the sections were rehydrated by 5 subsequent 2 min incubation steps in ethanol (p.A) of decreasing concentrations (100 %, 85 %, 70 %, 50 % and 30 % (v/v)). The slides were then washed 3 times for 1 min with TBS and blocked for 30 min in blocking solution (TBS, 1 % milk powder (w/v), 0.1 % Triton X-100 (v/v)). Within these 30 min, blocking solution was changed twice. Before incubation with the primary antibodies, the microscope slides were briefly dried. Primary antibodies were diluted to the relevant concentration in blocking solution in a total volume of 40 µl per slide and the solution was pipetted under cover slides that had been placed over the sections on little pieces of plasticine. Incubation was carried out in a wet chamber at 4 °C over night. Next day, the cover slides were removed and the microscope slides were washed for 30 min with blocking solution. Blocking solution was changed four times during the washing procedure. As secondary antibodies, Cy2 or Cy3 labeled conjugates (see Table 1) were used. Decoration was performed as described for the primary antibodies and the samples were incubated in the wet chamber for at least 45 min at room temperature in the dark. Incubation with the secondary antibodies was followed by extensive washing with blocking solution for 30 min. The solution was changed eight times and all the washing steps were carried out in the dark. Last, the slides where washed three times for 1 min with TBS in the dark. Then they were dried briefly and mounted in 50 % glycerol in TBS. Microscopy was performed at the Axioskop FL epifluorescence microscope (Zeiss) using the Zeiss filter sets no. 46 (Cy2, excitation: BP 500/20, beam splitter: FT 515, emission: BP 535/30) and no. 15 (Cy3, excitation: BP 546/12, beam splitter: FT 580, emission: LP 590).

Table 1 Primary and secondary antibodies used for immunolocalizations.

	Antibodies	Dilution
anti-RS6	affinity purified from mouse monoclonal antiserum (Meyer *et al.*, 2004; Khan *et al.*, 2007)	1:10
anti-GFP	IgG fraction purified from rabbit polyclonal antiserum (Pineda Antikörper-Service)	1:100
anti-mouse-Cy3	Cy3-conjugated AffiniPure goat anti-mouse IgG (Dianova)	1:80
anti-rabbit-Cy2	Cy2-conjugated AffiniPure goat anit-rabbit IgG (Dianova)	1:40

TBS:

50 mM Tris-Cl pH 7.5, 150 mM NaCl

7.7 Work with *X. laevis* oocytes

7.7.1 Oocyte material

X. laevis oocytes of stages V and VI that were ready-to-use for injection were provided by Prof. Dr. Hannelore Daniel from the Research Department of Food and Nutrition at the Center of Life and Food Sciences Weihenstephan on a weekly basis. The oocytes were kept at 16 °C in Barth's solution (pH 7.4) supplemented with 0.2 % BSA (w/v) and 50 µg/l gentamycin.

Barth's solution:

88 mM NaCl, 1 mM KCl, 2.4 mM $NaHCO_3$, 10 mM HEPES-NaOH, 0.33 mM $Ca(NO_3)_2$ x 4 H_2O, 0.41 mM $CaCl_2$ x 2 H_2O, 0.82 mM $MgSO_4$ x 7 H_2O, pH was adjusted to 7.4 with NaOH

7.7.2 Synthesis of mRNA for injection

mRNA for injection into oocytes was synthesized by *in vitro* transcription. All cDNAs were cloned into the pOO2 (Ludewig *et al.,* 2002) plasmid by Zourelidou *et al.* (unpublished). The pOO2 plasmid contains a SP6 RNA polymerase promoter sequence followed by a MCS for insertion of the cDNA and the 3'-UTR of the *X. laevis* major beta-globin gene that causes enhanced stability of the mRNA in oocytes. In 3' position of the beta-globin gene fragment, a sequence fragment with multiple adenines that will lead to polyadenylation of the mRNA is inserted into the vector. Before starting the transcription reaction, 15 μg of the plasmids were linearized in an overnight digestion with an enzyme that cuts directly behind the poly-A sequence in order to prevent to long transcripts in the *in vitro* reaction. The linearized vector was purified by phenol/chloroform extraction and DNA concentration was determined using a NanoDrop ND1000 (Thermo Scientific). 1 μg of the linear DNA was used for *in vitro* synthesis of capped mRNA with the mMessage mMachine® Kit (Ambion) following the manufacturer's instructions. In order to achieve high yield, the reaction was incubated for 2 hrs at 37 °C as recommended for SP6 reactions. After mRNA synthesis, template DNA was removed by adding 1 μl of TURBO DNase to the sample and incubating for 15 min at 37 °C. Subsequently, the mRNA was purified from the transcription reaction with the MEGAclear™ Kit (Ambion) following the manufacturer's instructions. The mRNA was eluted in 50 μl of elution buffer and the concentration was measured at the NanoDrop ND1000. The quality of the mRNA was checked by loading 2 μl of the sample on a 1 % agarose gel.

7.7.3 mRNA injection

For transient heterologous expression of proteins in oocytes, purified mRNA that was obtained as described in 7.7.2 was injected into the oocytes with a Nanoject II (Drummond Scientific Company) the day after the oocytes were isolated from *X. laevis* females. Injection needles were pulled from Nanoject II 3.5" replacement glass capillaries (Drummond Scientific Company) at a P-97 Flaming/Brown micropipette puller (Sutter Instrument) with the following settings: velocity = 120, heat = 500, pull = 30, time = 200. Pulled capillaries were broken so that the aperture at the tip was app. 20 μm. Before injection, mRNAs that encoded for PIN proteins were diluted to a concentration of 300 ng/μl; mRNAs encoding for

kinases where diluted to 150 ng/µl. If PIN- and kinase-encoding mRNAs were co-injected, the dilutions were mixed in a ratio of 1:1, if a PIN mRNA was injected alone, the sample was mixed 1:1 with RNase-free H_2O. Each oocyte was injected with app. 50 nl of mRNA solution or H_2O only in case of control oocytes. After injection, oocytes were transferred to Barth's solution supplemented with 0.2 % BSA (w/v) and 50 µg/l gentamycin and were kept at 16 °C.

7.7.4 Efflux assay with [^{3}H-IAA]

For measuring IAA efflux from oocytes, [^{3}H]-labeled IAA was injected into oocytes and the decrease of radioactivity over time was determined. Efflux assays were performed 4 days after mRNA injection (see 7.7.3). During this time, buffer solution was changed every day and dead oocytes were sorted out. The day before the efflux experiments, oocytes were put in Barth's solution with 50 µg/l gentamycin (Barth's + Gent) but without BSA. For the efflux assay, [^{3}H]-IAA with a specific activity of 20 Ci/mmol and a concentration of 1µCi/µl (American Radiolabeled Chemicals) was diluted 1:5 in Barth's + Gent and app. 50 nl of this dilution were injected into each oocyte, resulting in an internal [^{3}H]-IAA concentration between 1 µM and 1.5µM. When NPA was co-injected, it was diluted to the relevant concentration in the injection solution from a 10 mM stock in DMSO. The solution for injection of control oocytes was supplemented with the equivalent amount of DMSO. Injection on a precooled metal block was performed as described for mRNA in chapter 7.7.3. 10 to 12 oocytes were injected per time point and 4 to 5 time points were measured. After having injected the oocytes for one time point, they were immediately transferred to 3 ml ice-cold Barth's + Gent in one well of a 12-well plate and incubated on ice for 10 min to allow diffusion of the substrate and closure of the injection wound. Afterwards, they were washed in 3 ml ice-cold Barth's + Gent. For sampling of time point 0 min, individual oocytes were transferred directly from the washing solution to scintillation vials. For sampling the other time points, oocytes were transferred from the washing solution to 3 ml Barth's + Gent in a new 12-well plate at room temperature. If required, the solution was supplemented with 10 µM NPA out of a 10 mM stock in DMSO or with the equivalent amount of DMSO only as a control. After the desired incubation time, the oocytes were again washed in 3 ml Barth's + Gent and transferred to scintillation vials individually. By addition of 100 µl of 10 % SDS (w/v) and subsequent incubation for at least 15 min oocytes were dissolved. The scintillation vials

were then filled with 5 ml of scintillation cocktail (Rotiszint® eco plus, Roth) and vortexed rigorously. The amount of radioactivity in each oocyte was determined by liquid scintillation counting in a Beckman LS 6000 SC counter.

Blotting of data and statistical analysis was performed using the SigmaPlot 11.0 software (Systat Software Inc) with default settings.

7.7.5 Membrane preparation from oocytes

Isolation of proteins from *X. laevis* oocytes and separation of membrane proteins from cytosolic proteins was basically done as described by Bröer (2010). Briefly, up to 25 oocytes were homogenized in homogenization buffer by trituration with a blue tip on ice. Unless stated otherwise, 40 µl of homogenization buffer were used per oocyte. The homogenate was centrifuged at 2000 x g for 10 min at 4 °C and the supernatant was transferred to a 1.5 ml polyallomer microfuge® tube (Beckman Instruments). Membrane proteins were pelleted at 150,000 x g for 30 min at 4 °C in a Beckman Optima™ TL ultracentrifuge. After centrifugation, the supernatant was transferred to a new eppendorf cup and the pellet was resuspended in homogenization buffer supplemented with 4 % SDS (w/v) in a volume of 8 µl per initially used oocyte. In case of subsequent analysis of the phosphorylation status on a Western Blot, the homogenization buffer was supplemented with phophatase inhibitors (PhosStop phophatase inhibitor cocktail tablets, Roche) and the samples were immediately subjected to SDS-PAGE. Otherwise, samples were stored at -20 °C.

<u>Homogenization buffer:</u>

50 mM Tris-Cl pH 7,5, 100 mM NaCl, 1mM EDTA, 1 mM Pefabloc

7.7.6 Western Blot analysis

7.7.6.1 SDS-PAGE

Separation of proteins was achieved by SDS-PAGE according to Laemmli (Laemmli, 1970) in a *Protean Cell III* (BioRad). SDS-PAGE was performed at currents between 160 and 200 V on either 8% or 10 % acrylamide gels. Before loading, samples were mixed with 1/6 of 6 fold loading dye. Samples with cytosolic proteins were boiled for 5 min at 95 °C whereas samples containing membrane fractions were incubated for 15 min at 42 °C.

Resolving gel:

0,375 M Tris-Cl pH 8.8, X % 30 % Acrylamide/0.8 % Bisacrylamide, 0.1 % SDS (w/v), 0.05 % TEMED (v/v), 300 µg/ml APS

Stacking gel:

0.125 M Tris-Cl pH 6.8, 5 % 30 % Acrylamide/0.8 % Bisacrylamide, 0.1 % SDS (w/v), 0.04 % TEMED (v/v), 450 µg/ml APS

6x loading dye:

250 m M Tris-Cl pH 6.8, 50 % Glycerol (v/v), 10 % SDS (w/v), 5 % EtSH (v/v), 0.03 % Bromphenolblue (w/v)

SDS running buffer:

25 mM Tris-Base, 192 mM Glycine, 0.1 % SDS (v/v)

7.7.6.2 Wet Blot

Proteins that had been separated by SDS-PAGE before were transferred onto a nitrocellulose membrane in a *Protean Cell III* (BioRad) via Wet Blot procedure. The blot was assembled according to the manufacturer's instructions and transfer was done for 90 min at 150 mA. After blotting, the membrane was shortly stained with Ponceau in order to mark the lanes and subsequently destained with H_2O bidest. For saturation of unspecific binding sites, the membrane was incubated in blocking solution (TBS, 5 % milk powder (w/v), 0.2 % Tween (v/v)) for at least 45 min. After washing the membrane 3 times for 10 min in TBS, it was

incubated with the primary antibody in the appropriate dilution in 5 ml TBS with 1 % milk powder (w/v) at 4 °C over night. Next day, the membrane was washed 3 times with TBS-T (TBS, 0.2 % Tween (v/v)) and was then incubated with the secondary antibody for 60 min at room temperature. Afterwards, the membrane was washed with washing solution (TBS, 1 % milk powder (w/v), 0.2 % Tween (v/v)) for 15 min, followed by two 10 min washing steps with TBS-T and TBS, respectively. For detection of antigen-antibody-HRP complexes, the enhancer solution HRP-juice (PJK GmbH) was used.

Table 2 Primary and secondary antibodies used for Western Blot analysis

Antibodies		Dilution
anti-GFP	IgG fraction purified from rabbit polyclonal antiserum (Pineda Antikörper-Service)	1:2000
anti-PIN1	crude sheep antiserum (NASC N782245)	1:5000
anti-PIN3	crude sheep antiserum (NASC N782251)	1:3000
anti-UNC	IgG fraction purified from rabbit polyclonal antiserum (Enugutti *et al.*, 2012)	1:2000
anti-PHOT1	rabbit polyclonal antiserum (Inoue *et al.*, 2008)	1:1000
anti-PHOT1-pS-851	rabbit polyclonal antiserum (Inoue *et al.*, 2008)	1:1000
anti-rabbit	goat anti-rabbit IgG-HRP (Santa Cruz)	1:1000 to 1:5000
anti-sheep	donkey anti-sheep IgG-HRP (Dianova)	1:5000

Transfer buffer:

48 mM Tris-Base, 39 mM Glycine, 20 % Methanol (v/v), 0.037 % SDS (w/v)

8   Bibliography

Absmanner, B., Stadler, R. and Hammes, U.Z. (2013). "Phloem development in nematode-induced feeding sites: The implications of auxin and cytokinin." Front. Plant Sci. 4:241.

Aida, M., Beis, D., Heidstra, R., Willemsen, V., Blilou, I., Galinha, C., Nussaume, L., Noh, Y.-S., Amasino, R. and Scheres, B. (2004). "The PLETHORA Genes Mediate Patterning of the Arabidopsis Root Stem Cell Niche." Cell 119(1): 109-120.

Aloni, R., Pradel, K. and Ullrich, C. (1995). "The three-dimensional structure of vascular tissues in Agrobacterium tumefaciens-induced crown galls and in the host stems of Ricinus communis L." Planta 196(3): 597-605.

An, H., Roussot, C., Suarez-Lopez, P., Corbesier, L., Vincent, C., Pineiro, M., Hepworth, S., Mouradov, A., Justin, S., Turnbull, C. and Coupland, G. (2004). "CONSTANS acts in the phloem to regulate a systemic signal that induces photoperiodic flowering of Arabidopsis." Development 131(15): 3615-3626.

Andersen, J. B., Sternberg, C., Poulsen, L. K., Bjorn, S. P., Givskov, M. and Molin, S. (1998). "New unstable variants of green fluorescent protein for studies of transient gene expression in bacteria." Appl Environ Microbiol 64(6): 2240-2246.

Balasubramanian, M. and Rangaswami, G. (1962). "Presence of indole compound in nematode galls." Nature 194: 774-775.

Barbez, E., Kubes, M., Rolcik, J., Beziat, C., Pencik, A., Wang, B., Rosquete, M. R., Zhu, J., Dobrev, P. I., Lee, Y., Zazimalova, E., Petrasek, J., Geisler, M., Friml, J. and Kleine-Vehn, J. (2012). "A novel putative auxin carrier family regulates intracellular auxin homeostasis in plants." Nature 485(7396): 119-122.

Barker, K. R. and Koenning, S. R. (1998). "Developing sustainable systems for nematode management." Annu Rev Phytopathol 36: 165-205.

Bauby, H., Divol, F., Truernit, E., Grandjean, O. and Palauqui, J. C. (2007). "Protophloem differentiation in early Arabidopsis thaliana development." Plant Cell Physiol 48(1): 97-109.

Benjamins, R., Quint, A., Weijers, D., Hooykaas, P. and Offringa, R. (2001). "The PINOID protein kinase regulates organ development in Arabidopsis by enhancing polar auxin transport." Development 128(20): 4057-4067.

Benkova, E., Michniewicz, M., Sauer, M., Teichmann, T., Seifertova, D., Jurgens, G. and Friml, J. (2003). "Local, efflux-dependent auxin gradients as a common module for plant organ formation." Cell 115(5): 591-602.

Berleth, T. and Jürgens, G. (1993). "The role of the monopteros gene in organising the basal body region of the Arabidopsis embryo." Development 118: 575-587.

Bird, A. F. (1962). "The Inducement of Giant Cells By Meloidogyne Javanica." Nematologica 8(1): 1-10.

Bird, A. F. and Loveys, B. R. (1980). "The involvement of cytokinins in a host-parasite relationship between the tomato (Lycopersicon esculentum) and a nematode (Meloidogyne javanica)." Parasitology 80(03): 497-505.

Bird, D. M. (1996). "Manipulation of host gene expression by root-knot nematodes." The Journal of Parasitology 82: 881-888.

Bishopp, A., Benkova, E. and Helariutta, Y. (2011a). "Sending mixed messages: auxin-cytokinin crosstalk in roots." Curr Opin Plant Biol 14(1): 10-16.

Bishopp, A., Help, H., El-Showk, S., Weijers, D., Scheres, B., Friml, J., Benkova, E., Mahonen, A. P. and Helariutta, Y. (2011b). "A Mutually Inhibitory Interaction between Auxin and Cytokinin Specifies Vascular Pattern in Roots." Current Biology 21(11): 917-926.

Bishopp, A., Lehesranta, S., Vaten, A., Help, H., El-Showk, S., Scheres, B., Helariutta, K., Mähönen, A. P., Sakakibara, H. and Helariutta, Y. (2011c). "Phloem-Transported Cytokinin Regulates Polar Auxin Transport and Maintains Vascular Pattern in the Root Meristem." Current Biology 21(11): 927-932.

Blakeslee, J. J., Bandyopadhyay, A., Lee, O. R., Mravec, J., Titapiwatanakun, B., Sauer, M., Makam, S. N., Cheng, Y., Bouchard, R., Adamec, J. A., Geisler, M., Nagashima, A., Sakai, T., Martinoia, E., Friml, J. Ã., Peer, W. A. and Murphy, A. S. (2007). "Interactions among PIN-FORMED and P-Glycoprotein Auxin Transporters in Arabidopsis." The Plant Cell Online 19(1): 131-147.

Bleve-Zacheo, T. and Melillo, M. T. (1997). The biology of giant-cells. Cellular and Molecular Aspects of Plant-Nematode Interactions. C. Fenoll, F. M. W. Grundler and S. A. Ohl. Dordrecht, The Netherlands, Kluwer Academic Publishers: 65-79.

Blilou, I., Xu, J., Wildwater, M., Willemsen, V., Paponov, I., Friml, J., Heidstra, R., Aida, M., Palme, K. and Scheres, B. (2005). "The PIN auxin efflux facilitator network controls growth and patterning in Arabidopsis roots." Nature 433(7021): 39-44.

Bockenhoff, A., Prior, D. A., Grundler, F. M. and Oparka, K. J. (1996). "Induction of phloem unloading in Arabidopsis thaliana roots by the parasitic nematode Heterodera schachtii." Plant Physiol 112(4): 1421-1427.

Bögre, L., Ökresz, L., Henriques, R. and Anthony, R. G. (2003). "Growth signalling pathways in Arabidopsis and the AGC protein kinases." Trends in Plant Science 8(9): 424-431.

Bonke, M., Thitamadee, S., Mahonen, A. P., Hauser, M.-T. and Helariutta, Y. (2003). "APL regulates vascular tissue identity in Arabidopsis." Nature 426(6963): 181-186.

Boorer, K. J., Frommer, W. B., Bush, D. R., Kreman, M., Loo, D. D. and Wright, E. M. (1996). "Kinetics and specificity of a H+/amino acid transporter from Arabidopsis thaliana." J Biol Chem 271(4): 2213-2220.

Bröer, S. (2010). *Xenopus laevis* Oocytes. Membrane Transporters in Drug Discovery and Development, Methods and Protocols. Q. Yan, Humama Press: 295-310.

Cambridge, A. and Morris, D. (1996). "Transfer of exogenous auxin from the phloem to the polar auxin transport pathway in pea (Pisum sativum L.)." Planta 199(4): 583-588.

Chapman, E. J. and Estelle, M. (2009). "Mechanism of Auxin-Regulated Gene Expression in Plants." Annu Rev Genet 43: 265–285.

Chen, R., Hilson, P., Sedbrook, J., Rosen, E., Caspar, T. and Masson, P. H. (1998). "The Arabidopsis thaliana AGRAVITROPIC 1 gene encodes a component of the polar-auxin-transport efflux carrier." Proceedings of the National Academy of Sciences 95(25): 15112-15117.

Cox, D. N. and Muday, G. K. (1994). "NPA binding activity is peripheral to the plasma membrane and is associated with the cytoskeleton." The Plant Cell Online 6(12): 1941-1953.

D'Agostino, I. B., Deruere, J. and Kieber, J. J. (2000). "Characterization of the response of the Arabidopsis response regulator gene family to cytokinin." Plant Physiol 124(4): 1706-1717.

Dai, M., Zhang, C., Kania, U., Chen, F., Xue, Q., McCray, T., Li, G., Qin, G., Wakeley, M., Terzaghi, W., Wan, J., Zhao, Y., Xu, J., Friml, J. Ã., Deng, X. W. and Wang, H. (2012). "A PP6-Type Phosphatase Holoenzyme Directly Regulates PIN Phosphorylation and Auxin Efflux in Arabidopsis." The Plant Cell Online 24(6): 2497-2514.

Darwin, C. and Darwin, F. (1880). The power of movement in plants. London, John Murray.

Davies, P. J. (2010). The Plant Hormones: Their Nature, Occurrence, and Functions. Plant Hormones. P. Davies, Springer Netherlands: 1-15.

Davis, E. L., Hussey, R. S., Baum, T. J., Bakker, J., Schots, A., Rosso, M. N. and Abad, P. (2000). "Nematode Parasitism Genes." Annu Rev Phytopathol 38: 365-396.

de Almeida Engler, J., Favery, B., Engler, G. and Abad, P. (2005). "Loss of susceptibility as an alternative for nematode resistance." Curr Opin Biotechnol 16(2): 112-117.

De Meutter, J., Tytgat, T., Witters, E., Gheysen, G., Van Onckelen, H. and Gheysen, G. (2003). "Identification of cytokinins produced by the plant parasitic nematodes Heterodera schachtii and Meloidogyne incognita." Molecular Plant Pathology 4(4): 271-277.

Decraemer, W. and Hunt, D. J. (2006). Structure and classification. Plant nematology R. N. Perry and M. Moens, CAB eBooks: 3-32

Delbarre, A., Müller, P. and Guern, J. (1998). "Short-Lived and Phosphorylated Proteins Contribute to Carrier-Mediated Efflux, but Not to Influx, of Auxin in Suspension-Cultured Tobacco Cells." Plant Physiology 116(2): 833-844.

Delbarre, A., Müller, P., Imhoff, V. and Guern, J. (1996). "Comparison of mechanisms controlling uptake and accumulation of 2,4-dichlorophenoxy acetic acid, naphthalene-1-acetic acid, and indole-3-acetic acid in suspension-cultured tobacco cells." Planta 198(4): 532-541.

Dello Ioio, R., Linhares, F. S., Scacchi, E., Casamitjana-Martinez, E., Heidstra, R., Costantino, P. and Sabatini, S. (2007). "Cytokinins Determine Arabidopsis Root-Meristem Size by Controlling Cell Differentiation." Current Biology 17(8): 678-682.

Dharmasiri, N., Dharmasiri, S. and Estelle, M. (2005). "The F-box protein TIR1 is an auxin receptor." Nature 435(7041): 441-445.

Dhonukshe, P., Huang, F., Galvan-Ampudia, C. S., Mähönen, A. P., Kleine-Vehn, J., Xu, J., Quint, A., Prasad, K., Friml, J., Scheres, B. and Offringa, R. (2010). "Plasma membrane-bound AGC3 kinases phosphorylate PIN auxin carriers at TPRXS(N/S) motifs to direct apical PIN recycling." Development 137(19): 3245-3255.

Dhonukshe, P., Tanaka, H., Goh, T., Ebine, K., Mahonen, A. P., Prasad, K., Blilou, I., Geldner, N., Xu, J., Uemura, T., Chory, J., Ueda, T., Nakano, A., Scheres, B. and Friml, J. (2008). "Generation of cell polarity in plants links endocytosis, auxin distribution and cell fate decisions." Nature 456(7224): 962-966.

Ding, Z., Galvan-Ampudia, C. S., Demarsy, E., Langowski, L., Kleine-Vehn, J., Fan, Y., Morita, M. T., Tasaka, M., Fankhauser, C., Offringa, R. and Friml, J. (2011). "Light-mediated polarization of the PIN3 auxin transporter for the phototropic response in Arabidopsis." Nat

Cell Biol 13(4): 447-452.

Ding, Z. J., Wang, B. J., Moreno, I., Duplakova, N., Simon, S., Carraro, N., Reemmer, J., Pencik, A., Chen, X., Tejos, R., Skupa, P., Pollmann, S., Mravec, J., Petrasek, J., Zazimalova, E., Honys, D., Rolcik, J., Murphy, A., Orellana, A., Geisler, M. and Friml, J. (2012). "ER-localized auxin transporter PIN8 regulates auxin homeostasis and male gametophyte development in Arabidopsis." Nature Communications 3: 941.

Dixon, M. W., Jacobson, J. A., Cady, C. T. and Muday, G. K. (1996). "Cytoplasmic Orientation of the Naphthylphthalamic Acid-Binding Protein in Zucchini Plasma Membrane Vesicles." Plant Physiology 112(1): 421-432.

Dolan, L., Janmaat, K., Willemsen, V., Linstead, P., Poethig, S., Roberts, K. and Scheres, B. (1993). "Cellular organisation of the Arabidopsis thaliana root." Development 119: 71-84.

Donaldson, J. G. and Jackson, C. L. (2000). "Regulators and effectors of the ARF GTPases." Curr Opin Cell Biol 12(4): 475-482.

Donner, T. J. and Scarpella, E. (2009). "Auxin-transport-dependent leaf vein formationThis paper is one of a selection published in a Special Issue comprising papers presented at the 50th Annual Meeting of the Canadian Society of Plant Physiologists (CSPP) held at the University of Ottawa, Ontario, in June 2008." Botany 87(7): 678-684.

Elo, A., Immanen, J., Nieminen, K. and Helariutta, Y. (2009). "Stem cell function during plant vascular development." Seminars in Cell & Developmental Biology 20(9): 1097-1106.

Enugutti, B., Kirchhelle, C., Oelschner, M., Torres Ruiz, R. A., Schliebner, I., Leister, D. and Schneitz, K. (2012). "Regulation of planar growth by the Arabidopsis AGC protein kinase UNICORN." Proc Natl Acad Sci U S A 109(37): 15060-15065.

Esau, K. (1965). "Vascular differentiation in plants." New York, Holt, Rinehart, and Winston.

Esau, K. (1969). „The phloem." Berlin, Stuttgart, Gebr. Borntraeger.

Feraru, E. and Friml, J. (2008). "PIN polar targeting." Plant Physiol 147(4): 1553-1559.

Fester, T., Berg, R. H. and Taylor, C. G. (2008). "An easy method using glutaraldehyde-introduced fluorescence for the microscopic analysis of plant biotrophic interactions." Journal of Microscopy 231(2): 342-348.

Friml, J. (2003). "Auxin transport — shaping the plant." Current Opinion in Plant Biology 6(1): 7-12.

Friml, J., Benkova, E., Blilou, I., Wisniewska, J., Hamann, T., Ljung, K., Woody, S., Sandberg, G., Scheres, B., Jurgens, G. and Palme, K. (2002a). "AtPIN4 mediates sink-driven auxin gradients and root patterning in Arabidopsis." Cell 108(5): 661-673.

Friml, J., Vieten, A., Sauer, M., Weijers, D., Schwarz, H., Hamann, T., Offringa, R. and Jurgens, G. (2003). "Efflux-dependent auxin gradients establish the apical-basal axis of Arabidopsis." Nature 426(6963): 147-153.

Friml, J., Wisniewska, J., Benkova, E., Mendgen, K. and Palme, K. (2002b). "Lateral relocation of auxin efflux regulator PIN3 mediates tropism in Arabidopsis." Nature 415(6873): 806-809.

Friml, J., Yang, X., Michniewicz, M., Weijers, D., Quint, A., Tietz, O., Benjamins, R., Ouwerkerk, P. B. F., Ljung, K., Sandberg, G., Hooykaas, P. J. J., Palme, K. and Offringa, R. (2004). "A PINOID-Dependent Binary Switch in Apical-Basal PIN Polar Targeting Directs Auxin Efflux." Science 306(5697): 862-865.

Galvan-Ampudia, C. S. and Offringa, R. (2007). "Plant evolution: AGC kinases tell the auxin tale." Trends Plant Sci 12(12): 541-547.

Gälweiler, L., Guan, C., Müller, A., Wisman, E., Mendgen, K., Yephremov, A. and Palme, K. (1998). "Regulation of polar auxin transport by AtPIN1 in Arabidopsis vascular tissue." Science 282(5397): 2226-2230.

Geisler, M., Blakeslee, J. J., Bouchard, R., Lee, O. R., Vincenzetti, V., Bandyopadhyay, A., Titapiwatanakun, B., Peer, W. A., Bailly, A., Richards, E. L., Ejendal, K. F. K., Smith, A. P., Baroux, C., Grossniklaus, U., Müller, A., Hrycyna, C. A., Dudler, R., Murphy, A. S. and Martinoia, E. (2005). "Cellular efflux of auxin catalyzed by the Arabidopsis MDR/PGP transporter AtPGP1." The Plant Journal 44(2): 179-194.

Geldner, N., Friml, J., Stierhof, Y.-D., Jurgens, G. and Palme, K. (2001). "Auxin transport inhibitors block PIN1 cycling and vesicle trafficking." Nature 413(6854): 425-428.

Gheysen, G. and Fenoll, C. (2002). "Gene expression in nematode feeding sites." Annu Rev Phytopathol 40: 191-219.

Golinowski, W., Grundler, F. M. W. and Sobczak, M. (1996). "Changes in the structure ofArabidopsis thaliana during female development of the plant-parasitic nematode Heterodera schachtii." Protoplasma 194(1-2): 103-116.

Golinowski, W., Sobczak, M., Kurek, W. and Grymaszewska, G. (1997). The structure of syncytia. Cellular and Molecular Aspects of Plant-Nematode Interactions. C. Fenoll, F. M. W.

Grundler and S. A. Ohl. Dordrecht, The Netherlands, Kluwer Academic Publishers: 80-97.

Goverse, A., Overmars, H., Engelbertink, J., Schots, A., Bakker, J. and Helder, J. (2000). "Both induction and morphogenesis of cyst nematode feeding cells are mediated by auxin." Mol Plant Microbe Interact 13(10): 1121-1129.

Grunewald, W., Cannoot, B., Friml, J. and Gheysen, G. (2009a). "Parasitic nematodes modulate PIN-mediated auxin transport to facilitate infection." PLoS Pathog 5(1): e1000266.

Grunewald, W. and Friml, J. (2010). "The march of the PINs: developmental plasticity by dynamic polar targeting in plant cells." Embo J 29(16): 2700-2714.

Grunewald, W., van Noorden, G., Van Isterdael, G., Beeckman, T., Gheysen, G. and Mathesius, U. (2009b). "Manipulation of auxin transport in plant roots during Rhizobium symbiosis and nematode parasitism." Plant Cell 21(9): 2553-2562.

Hamann, T., Benkova, E., Bäurle, I., Kientz, M. and Jürgens, G. (2002). "The Arabidopsis BODENLOS gene encodes an auxin response protein inhibiting MONOPTEROS-mediated embryo patterning." Genes & Development 16(13): 1610-1615.

Hamann, T., Mayer, U. and Jurgens, G. (1999). "The auxin-insensitive bodenlos mutation affects primary root formation and apical-basal patterning in the Arabidopsis embryo." Development 126(7): 1387-1395.

Hammes, U. Z., Schachtman, D. P., Berg, R. H., Nielsen, E., Koch, W., McIntyre, L. M. and Taylor, C. G. (2005). "Nematode-induced changes of transporter gene expression in Arabidopsis roots." Mol Plant Microbe Interact 18(12): 1247-1257.

Hardtke, C. S. and Berleth, T. (1998). "The Arabidopsis gene MONOPTEROS encodes a transcription factor mediating embryo axis formation and vascular development." EMBO J 17(5): 1405-1411.

Hobbie, L. and Estelle, M. (1995). "The axr4 auxin-resistant mutants of Arabidopsis thaliana define a gene important for root gravitropism and lateral root initiation." Plant J 7(2): 211-220.

Hoth, S., Schneidereit, A., Lauterbach, C., Scholz-Starke, J. and Sauer, N. (2005). "Nematode infection triggers the de novo formation of unloading phloem that allows macromolecular trafficking of green fluorescent protein into syncytia." Plant Physiol 138(1): 383-392.

Hoth, S., Stadler, R., Sauer, N. and Hammes, U. Z. (2008). "Differential vascularization of nematode-induced feeding sites." Proc Natl Acad Sci U S A 105(34): 12617-12622.

Huang, F., Kemel Zago, M., Abas, L., van Marion, A., GalvÃ¡n-Ampudia, C. S. and Offringa, R. (2010). "Phosphorylation of Conserved PIN Motifs Directs Arabidopsis PIN1 Polarity and Auxin Transport." The Plant Cell Online 22(4): 1129-1142.

Hussey, R. and Barker, K. (1973). "A comparison of methods of collecting inocula of Meloidogyne spp., including a new technique." Plant Dis Rep 57: 1025-1028.

Hussey, R. S. and Grundler, F. M. W. (1998). Nematode parasitism of plants. The physiology of freeliving and plant-parasitic nematodes. R. N. Perry and D. J. Wright. Wallingford, CABI publishing**:** 213-243.

Hutangura, P., Mathesius, U., Jones, M. G. K. and Rolfe, B. G. (1999). "Auxin induction is a trigger for root gall formation caused by root-knot nematodes in white clover and is associated with the activation of the flavonoid pathway." Functional Plant Biology 26(3): 221-231.

Imlau, A., Truernit, E. and Sauer, N. (1999). "Cell-to-cell and long-distance trafficking of the green fluorescent protein in the phloem and symplastic unloading of the protein into sink tissues." Plant Cell 11(3): 309-322.

Inoue, S., Kinoshita, T., Matsumoto, M., Nakayama, K. I., Doi, M. and Shimazaki, K. (2008). "Blue light-induced autophosphorylation of phototropin is a primary step for signaling." Proc Natl Acad Sci U S A 105(14): 5626-5631.

Ioio, R. D., Nakamura, K., Moubayidin, L., Perilli, S., Taniguchi, M., Morita, M. T., Aoyama, T., Costantino, P. and Sabatini, S. (2008). "A Genetic Framework for the Control of Cell Division and Differentiation in the Root Meristem." Science 322(5906): 1380-1384.

Johnson, R. N. and Viglierchio, D. R. (1969). "A growth promoting substance occuring in an extract prepared from *Heterodera schachtii* larvae. ." Nematologica 15: 159-160.

Jones, M. G. and Northcote, D. H. (1972). "Nematode-induced syncytium--a multinucleate transfer cell." J Cell Sci 10(3): 789-809.

Jones, M. G. and Payne, H. L. (1978). "Early stages of nematode-induced giant-cell formation in roots of Impatiens balsamina." J Nematol 10(1): 70-84.

Jones, M. G. K. (1981). "Host cell responses to endoparasitic nematode attack: structure and function of giant cells and syncytia*." Annals of Applied Biology 97(3): 353-372.

Juergensen, K., Scholz-Starke, J., Sauer, N., Hess, P., van Bel, A. J. and Grundler, F. M. (2003). "The companion cell-specific Arabidopsis disaccharide carrier AtSUC2 is expressed in nematode-induced syncytia." Plant Physiol 131(1): 61-69.

Karczmarek, A., Overmars, H., Helder, J. and Goverse, A. (2004). "Feeding cell development by cyst and root-knot nematodes involves a similar early, local and transient activation of a specific auxin-inducible promoter element." Mol Plant Pathol 5(4): 343-346.

Katekar, G. F. and Geissler, A. E. (1980). "Auxin Transport Inhibitors: IV. Evidence of a common mode of action for a proposed class of auxin transport inhibitors: The phytotropins." Plant Physiology 66(6): 1190-1195.

Khan, J. A., Wang, Q., Sjolund, R. D., Schulz, A. and Thompson, G. A. (2007). "An early nodulin-like protein accumulates in the sieve element plasma membrane of Arabidopsis." Plant Physiol 143(4): 1576-1589.

Kleine-Vehn, J., Dhonukshe, P., Sauer, M., Brewer, P. B., Wisniewska, J., Paciorek, T., Benkova, E. and Friml, J. (2008). "ARF GEF-dependent transcytosis and polar delivery of PIN auxin carriers in Arabidopsis." Current Biology 18(7): 526-531.

Kleine-Vehn, J. and Friml, J. (2008). "Polar targeting and endocytic recycling in auxin-dependent plant development." Annu Rev Cell Dev Biol 24: 447-473.

Kleine-Vehn, J., Huang, F., Naramoto, S., Zhang, J., Michniewicz, M., Offringa, R. and Friml, J. (2009). "PIN auxin efflux carrier polarity is regulated by PINOID kinase-mediated recruitment into GNOM-independent trafficking in Arabidopsis." Plant Cell 21(12): 3839-3849.

Kögl, F., Erxleben, H. and Haagen-Smith, A. J. (1934). "Über die Isolierung der Auxine a und b aus pflanzlichen Materialien. IX. Mitteilung. ." Zeitschrift

für Physiologische Chemie 243: 209–226.

Laemmli, U. K. (1970). "Cleavage of structural proteins during the assembly of the head of bacteriophage T4." Nature 227(5259): 680-685.

Lee, S. H. and Cho, H. T. (2006). "PINOID positively regulates auxin efflux in Arabidopsis root hair cells and tobacco cells." Plant Cell 18(7): 1604-1616.

Leibfried, A., To, J. P. C., Busch, W., Stehling, S., Kehle, A., Demar, M., Kieber, J. J. and Lohmann, J. U. (2005). "WUSCHEL controls meristem function by direct regulation of cytokinin-inducible response regulators." Nature 438(7071): 1172-1175.

Ljung, K., Bhalerao, R. P. and Sandberg, G. (2001). "Sites and homeostatic control of auxin biosynthesis in Arabidopsis during vegetative growth." The Plant Journal 28(4): 465-474.

Ljung, K., Hull, A. K., Celenza, J., Yamada, M., Estelle, M., Normanly, J. and Sandberg, G. (2005). "Sites and Regulation of Auxin Biosynthesis in Arabidopsis Roots." The Plant Cell

Online 17(4): 1090-1104.

Lohar, D. P., Schaff, J. E., Laskey, J. G., Kieber, J. J., Bilyeu, K. D. and Bird, D. M. (2004). "Cytokinins play opposite roles in lateral root formation, and nematode and Rhizobial symbioses." The Plant Journal 38(2): 203-214.

Luschnig, C., Gaxiola, R. A., Grisafi, P. and Fink, G. R. (1998). "EIR1, a root-specific protein involved in auxin transport, is required for gravitropism in Arabidopsis thaliana." Genes Dev 12(14): 2175-2187.

Mähönen, A. P., Bonke, M., Kauppinen, L., Riikonen, M., Benfey, P. N. and Helariutta, Y. (2000). "A novel two-component hybrid molecule regulates vascular morphogenesis of the Arabidopsis root." Genes & Development 14(23): 2938-2943.

Mano, Y. and Nemoto, K. (2012). "The pathway of auxin biosynthesis in plants." Journal of Experimental Botany 63(8): 2853-2872.

Marchant, A., Bhalerao, R., Casimiro, I., Eklof, J., Casero, P. J., Bennett, M. and Sandberg, G. (2002). "AUX1 promotes lateral root formation by facilitating indole-3-acetic acid distribution between sink and source tissues in the Arabidopsis seedling." Plant Cell 14(3): 589-597.

Marchant, A., Kargul, J., May, S. T., Müller, P., Delbarre, A., Perrot-Rechenmann, C. and Bennett, M. J. (1999). "AUX1 regulates root gravitropism in Arabidopsis by facilitating auxin uptake within root apical tissues." EMBO J 18(8): 2066-2073.

Marella, H. H., Nielsen, E., Schachtman, D. P. and Taylor, C. G. (2013). "The Amino Acid Permeases AAP3 and AAP6 Are Involved in Root-Knot Nematode Parasitism of Arabidopsis." Molecular Plant-Microbe Interactions 26(1): 44-54.

Mazarei, M., Lennon, K. A., Puthoff, D. P., Rodermel, S. R. and Baum, T. J. (2003). "Expression of an Arabidopsis phosphoglycerate mutase homologue is localized to apical meristems, regulated by hormones, and induced by sedentary plant-parasitic nematodes." Plant Mol Biol 53(4): 513-530.

McClure, M. A. (1977). "Meloidogyne incognita: a metabolic sink." J Nematol 9(1): 88-90.

Meyer, S., Lauterbach, C., Niedermeier, M., Barth, I., Sjolund, R. D. and Sauer, N. (2004). "Wounding enhances expression of AtSUC3, a sucrose transporter from Arabidopsis sieve elements and sink tissues." Plant Physiol 134(2): 684-693.

Michniewicz, M., Zago, M. K., Abas, L., Weijers, D., Schweighofer, A., Meskiene, I., Heisler, M. G., Ohno, C., Zhang, J., Huang, F., Schwab, R., Weigel, D., Meyerowitz, E. M., Luschnig,

C., Offringa, R. and Friml, J. (2007). "Antagonistic Regulation of PIN Phosphorylation by PP2A and PINOID Directs Auxin Flux." Cell 130(6): 1044-1056.

Morris, D. (2000). "Transmembrane auxin carrier systems - dynamic regulators of polar auxin transport." Plant Growth Regulation 32(2-3): 161-172.

Moubayidin, L., Perilli, S., Dello Ioio, R., Di Mambro, R., Costantino, P. and Sabatini, S. (2010). "The Rate of Cell Differentiation Controls the Arabidopsis Root Meristem Growth Phase." Current Biology 20(12): 1138-1143.

Mravec, J., Skupa, P., Bailly, A., Hoyerova, K., Krecek, P., Bielach, A., Petrasek, J., Zhang, J., Gaykova, V., Stierhof, Y.-D., Dobrev, P. I., Schwarzerova, K., Rolcik, J., Seifertova, D., Luschnig, C., Benkova, E., Zazimalova, E., Geisler, M. and Friml, J. (2009). "Subcellular homeostasis of phytohormone auxin is mediated by the ER-localized PIN5 transporter." Nature 459(7250): 1136-1140.

Müller, A., Guan, C., Gälweiler, L., Tanzler, P., Huijser, P., Marchant, A., Parry, G., Bennett, M., Wisman, E. and Palme, K. (1998). "AtPIN2 defines a locus of Arabidopsis for root gravitropism control." EMBO J 17(23): 6903-6911.

Müller, B. and Sheen, J. (2007a). "Advances in cytokinin signaling." Science 318(5847): 68-69.

Müller, B. and Sheen, J. (2007b). "Arabidopsis Cytokinin Signaling Pathway." Sci. STKE 2007 (407)

Müller, B. and Sheen, J. (2008). "Cytokinin and auxin interaction in root stem-cell specification during early embryogenesis." Nature 453(7198): 1094-1097.

Offler, C. E., McCurdy, D. W., Patrick, J. W. and Talbot, M. J. (2002). "Transfer Cells: Cells specialized for a special purpose." Annu. Rev. Plant Biol. 54: 431–454

Okada, K., Ueda, J., Komaki, M. K., Bell, C. J. and Shimura, Y. (1991). "Requirement of the Auxin Polar Transport System in Early Stages of Arabidopsis Floral Bud Formation." The Plant Cell Online 3(7): 677-684.

Ottenschläger, I., Wolff, P., Wolverton, C., Bhalerao, R. P., Sandberg, G., Ishikawa, H., Evans, M. and Palme, K. (2003). "Gravity-regulated differential auxin transport from columella to lateral root cap cells." Proc Natl Acad Sci U S A 100(5): 2987-2991.

Palme, K. and Gälweiler, L. (1999). "PIN-pointing the molecular basis of auxin transport." Curr Opin Plant Biol 2(5): 375-381.

Paponov, I. A., Teale, W. D., Trebar, M., Blilou, I. and Palme, K. (2005). "The PIN auxin efflux facilitators: evolutionary and functional perspectives." Trends in Plant Science 10(4): 170-177.

Peret, B., De Rybel, B., Casimiro, I., Benkova, E., Swarup, R., Laplaze, L., Beeckman, T. and Bennett, M. J. (2009). "Arabidopsis lateral root development: an emerging story." Trends Plant Sci 14(7): 399-408.

Perilli, S., Di Mambro, R. and Sabatini, S. (2012). "Growth and development of the root apical meristem." Current Opinion in Plant Biology 15(1): 17-23.

Perilli, S., Moubayidin, L. and Sabatini, S. (2010). "The molecular basis of cytokinin function." Current Opinion in Plant Biology 13(1): 21-26.

Petersson, S. V., Johansson, A. I., Kowalczyk, M., Makoveychuk, A., Wang, J. Y., Moritz, T., Grebe, M., Benfey, P. N., Sandberg, G. r. and Ljung, K. (2009). "An Auxin Gradient and Maximum in the Arabidopsis Root Apex Shown by High-Resolution Cell-Specific Analysis of IAA Distribution and Synthesis." The Plant Cell Online 21(6): 1659-1668.

Petrasek, J. and Friml, J. (2009). "Auxin transport routes in plant development." Development 136(16): 2675-2688.

Petrasek, J., Mravec, J., Bouchard, R., Blakeslee, J. J., Abas, M., Seifertova, D., Wisniewska, J., Tadele, Z., Kubes, M., Covanova, M., Dhonukshe, P., Skupa, P., Benkova, E., Perry, L., Krecek, P., Lee, O. R., Fink, G. R., Geisler, M., Murphy, A. S., Luschnig, C., Zazimalova, E. and Friml, J. (2006). "PIN Proteins Perform a Rate-Limiting Function in Cellular Auxin Efflux." Science 312(5775): 914-918.

Przemeck, G. K., Mattsson, J., Hardtke, C. S., Sung, Z. R. and Berleth, T. (1996). "Studies on the role of the Arabidopsis gene MONOPTEROS in vascular development and plant cell axialization." Planta 200(2): 229-237.

Rademacher, E. H. and Offringa, R. (2012). "Evolutionary Adaptations of Plant AGC Kinases: From Light Signaling to Cell Polarity Regulation." Front Plant Sci 3: 250.

Rakusová, H., Gallego-Bartolomé, J., Vanstraelen, M., Robert, H. S., Alabadí, D., Blázquez, M. A., Benková, E. and Friml, J. (2011). "Polarization of PIN3-dependent auxin transport for hypocotyl gravitropic response in Arabidopsis thaliana." The Plant Journal 67(5): 817-826.

Redig, P., Shaul, O., Inze, D., Van Montagu, M. and Van Onckelen, H. (1996). "Levels of endogenous cytokinins, indole-3-acetic acid and abscisic acid during the cell cycle of synchronized tobacco BY-2 cells." FEBS Lett 391(1-2): 175-180.

Rubery, P. H. (1990). "Phytotropins: receptors and endogenous ligands. Hormone Perception and Signal Transduction in Animals and Plants." Cambridge: Company of Biologists. Roberts, J., Kirk, C. and M. Venis. pp. 119–146.

Ruegger, M., Dewey, E., Gray, W. M., Hobbie, L., Turner, J. and Estelle, M. (1998). "The TIR1 protein of Arabidopsis functions in auxin response and is related to human SKP2 and yeast Grr1p." Genes & Development 12(2): 198-207.

Sabatini, S., Beis, D., Wolkenfelt, H., Murfett, J., Guilfoyle, T., Malamy, J., Benfey, P., Leyser, O., Bechtold, N., Weisbeek, P. and Scheres, B. (1999). "An Auxin-Dependent Distal Organizer of Pattern and Polarity in the Arabidopsis Root." Cell 99(5): 463-472.

Sachs, T. and Woolhouse, H. W. (1981). The Control of the Patterned Differentiation of Vascular Tissues. Advances in Botanical Research, Academic Press. Volume 9**:** 151-262.

Sakai, T., Kagawa, T., Kasahara, M., Swartz, T. E., Christie, J. M., Briggs, W. R., Wada, M. and Okada, K. (2001). "Arabidopsis nph1 and npl1: Blue light receptors that mediate both phototropism and chloroplast relocation." Proceedings of the National Academy of Sciences 98(12): 6969-6974.

Sambrook, J., Fritsch, E. F. and Maniatis, T. (1989). Molecular cloning: A laboratory manual. Cold Spring Harbor, New York, Cold Spring Harbor Laboratory Press.

Santelia, D., Vincenzetti, V., Azzarello, E., Bovet, L., Fukao, Y., Düchtig, P., Mancuso, S., Martinoia, E. and Geisler, M. (2005). "MDR-like ABC transporter AtPGP4 is involved in auxin-mediated lateral root and root hair development." FEBS Letters 579(24): 5399-5406.

Santner, A. and Estelle, M. (2009). "Recent advances and emerging trends in plant hormone signalling." Nature 459(7250): 1071-1078.

Sasser, J. N. (1980). "Root-knot nematodes: A global menace to crop production." Plant Dis 64: 36-41.

Sauer, M., Robert, S. and Kleine-Vehn, J. (2013). "Auxin: simply complicated." J Exp Bot 64(9): 2565-2577.

Scarpella, E., Marcos, D., Friml, J. and Berleth, T. (2006a). "Control of leaf vascular patterning by polar auxin transport." Genes & Development 20(8): 1015-1027.

Scarpella, E., Marcos, D., Friml, J. and Berleth, T. (2006b). "Control of leaf vascular patterning by polar auxin transport." Genes Dev 20(8): 1015-1027.

Scheres, B., Di Laurenzio, L., Willemsen, V., Hauser, M. T., Janmaat, K., Weisbeek, P. and Benfey, P. N. (1995). "Mutations affecting the radial organisation of the Arabidopsis root display specific defects throughout the embryonic axis." Development 121: 53-62.

Scheres, B., Wolkenfelt, H., Willemsen, V., Terlouw, M., Lawson, E., Dean, C. and Weisbeek, P. (1994). "Embryonic origin of the Arabidopsis primary root and root meristem initials" Development 120: 2475-2487.

Sijmons, P. C., Grundler, F. M. W., von Mende, N., Burrows, P. R. and Wyss, U. (1991). "Arabidopsis thaliana as a new model host for plant-parasitic nematodes." The Plant Journal 1(2): 245-254.

Skoog, F. and Miller, C. O. (1957). "Chemical regulation of growth and organ formation in plant tissue scultured in vitro." Symp. Soc. Exp. Biol. 11: 118-131.

Stadler, R. and Sauer, N. (1996). " The Arabidopsis thaliana AtSUC2 gene is specifically expressed in companion cells." Bot. Acta 109: 299-306.

Steinmann, T., Geldner, N., Grebe, M., Mangold, S., Jackson, C. L., Paris, S., Gälweiler, L., Palme, K. and Jürgens, G. (1999). "Coordinated Polar Localization of Auxin Efflux Carrier PIN1 by GNOM ARF GEF." Science 286(5438): 316-318.

Sussman, M. R. and Gardner, G. (1980). "Solubilization of the Receptor for N-1-Naphthylphthalamic Acid." Plant Physiology 66(6): 1074-1078.

Swarup, K., Benkova, E., Swarup, R., Casimiro, I., Peret, B., Yang, Y., Parry, G., Nielsen, E., De Smet, I., Vanneste, S., Levesque, M. P., Carrier, D., James, N., Calvo, V., Ljung, K., Kramer, E., Roberts, R., Graham, N., Marillonnet, S., Patel, K., Jones, J. D., Taylor, C. G., Schachtman, D. P., May, S., Sandberg, G., Benfey, P., Friml, J., Kerr, I., Beeckman, T., Laplaze, L. and Bennett, M. J. (2008). "The auxin influx carrier LAX3 promotes lateral root emergence." Nat Cell Biol 10(8): 946-954.

Tanaka, H., Dhonukshe, P., Brewer, P. B. and Friml, J. (2006). "Spatiotemporal asymmetric auxin distribution: a means to coordinate plant development." Cellular and Molecular Life Sciences CMLS 63(23): 2738-2754.

Terasaka, K., Blakeslee, J. J., Titapiwatanakun, B., Peer, W. A., Bandyopadhyay, A., Makam, S. N., Lee, O. R., Richards, E. L., Murphy, A. S., Sato, F. and Yazaki, K. (2005). "PGP4, an ATP Binding Cassette P-Glycoprotein, Catalyzes Auxin Transport in Arabidopsis thaliana Roots." The Plant Cell Online 17(11): 2922-2939.

Titapiwatanakun, B., Blakeslee, J. J., Bandyopadhyay, A., Yang, H., Mravec, J., Sauer, M., Cheng, Y., Adamec, J., Nagashima, A., Geisler, M., Sakai, T., Friml, J., Peer, W. A. and Murphy, A. S. (2009). "ABCB19/PGP19 stabilises PIN1 in membrane microdomains in Arabidopsis." The Plant Journal 57(1): 27-44.

To, J. P., Haberer, G., Ferreira, F. J., Deruere, J., Mason, M. G., Schaller, G. E., Alonso, J. M., Ecker, J. R. and Kieber, J. J. (2004). "Type-A Arabidopsis response regulators are partially redundant negative regulators of cytokinin signaling." Plant Cell 16(3): 658-671.

To, J. P. C. and Kieber, J. J. (2008). "Cytokinin signaling: two-components and more." Trends in Plant Science 13: 85-92.

Torres-Ruiz, R. A. and Jürgens, G. (1994). "Mutations in the FASS gene uncouple pattern formation and morphogenesis in Arabidopsis development." Development 120: 2967-2978.

Trudgill, D. L. (1972). "Influence of Feeding Duration On Moulting and Sex Determination of Meloidogyne Incognita." Nematologica 18(4): 476-481.

Trudgill, D. L. and Blok, V. C. (2001). "Apomictic, polyphagous root-knot nematodes: exceptionally successful and damaging biotrophic root pathogens." Annu Rev Phytopathol 39: 53-77.

Ullrich, C. I. and Aloni, R. (2000). "Vascularization is a general requirement for growth of plant and animal tumours." Journal of Experimental Botany 51(353): 1951-1960.

Ulmasov, T., Liu, Z. B., Hagen, G. and Guilfoyle, T. J. (1995). "Composite structure of auxin response elements." The Plant Cell Online 7(10): 1611-1623.

Ulmasov, T., Murfett, J., Hagen, G. and Guilfoyle, T. J. (1997). "Aux/IAA proteins repress expression of reporter genes containing natural and highly active synthetic auxin response elements." Plant Cell 9(11): 1963-1971.

van den Berg, C., Willemsen, V. H., W.; , Weisbeek, P. and Scheres, B. J. G. (1995). "Cell fate in the Arabidopsis root meristem determined by directional signalling." Nature 378(6552): 62-65.

Vanneste, S. and Friml, J. (2009). "Auxin: A Trigger for Change in Plant Development." Cell 136(6): 1005-1016.

Vieten, A., Sauer, M., Brewer, P. B. and Friml, J. (2007). "Molecular and cellular aspects of auxin-transport-mediated development." Trends Plant Sci 12(4): 160-168.

Weijers, D. and Jürgens, G. (2005). "Auxin and embryo axis formation: the ends in sight?" Current Opinion in Plant Biology 8(1): 32-37.

Went, F. W. and Thimann, K. V. (1937). "Phytohormones." New York, Macmillan.

Wenzel, C. L., Schuetz, M., Yu, Q. and Mattsson, J. (2007). "Dynamics of MONOPTEROS and PIN-FORMED1 expression during leaf vein pattern formation in Arabidopsis thaliana." The Plant Journal 49(3): 387-398.

Werner, D. (2011)." Symplastische Kopplung in Arabidopsis thaliana: Untersuchungen zur Phloementladung sowie Entstehung und Verteilung von Plasmodesmata." Naturwissenschaftliche Fakultät Erlangen, Friedrich-Alexander-Universität Erlangen-Nürnberg.

Williamson, V. M. and Gleason, C. A. (2003). "Plant-nematode interactions." Curr Opin Plant Biol 6(4): 327-333.

Willige, B. C., Ahlers, S., Zourelidou, M., Barbosa, I. C. R., emarsy, E., Trevisan, M., Davis, P. A., Roelfsema, M. R. G., Hangarter, R., Fankhauser, C. and Schwechheimer, C. (2013). "D6PK AAGCVIII kinases are required for auxin transport and phototropic hypocotyl bending." The Plant Cell 25(5): 1674-1688.

Woodward, A. W. and Bartel, B. (2005). "Auxin: Regulation, Action, and Interaction." Annals of Botany 95(5): 707-735.

Wyss, U. (1997). "Root parasitic nematodes: An overview. Cellular and molecular aspects of plant-nematode interaction." C. Fenoll, F. M. W. Grundler and S. A. Ohl. Dordrecht 5–22, Kluwer Academic Publishers: 5–22.

Wyss, U., Grundler, F. and Munch, A. (1992). "The parasitic behaviour of second stage juveniles of *Meloidogyne incognita* in roots of *Arabidopis thaliana*" Nematologica 38: 98-111

Yang, H. and Murphy, A. S. (2009). "Functional expression and characterization of Arabidopsis ABCB, AUX 1 and PIN auxin transporters in Schizosaccharomyces pombe." The Plant Journal 59(1): 179-191.

Yang, Y., Hammes, U. Z., Taylor, C. G., Schachtman, D. P. and Nielsen, E. (2006). "High-affinity auxin transport by the AUX1 influx carrier protein." Curr Biol 16(11): 1123-1127.

Yu, P. K. and Viglierchio, D. R. (1964). "Plant growth substances and parasitic nematodes. I. Root knot nematodes and tomato." Experimental Parasitology 15(3): 242-248.

Zazimalova, E., Krecek, P., Skupa, P., Hoyerova, K. and Petrasek, J. (2007). "Polar transport of the plant hormone auxin" the role of PIN-FORMED (PIN) proteins." Cellular and Molecular Life Sciences 64(13): 1621-1637.

Zazimalova, E., Murphy, A. S., Yang, H., Hoyerova, K. and Hosek, P. (2010). "Auxin transporters--why so many?" Cold Spring Harb Perspect Biol 2(3): a001552.

Zegzouti, H., Li, W., Lorenz, T. C., Xie, M., Payne, C. T., Smith, K., Glenny, S., Payne, G. S. and Christensen, S. K. (2006). "Structural and Functional Insights into the Regulation of Arabidopsis AGC VIIIa Kinases." Journal of Biological Chemistry 281(46): 35520-35530.

Zhang, K., Letham, D. and John, P. L. (1996). "Cytokinin controls the cell cycle at mitosis by stimulating the tyrosine dephosphorylation and activation of p34cdc2-like H1 histone kinase." Planta 200(1): 2-12.

Zourelidou, M., Müller, I., Willige, B. C., Nill, C., Jikumaru, Y., Li, H. and Schwechheimer, C. (2009). "The polarly localized D6 PROTEIN KINASE is required for efficient auxin transport in Arabidopsis thaliana." Development 136(4): 627-636.

Eidesstattliche Erklärung

Ich erkläre hiermit an Eides statt, dass ich die vorliegende Arbeit ohne unzulässige Hilfe Dritter und ohne Benutzung anderer als der angegebenen Hilfsmittel angefertigt habe.

Die aus anderen Quellen direkt oder indirekt übernommenen Daten und Konzepte sind durch Angabe des Literaturzitats gekennzeichnet.

Birgit Absmanner

Regensburg, den 20.6.2013